The Performance of Reinforced Concrete

External Beam-Column Joints Subjected to

Non-reversing Cyclic Loading.

By

GRAHAM ALAN BROWN B.E.(Hons)

Civil Engineering Department
University of Adelaide.

This thesis was submitted in March 1979 as
2/3 of the requirement for a Master of
Engineering Science degree at the University
of Adelaide.

Supervisor : Dr M. J. S. Hirst.

C O N T E N T S

Contents Continued...

Contents continued....   <u>Page</u>

S U M M A R Y

Since the occurrence of a devasting cyclone over Darwin in December 1974, there has been increased interest locally in the fatigue performance of materials and structures at high intensity loads. This research programme has tested reinforced concrete T-joints under these conditions and forms part of a wider research programme at the University of Adelaide into general joint performance.

Previous research on the T-joint has shown that standard designs used in construction are often weaker than the connected members unless special precautions are taken. Tests were undertaken to determine the effect of the load distribution and magnitude on the static and fatigue performance of a joint commonly used in practice. The results indicate that it is possible to construct a joint that will maintain a load sufficient to yield the reinforcement either to a large static deflection or to at least 40,000 cycles when tested in fatigue. Variations of the load distribution and magnitude were found to have no effect to at least 40,000 load cycles.

Further tests were conducted to determine the effect of variations of the reinforcement layout, bond length and load distribution. It was found that these parameters can have a large effect on the performance of the T-joint and that specimens designed in accordance with Australian Standard AS 1480 Concrete Structures Code may not perform satisfactorily under static or fatigue loads. With a large compressive column load the performance of some joints was improved because of increased steel bond strength and reduced tensile stress on the joint block diagonal.

A complementary theoretical investigation resulted in an improved model to predict joint block cracking. Linear and non-linear

finite element models of the T-joint were also developed.
These 3 models were used with varying amounts of success to
predict the performance of the specimens under test.

This Thesis contains no material which has been accepted for the award of any other degree or diploma in any university and that to the best of the candidate's knowledge and belief the thesis contains no material previously published or written by another person, except when due reference is made in the text of the thesis.

Graham Alan Brown.

GLOSSARY OF TERMS AND NOTATION

Figure 1.1	Defines the terms used to describe the parts of the T-joint.
"D"	The overall depth of the member.
"joint block model"	A simplified description of the joint block structure in terms of 1 or 2-dimensional members.
"load/force distribution"	One of a possible set of loads/forces which are applied to the joint or joint block.
"joint efficiency"	The ratio of the strength of the joint to the calculated flexural strength of the beam.
"cracking moment (M_{cr})"	The moment in the beam at the centre of the joint which will cause the joint block to crack on the primary diagonal.
"yield moment (M_y)"	The moment in the beam at the centre of the joint which will cause a plastic hinge to form in the joint block or adjacent beam.
"ultimate moment (M_u)"	The maximum moment that the joint will carry in terms of the beam moment at the centre of the joint block.

Additional description of the notation is given in Chapter 3 where it is first used.
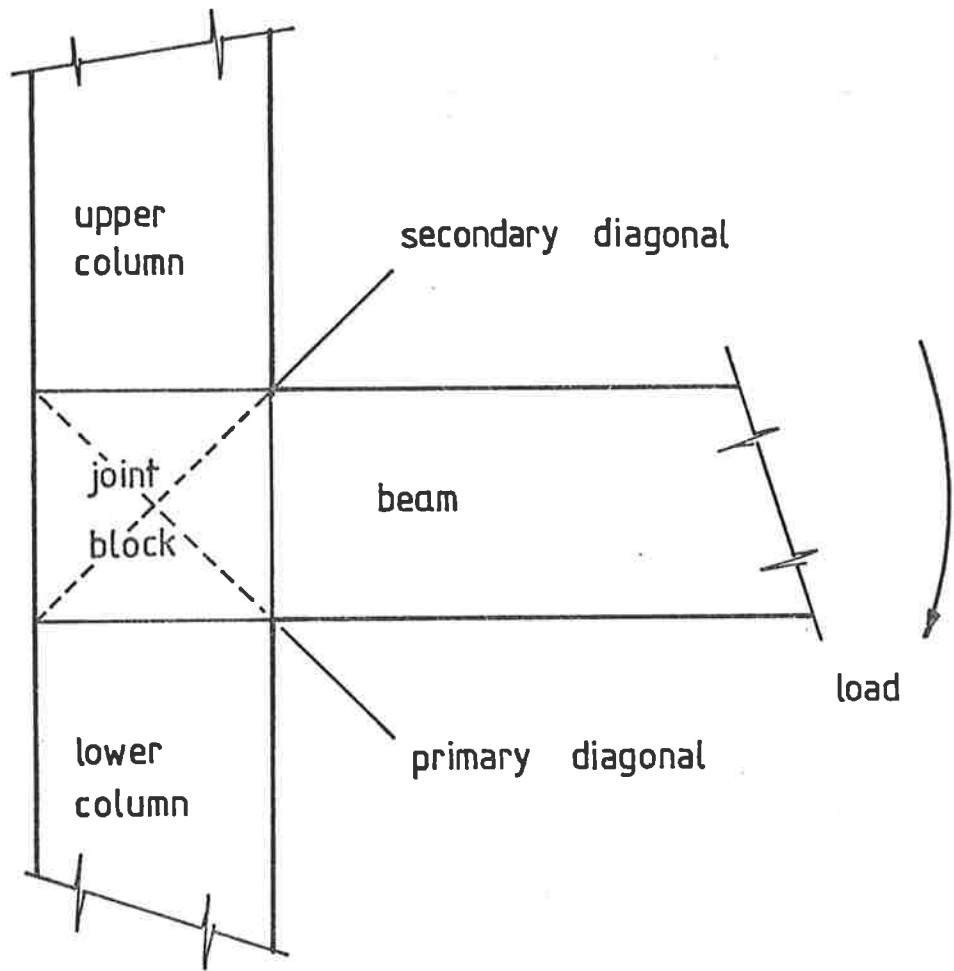
FIGURE 1.1   T-joint terms.

1.   INTRODUCTION

When engineers design a reinforced concrete structure they often assume that if standard reinforcement details are used the joints are as strong and ductile as the members they connect. This assumption is known to be incorrect in some circumstances, especially for the T-joint formed by the connection between a column and a beam. One of the many examples of the T-joint occurs in the exterior walls of multi-story buildings.

Since the weakness of the T-joint has been recognised there have been extensive investigations to determine the modes of failure and performance parameters under static and seismic loads[1][2][3][9][10][11][12]. Several failure modes were found, the common one being diagonal cracking of the joint block as shown in Figure 1.2. The performance of the joint after the formation of the crack varied from a rapid collapse to very ductile. Specimens collapsed due to loss of bond on the reinforcement in the joint block and inability to form a compressive strut on the primary diagonal. The significance of the failure of the joint(s) depends on the type of loading and the location of the joint(s) within the structure.

Under static load the joint must resist the load and remain visually acceptable. Thus the formation of a diagonal crack in the joint block would often violate service criteria. In practice, only a few cases of T-joint failure have been observed under static load[1]. The low number of failures and the absence of joints which have collapsed is due to the redistribution of forces within the structure. The loss of stiffness in a small number of joints, because of the formation of a crack, can be hidden because of the redistribution of moment to a stiffer part of the structure. A joint which subsequently loses strength at a greater deflection is thus prevented from collapsing. This reduces the risk of collapse of the whole
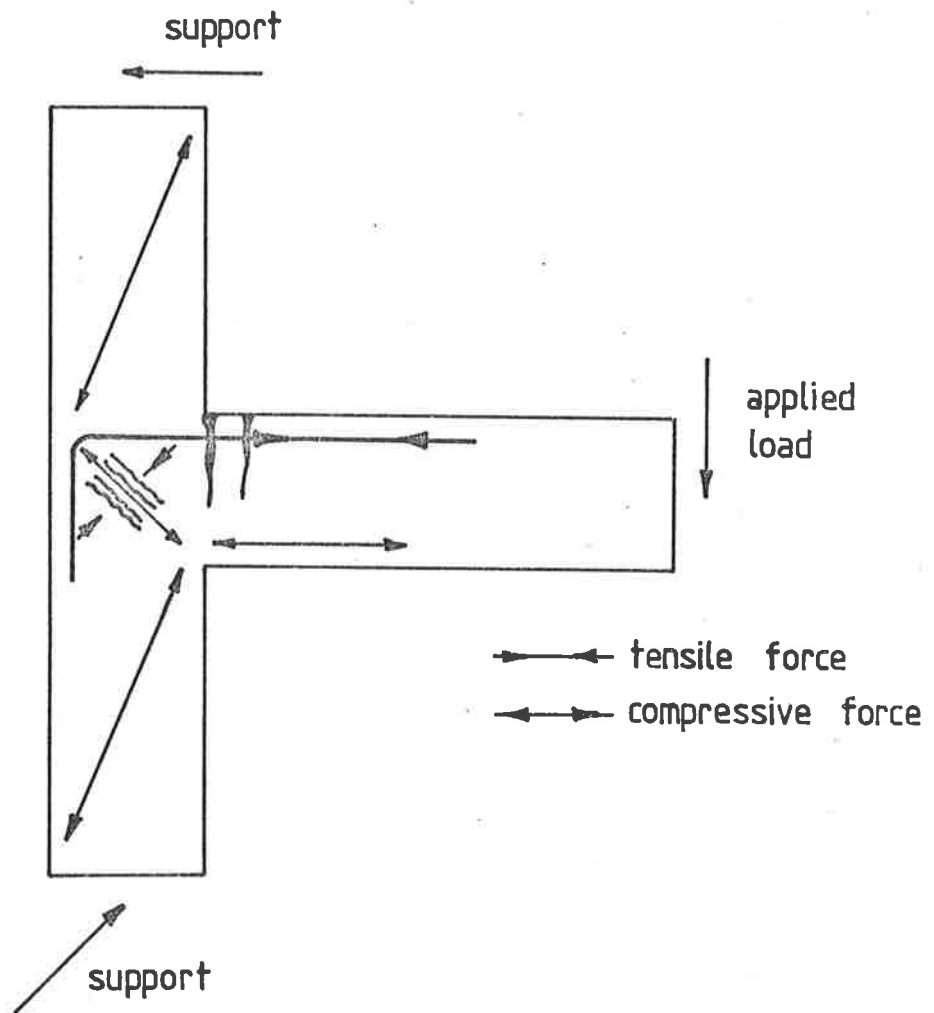
FIGURE 1.2   The force system that causes
diagonal cracking of the joint block.

structure and minimises joint damage.

Under seismic loading the joint is subjected to large reversing forces. To allow the structure to absorb the energy from the earthquake the joints are designed to undergo large plastic deformations. The very severe seismic loading has resulted in more failures of T-joints than have been observed under static loads [13][14][15]. One of the design aims is to minimise the plastic deformations in the joint block. This helps to maintain the strength of the joint and minimise damage. The appearance of the joint after a severe earthquake is generally of secondary importance to strength. The experimental research indicates that failure of the joint block is often by the formation of diagonal joint block cracks and subsequent loss of shear strength. Because the loading is bi-directional the cracks form on both diagonals. Cycling of the load causes rapid disintegration of the joint and a loss of strength. Bond failure on the steel reinforcing often occurs because of the degradation of the surrounding concrete and the large steel forces. Researchers have now determined the major parameters which control the performance of the T-joint under static and seismic load. This enables joints to be designed which have greatly improved performance under static or seismic loads.

However, the occurrence of a cyclone in Northern Australia which devastated the City of Darwin has prompted a large amount of interest in the fatigue performance of materials and structures at high intensity loads. The geographic and demographic distribution of cities and towns in the cyclonic areas of Australia results in a reduced demand for prime commercial land. Thus, most multi-storey buildings would be less than 5 stories high. Often it is possible to resist the lateral wind load in the columns rather than by a stiff central core as is done in tall

slender buildings. For those buildings where the proportion of T-joints is significant, the T-joint performance could have a large effect on the overall performance of the structure, although there are no known failures of T-joints due to wind loading. This may be because of the brick cladding and rigid interior panel walls which greatly increase the stiffness over that of the bare frame and reduce the sway of the building. However, there is an increasing trend to reduce this additional stiffness for economy which may thus result in fatigue failure of the joints.

Only a small percentage of the cyclones affecting these structures would be expected to be of such intensity that they would cause damage. However, during the life of the structure the accumulating damage may result in collapse. There was no previous knowledge on the performance of the T-joint under fatigue loading other than what could be interpolated from the static and seismic performance. Because of the increasing dependance on the integrity of the building frame and the revived awareness of the damage caused by cyclones it is important that the fatigue performance of the T-joint and probability of failure is known.

For a joint to have satisfactory fatigue performance it must have adequate strength, as for static loading. It is also necessary that the joint is able to resist this load after many load cycles. Unlike seismic loading, the direction of the cyclonic loading may be patterned and may not reverse every cycle. Thus the adoption of seismic joint designs to resist cyclonic fatigue loads may result in overdesigned and uneconomic structures. Conversely, the static design methods used at present for cyclonic loading may result in failure.

In order to provide the necessary fatigue design data a research programme was begun to study the performance of the T-joint when subjected

to cyclonic loading. The work included in this thesis is a preliminary investigation to determine some of the critical design parameters and to evaluate a reinforcement layout used commonly in practice. These aims were to be achieved by a testing programme and a theoretical analysis. It was expected that the performance of the joint under cyclonic loading would be a median of that due to static and seismic loading. However, because of the preliminary nature of this part of the work in the overall programme it was designed to provide broad qualitative results and not necessarily detailed quantitative design recommendations.

2. LITERATURE REVIEW

The performance of the T-joint under cyclonic or fatigue loading had not previously been investigated. To obtain information on the likely fatigue performance of the T-joint literature on related topics was studied. These topics being the performance of the T-joint under static and seismic loading and the fatigue performance of the joint components.

2.1 Static Performance of the T-Joint

Two significant independant investigations have been made into the static performance of T-joints. Investigations conducted by Taylor, Clarke and Somerville[1][2] in England and Nilsson and Losberg[3] in Sweden were parts of larger research programmes on joints conducted in each of the countries. The tests were similar in the type of experimentation and results obtained. The main points can be summarised as follows:

(1) The characteristic failure mode of the T-joint
     is the formation of a crack on the primary
     diagonal (see Figure 1.2). The collapse
     mechanism depends on the reinforcement
     layout. Collapse can occur by the shear failure
     of the joint block due to the diagonal crack
     or by crushing of the concrete parallel to the
     diagonal crack(s).
     Although the crack may form at a low load the
     specimen may resist an increased load without

collapsing. Significant beam hinging also occurs in the more efficient joints.

(2)   The static strength efficiency of the T-joint varies considerably depending on the reinforcement layout, amount and anchorage, and load distribution. The tests show that some reinforcement layouts have static efficiencies (joint strength/member strength) as low as 24 per cent.

(3)   The joint forces can be modelled with a simplified force system. This enables the joint block cracking load to be predicted.

The relevant results from each of the research programmes are discussed further on the following pages.

Figure 2.1 shows T-joints which are typical of those used in the tests of Nilsson[3], Somerville[1] and Taylor[2]. Each specimen consisted of a joint block and 3 stubmembers. The reinforcement was varied in each of the specimens. In addition, the tests simulated different load distributions on the joint by the use of different beam and column loads.

Although Nilsson implies that his tests modelled the connection between a bridge deck and the supporting wall his specimens only had a 200 mm thick joint block. It is expected these narrow specimens would give a conservative result compared to a wider joint. The specimens tested by Somerville[1] and Taylor[2] were meant to model an external beam-column joint in a building frame and were similar in size to those used by Nilsson.
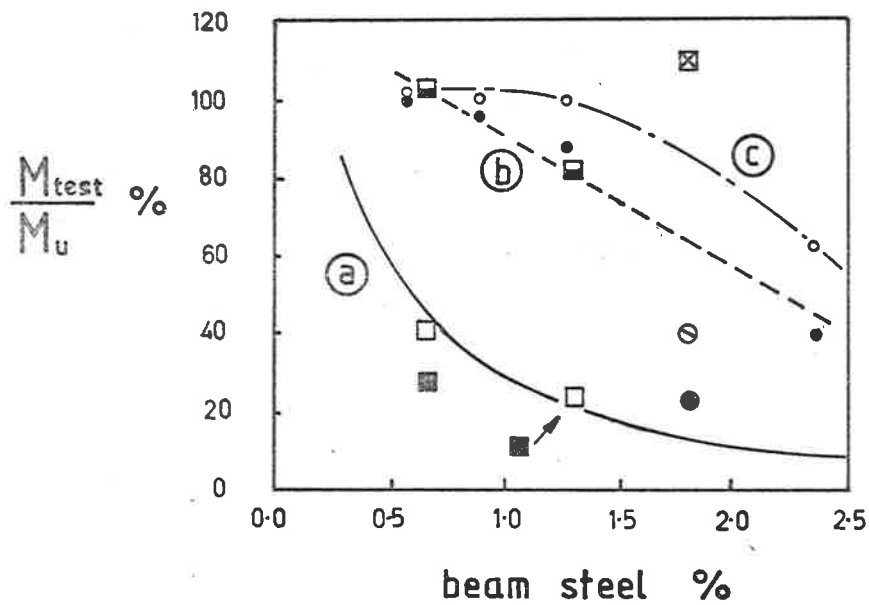
a   Nilsson's cracking model (590 MPa steel)
b   Somerville average cracking %
c   Somerville average failure %
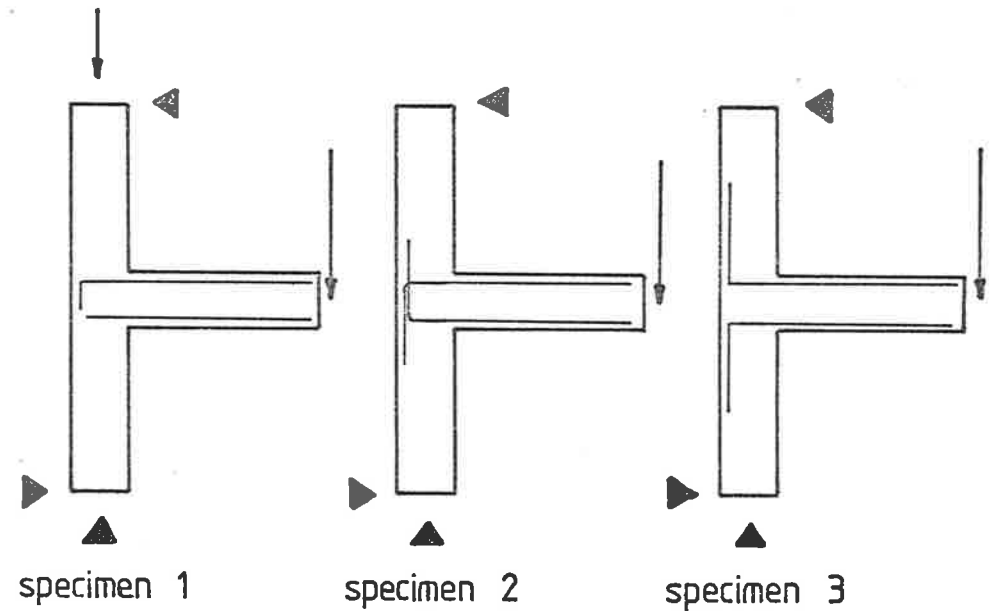
FIGURE 2.1   The effect of reinforcement variations on specimen performance.

The specimens tested by Nilsson contained no shear steel in the joint block or members. However, those tested by Somerville and Taylor contained a small amount. Only one ligature was within the joint block, the rest were evenly spaced at a distance equal to the depth of the column (6 mm ϕ ligatures at 145 mm c.c. throughout the column). Because the amount of shear steel is small it may be assumed to be unreinforced against shear in the joint block.

In the following discussion the members of both types of T-joint are defined such that the column is the continuous member and the beam is truncated at the joint block.

Nilsson and Taylor show that the diagonal joint block crack is a result of the shear stresses applied to the joint block by the connected members (see Figure 1.2). Although cracking of the joint would often be regarded as a failure, particularly with strict serviceability criteria, Somerville and Nilsson have shown that often the joints can carry an increased load (see Figure 2.1). In those specimens which did not collapse in the joint block, hinges formed in the members at the face of the joint block.

When the failure of the specimen occurred in the joint block Somerville[1] and Taylor[2] observed that crushing of the compressive diagonal (parallel to diagonal crack(s)) sometimes occurred. The crushing resulted in a loss of strength. Nilsson does not indicate the presence of this action. Taylor makes reference to bearing failures under the bend in the beam tension reinforcement for tests by Jirsa and Marques[4] in specimens where the beam steel was located outside of the column steel. As Taylor did not observe any bearing failures in his tests despite the calculated high bearing stresses, he concluded that the bearing capacity was considerably enhanced by the confinement of the ligatures around the column steel.

Taylor also recognised the presence of high bond stresses on the column bars where they pass through the joint block. Although no failures were observed by Taylor, concrete splitting has been observed under seismic loading[8].

Nilsson, Somerville and Taylor's results show that the formation of the crack and the collapse of the joints can occur within a wide range of efficiencies. Values of 24-110 per cent were recorded. Their results indicate that the parameters controlling the performance are reinforcement layout and percentage, the reinforcement anchorage and the load distribution.

Bending the beam tension steel in or out of the joint block produces a change of up to 85 per cent in joint efficiency. When the beam tension reinforcement is bent into the joint block the radial forces in the bend act directly on the compressive diagonal. Conversely, when the beam tension reinforcement is bent out of the joint block the compressive diagonal strut is resisted only by the surrounding concrete and column steel.

Variations in the reinforcement percentages have produced large variations in joint efficiencies. The results for Nilsson and Somerville's tests are shown in Figure 2.1. Although the test programmes used different loading conditions it is evident that 100 per cent joint efficiencies are achieved below a certain beam steel percentage. This is due to the reduction in beam strength below that of the joint block.

A significant difference between the specimens tested by Nilsson and those by Somerville and Taylor, was the position at which the bond length of the beam bars was considered to begin. Somerville's design assumed that bond was effective from the column face and Nilsson assumed that bond was effective from the bend in the steel except for those layouts that restricted the available bond length. The actual bond lengths used in each of the test programmes was not given in the literature. The collapse loads for the comparable specimens in

Figure 2.1 do not show conclusively the benefits of the increased bond
length used by Nilsson because of the small number of comparable tests,
and different member axial loads.

Taylor has considered the effect of lateral stress provided by the
column axial force on the bond of the beam tension steel. Tests were
made by Taylor on bars embedded in concrete and it was found that the
bond strength could be doubled by increasing the lateral compressive stress
to 30 MPa. Normally, without any column pre-stress, the beam tension
bars are subjected to lateral tensile stress where they enter the joint
block. This is considered by Park and Paulay[8] to reduce the effective
bond strength.

Nilsson has shown that compressive axial force in the beam will
increase the joint strength. Increases in ultimate strength of 15-25 per
cent were obtained. Although Somerville[1] and Taylor[2] considered the
significance of column axial load they only used one value of it to
represent the load from the upper floors of the building. Several other
investigations into the effect of column axial load on joint performance
have shown that it is significant[5][6]. Although these tests were not
made on T-joints they show the need for a full investigation into the
effect of member axial load on T-joints and the need to use a realistic
load distribution representative of that occurring in a real structure.

Nilsson and Taylor have both developed simple models of the joint
block stress distribution and structure. Taylor's model relates the
tensile stress in the joint block immediately prior to cracking to the
applied shear and normal stress distribution by using the principal stress
equation for a solid body. The pattern of forces around the joint block
is determined from the forces applied to the members and the geometry of

the joint. Nilsson has used an elastic analysis to show that the
distribution of the tensile stress on the plane of the crack is parabolic.
His model assumes that the plane of the crack is perpendicular to the
vector sum of the force in the beam tension steel and the tension force in
the inner column steel. The relationship between peak tensile stress
and the applied joint moment is found by integrating the tensile stress on
the potential crack plane and equating this to the forces applied to the
joint block. Both of these models have been used to predict the test
results. Because the models make no allowance for any strength increase
due to the steel reinforcement they must be a conservative solution.
Taylor has shown his test results in relation to the predicted cracking
loads. Although some predictions were close to the actual test values,
many of the test values were up to twice the predicted values. In all
instances the predicted values were a lower bound. Similarly, Nilsson
has shown that his model will predict the cracking load very closely for
the most inefficient reinforcement layouts. He indicates, although
without quantitative proof, that the more efficient joints crack at a load
higher than that predicted by the model. A detailed analysis and
discussion of Nilsson's model is given in Chapter 3.

The two research programmes have both reached similar conclusions
regarding the parameters controlling joint performance. However, because
of the small number of tests and the lack of comparable results there is
little quantitative information.

2.2 Seismic Performance of the T-joint

The seismic performance of the T-joint was included in the literature
review for the insight it could give to the more general question of
joint fatigue performance and in particular performance under cyclonic
loading.

Under seismic loading the joint must maintain adequate strength while undergoing large imposed deflections in two opposite directions. The ability to do this determines if the joint is satisfactory. Under seismic loading cracking of the joint is accepted since by undergoing large deflections the energy absorption capacity of the joint is greatly increased.

As might be expected, the parameters controlling seismic joint performance are principally those discussed in Section 2.1 on the static load performance of the T-joint. However, some of these parameters are now more important because of the severe nature of the loading. In addition, other parameters are now important in assessing joint performance.

The following discussion is principally concerned with the work by Hanson and Connor[11], and Park, Paulay and Megget[9][10]. The last three researchers were part of a team at the University of Canterbury in New Zealand which tested a particular series of specimens.

Failure of the joint can occur in the joint block or in the adjacent members. Park and Paulay state that in the tests at the University of Canterbury all 13 specimens failed in the joint block rather than in the beam. This was regarded as serious as it weakens the columns, and not just the beam, with resulting instability problems for the frame as a whole.

The lines of force in the joint block are as discussed for static loading but because the loading direction reverses periodically the joint block is subjected to cyclicly varying stresses and suffers rapid degradation. Park[9] describes the breakdown and failure of the joint block as follows:

(1)   Diagonal cracking occurs on the first cycle.

(2)   Reversed loading causes tension cracks to form on

the other diagonal of the joint block.

(3)   Small shear displacements across the crack (yielding
        of shear steel if present) causes grinding and
        uneven bearing when joint is loaded in reverse
        direction. This leads to the disintegration of
        the joint block with a large increase in volume.

(4)   Where transverse shear steel is present (usually
        standard for seismic design) crack sizes are reduced,
        and depending on its configuration, volume increases
        are reduced.

(5)   The deterioration of the joint block can result in
        loss of strength and stiffness which is usually
        considered a failure.

Megget concluded from his observations of the seismic tests that the joint
block collapses when it is unable to form a diagonal compressive strut.
Park[9] notes that failure of the joint may also result from bond failure
of the reinforcement. Hanson[11] also observed that where the column
cross-section was reduced assymetrically by concrete spalling, instability
may cause joint collapse.

The research conducted in New Zealand[9][10] at the University of
Canterbury and in America by Hanson and Connor[11] indicates that the
important performance parameters are;

(1)   steel layout

(2)   steel anchorage

(3)   shear steel

(4)   column axial load

(5)   side beams.

These parameters influence the stress pattern in the joint and/or increase the joints ability to carry the stresses.

A comparison of the New Zealand and the American test results reveals some interesting points. Park[9] concluded from his observations that where the column is narrow and lightly loaded the bond length on the beam steel should be provided from the bend in the reinforcement because of the poor bonding where the steel enters the joint block. This is due to the surrounding concrete often being in tension due to column bending, longitudinal splitting of the concrete and the possibility of lower quality concrete surrounding the steel because of sedimentation. They tested various anchorage conditions with bond lengths in accordance with ACI 318-71[17] recommendations where possible. Hanson considers that if the bond is provided from the face of the column in accordance with ACI 318-63[16] then bond strength is adequate. The two editions of the ACI code state the required bond length using different formulae. For the same strength of concrete and same size reinforcement the 1971 edition requires 18 per cent more bond length.

The difference in the performance of the T-joints in the different test programmes is explained by Megget and Park who consider the deflections imposed in Hanson's tests to be inadequate. As discussed previously, work by Taylor[2] has shown the lateral compressive stresses on the reinforcement significantly increase the bond strength. The New Zealand researchers had noted the possible increased joint shear strength due to the column loading but decided against its use because they were modelling joints in frames with low column loads. Although Hanson used different column loads he did not indicate it had any effect on bond strength.

Splitting along the column reinforcement in the joint block occurred in New Zealand tests[8]. This was attributed to the very high bond stresses caused by the rapid changes in steel reinforcement forces through

the joint block. These high bond stresses had been noted in the static
tests by Taylor but no damage was observed.

Joint block shear steel is normally only used in buildings subject
to seismic loading. The shear steel not only carries the large shear
forces but helps to contain the joint block. Park[9] says that shear
steel placed in accordance with ACI 318-71 is inadequate and that no
allowance should be made for the shear carried by the concrete in the
absence of column axial load. Some of Hanson's specimens used similar
amounts of shear steel but had more than twice the beam flexural strength.
Hanson showed that for his tests this level of shear steel was adequate.
As noted by Megget, the different results are due to the different
deflections imposed in the tests. The selection of the shear steel is
sometimes based on information gained from a rigid body analysis of the
cracked joint block. This is regarded by Park[9] as inadequate as not all
of the shear steel in the joint block yields. Thus the steel is not all
equally effective and this must be taken into account when prescribing
steel requirements.

In a real structure the T-joint is normally constrained by adjacent
beams at 90 degrees to the joint. Hanson says that his tests indicate
that in this situation the joint operates satisfactorily without shear steel.
Photographs taken during investigations into the effects of earthquakes
also indicate that joint performance may be improved by lateral
confinement[13][14][15].

The tests show the T-joints designed for seismic loading usually
perform well under static loading but lose strength under seismic loading.
In the joint tests discussed by Park, Paulay and Megget[9][10] and Hanson
and Connor[11] the joints had static efficiencies greater than 85 per cent

with the majority near 100 per cent. The seismic performance of the
joints varied from completely unsatisfactory to satisfactory. The
definition of satisfactory performance varied between the tests because
of the difference in the imposed joint ductilities. Park and Paulay[9] did
not consider any of their test specimens as having adequate performance,
as they all failed in the joint block. The best specimen maintained 80 per
cent of its initial yield strength at the end of the test. Some of the
specimens lost strength rapidly after the first plastic cycle and some
fell as low as 40 per cent at the end of the test. Hanson and Connor said
that some of their specimens (which had similar shear steel to that used
in the New Zealand tests), performed adequately. They noted that the
joints with reduced amounts of shear steel lost strength after a few load
cycles. As noted previously, the different performance for similar
specimens is due to the different imposed deflections, used in each of the
research programmes.

The seismic studies have isolated the parameters which control the
loss of strength and ductility. They highlight the importance of an
ultimate load analysis to ensure that a load path is available even if the
joint is no longer visually acceptable. This design philosophy appears
to be an acceptable criterion for severe cyclonic wind or fatigue loading.

2.3   Fatigue Performance of Joint Components

Investigations into the fatigue performance of plain and reinforced
concrete have been conducted since the late nineteenth century. Because
of the immense number of variables and the complex nature of their
interaction the fatigue of concrete is still not fully understood. The
performance parameters that have received a large amount of attention are
frequency, amplitude (stress range) and peak stress of the loading.

Conflicting conclusions are given regarding the effect of frequency of loading and the presence of a fatigue limit.

The effect of peak stress variations on plain concrete specimens and reinforced concrete beams is well proven.[18][19][20][21][22] All of this research shows that reduced peak stress values result in an increased fatigue life. Award[18] has shown the life of plain concrete specimens also depends on the stress range, a reduction in the stress range results in an increased life. Conflicting evidence and opinion is given to the presence of a fatigue limit for plain and reinforced concrete [21][22][25][27]. Those reports that give evidence of a fatigue limit give the limiting stress in the range of 50-70 per cent of the ultimate static strength. The author believes that much of the confusion exists because of the use of the logarithmic ordinate on the fatigue plots. All the research so far shows there is a very large increase in the number of cycles to failure around 70 per cent of the ultimate strength.

A similar situation exists with the effect of frequency (or stress rate) of loading on the fatigue life. The numerous researchers and reviews give conflicting significance to its importance[18][20][21][22][23][24].

Kesler's[23] results show that frequencies of 1-6 Hz have no significance. Similar results are given by Raithby and Galloway[20] for frequencies of 4-20 Hz. Research by Award and Hilsdorf[18], and Sparks and Menzies[24] at frequencies below 1 Hz give fatigue lives which are order dependant on the frequency. However, these tests used different waveforms for the loading. The tests at frequencies above 1 Hz were made with a sine wave pattern and those below 1 Hz were made with a sawtooth pattern. This possibly has some effect on the result but the author believes that the frequency variations are significant at low frequencies, (at least below 1 Hz). The above research workers appear to regard frequency and stress rate as the same parameter. However, none of their

tests were made with a squarewave loading pattern to determine if the frequency and stress rate were not always directly proportional.

It has been shown that various load patterns and rest periods will increase the strength of the specimen. Award and Hilsdorf[18] found that increases in the static strength of up to 5 per cent could be obtained after a specimen was tested to 30 per cent of the fatigue life. Hilsdorf and Kesler[26] found that if the smaller peak stress is cycled before the larger, an increase in fatigue life is obtained.

Different types of specimens fail in different modes and it is obvious that different stress patterns occur with each specimen. Tests by Chang and Kesler[25] indicated that the type of failure occurring in a flexural specimen depended on the magnitude of the peak stress at various locations. Thus a S/N curve for the specimen may consist of sections from several S/N curves for each of the possible failure modes. The significance of this is observed in confined cylinder compression tests by Takhar, Jordan and Gamble[28] who showed that lateral confinement produced a significant increase in the fatigue life. At peak stresses of 80 per cent of the ultimate, a two order increase is obtained with a confining pressure of approximately 30 per cent of the ultimate static compressive cylinder strength. Thus the correlation of test data from different types of specimens must be done with care because of the different three dimensional stress patterns involved.

Variations of moisture content, curing environment and age affects the static strength and fatigue life of the specimen [18][20][29]. Research by Raithbury and Galloway[20] shows that ovendried specimens have a significant increase in fatigue life over surface dried specimens. An unexpected result is that saturated specimens are shown to have a fatigue life between the other two cases. Award has shown that for

plain concrete cylinders in compression an increase in age from 7 to 90 days generally results in an increase in fatigue life of an order. Thus the amount of damage done to a structure by the fatigue loading might depend on the curing conditions, age and moisture content of the concrete.

The ability to predict the life of a fatigue specimen under varying stress ranges and loading frequencies would be an obvious advantage. Miner's[30] rule is an attempt to do this but in its original form is unable to cope with frequency variations. Hilsdorf[26] says that at high loads Miner's rule is unsafe and at low loads is conservative. Award[18] has developed a cumulative damage theory to account for the frequency/stress rate effects from the tests but no independant checks on this model are available.

The reinforced concrete can also collapse because of steel failure. ACI Committee 215[31] advise that failure of the reinforcement may be more critical because of a more rapid collapse with less warning. In high load low cycle fatigue the author considers that steel failure is unlikely. This is because large deflections and concrete cracking usually occur which increases the rate of failure of the concrete. The use of structural grade reinforcement also reduces the risk of steel failure in this situation because of its extremely good ductility and fatigue properties.

The development of mathematical models to predict the fatigue life of a structure is a long way off. This is because of the disagreement about the significance of the parameters and their interdependance, and because much of the test data for plain concrete cannot be applied directly to reinforced concrete.

2.4   SUMMARY

The literature survey has shown that the T-joints fatigue performance might depend principally on the reinforcement detailing and the distribution of the applied loads. It has also indicated that joint failure could occur by beam hinging, shear failure of the joint block and bond failure on the reinforcement. The fatigue failure of the reinforcement would not be expected.

3.   ELASTIC THEORETICAL ANALYSIS

In order to complement the experimental research discussed in Chapters 5 and 6, analytical methods were used to predict the general behaviour of the T-joint. In particular, the range of forces on a joint were found by analysing a typical building frame. Then the stress pattern in a T-joint was found from a linear finite element (F.E.) analysis. This study lead to a re-examination of an existing model to predict joint block cracking and its subsequent improvement. The above models are all elastic. Although the T-joint is only elastic for a small fraction of its total possible deflection the results were very useful in building up a general picture of the joint behaviour. The stress patterns show how the joint resists the applied loads and where failure is likely. The linear F.E. analysis was also used as a preliminary investigation prior to conducting the non-linear F.E. analysis discussed in Chapter 4.

3.1 Joint Forces in a Typical Building Frame

T-joints are used in many types of structures but more so in multi-storey buildings. A joint in a building frame is subjected to loads which depend on the frame layout, the spatial distribution and magnitude of the load, and the location of the joint in the frame. Some earlier research[2][3][5][6] has shown that the load distribution on a joint has an effect on its performance and so this was investigated prior to any other topics.

It is possible to describe the load distribution on a joint in terms of the load ratios M/P and M/V, and the shear spans of the columns.

Figure 3.1 indicates the position of these loads on the joint. This
research programme set out to determine the effect of different load
distributions and it was important to know the range of M/P and
M/V in building frames.   This was determined by analysing a building
frame of realistic member proportions which was loaded with combinations
of dead load (D.L.), live load (L.L.) and wind load (W.L.).

3.1.1 Analysis of a Typical Building Frame

The frame and section properties are shown in Figure 3.2. This
particular 4-storey, 4-bay frame, was chosen as it is typical of the
low-rise buildings erected for commercial occupancy in the cyclonic area
of Australia. Land costs in these areas would generally be less
significant than construction costs and high rise construction is
uneconomic. In frames where brick cladding and panel walls are used the
wind forces occurring at the joints are reduced because of the stiffness
of the brickwork in shear. However, this additional stiffness is often
neglected in design.

The load cases DL + LL + WL and DL + WL were assumed to give
the extreme values of M/P and M/V. The frame loads were obtained from
the AS1170[32][33] SAA Loading Code. The D.L. of the building was found
by estimating the weight of the bare frame, plus walls, cladding and
floors. (25 KN/m of beam plus 36 KN at each end of the beam). It was
assumed that the building would be used for offices, a motel or similar
occupancy. (a maximum live load of 4 KPa). The wind loading on the
frame was taken as that due to the wind velocity given in the AS1170[33]
code for the Darwin area. (a design wind pressure of 3.0 KPa with
factors of +0.8, -0.5 and -0.9 for the windward wall, leeward wall and
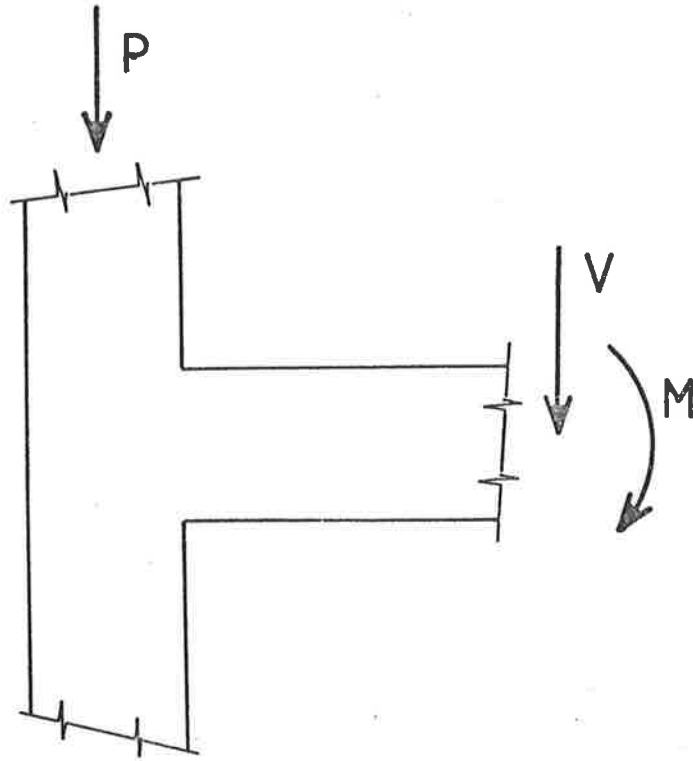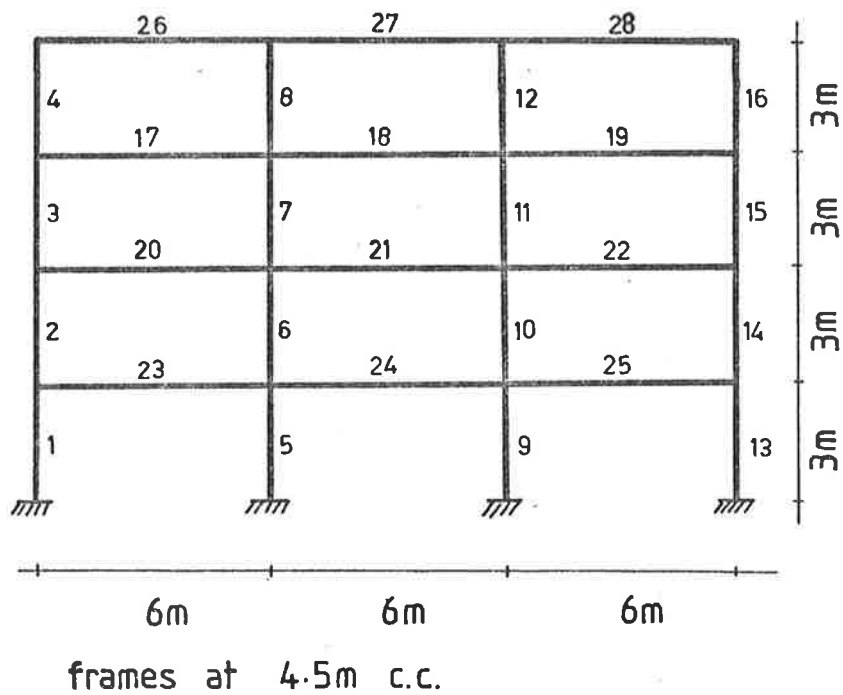roof respectively). Analysis of the frame was carried out by a

FIGURE 3.1   The forces used to describe
              the load distribution on a T-joint.

member	I_{xx} mm$^4 \div 10^6$	Area mm$^2 \div 10^6$
1,5,9,13	1·0	0·2
2,6,10,16	0·8	0·17
3,7,11,15	0·6	0·11
4,8,12,16	0·4	0·09
17,18,19	2·0	5·0 ●
20,21,22	2·0	5·0 ●
23,24,25	2·0	5·0 ●
26,27,28	2·0	5·0 ●

● Area of member increased to account
for in-plane stiffness of floor slab.

FIGURE 3.2   The frame used in the analysis to determine the
range of values of M/V and M/P .

structural analysis computer program called ACES developed by the South Australian Government Computer Centre.

3.1.2 Values of M/P and M/V for a T-joint

An inspection of the results of the frame analysis in Figure 3.3 shows that M/V lies between 0.01 and 1.41 metres for all locations within the frame. The AS1480[34] Concrete Structures Code gives M/V values between 1.0 and 1.2 metres. A value of 1.06 metres was chosen as representative and subsequently used in the experimental programme. The M/P values from the analysis indicate that a large range of values is likely to occur in a structure. Values of 0.0 to 8.0 metres were obtained. The test program used M/P values of 0.14 and 1.83 metres to determine any influence of column load. The difference in column axial stress for M/P values of 1.83 and 8.0 metres is small when compared to the difference between the column stresses resulting from M/P values of 0.14 and 1.83 metres. With the load distribution parameters determined the joint itself was then analysed.

3.2 Elastic Finite Element Analysis of a T-joint

An unloaded or lightly loaded joint can be regarded as a "homogeneous" uncracked structure containing reinforcement. At higher loads the concrete cracks and the steel slips in the concrete. However, despite this known limitation an elastic F.E. analysis was used to study the stress patterns in the uncracked joint for different M/P values and reinforcement layouts. The results of the analysis were used to verify and improve Nilsson's cracking model (Section 3.3 and 3.4) and to help determine the behaviour pattern of the joint.
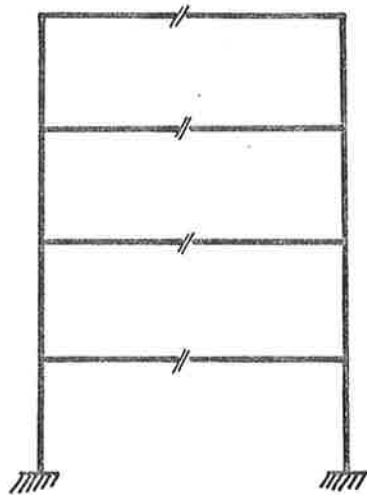
M/V	M/P
0·98	6·57
1·29	0·92
1·41	0·53
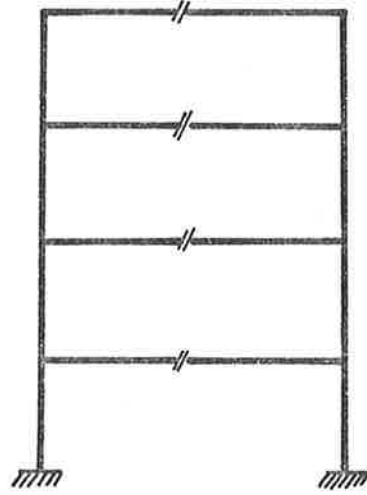
M/V	M/P
0·21	1·95
0·12	0·06
0·59	0·14

DL + WL

M/V	M/P
0·88	8·04
1·14	0·89
1·23	0·50

M/V	M/P
0·37	5·06
0·25	0·16
0·01	0·00

DL + LL + WL

FIGURE 3.3   M/P and M/V values in the typical frame. All values given in metres.

3.2.1   The F.E. Program

The program used to analyse the 2-D F.E. model was the structural analysis program called ACES which was run on the University of Adelaide CDC CYBER Computer. A 2-D model was used because of the impractical computer storage and time requirements for even a coarse 3-D mesh bearing in mind it is only an elastic analysis.

3.2.2   The F.E. Mesh

The mesh selected for the analysis is that shown in Figure 3.4. This 2-D model resulted from a study to determine the effect of different element layouts on the stress values predicted by the model. As was expected the different element layouts predicted stresses which were asymptotic. Figure 3.5 shows the results of the study based on the number and type of elements in the joint block. The results show that the use of the isoquadrilateral elements gave stresses approximately 10 per cent closer to the estimated asymptotic value than those from the element layout with a joint block represented by 100, 4-node square elements. However, the latter mesh was used because the difference in results did not justify the threefold increase in computing time and the results obtained from the 4-node rectangular elements were considered adequate. Preliminary computer runs were also made with the applied loads represented by point or distributed loads. This was done to check that the specimens members were of a sufficient length so that joint block stresses were independant of the load distribution at the loaded points. The overall dimensions of the model were chosen to be as representative as possible of a real joint within the limitations of the program.

Steel reinforcement was included in the model in the form of bar elements. Values of 1.8 and 2.9 per cent were used for the beam
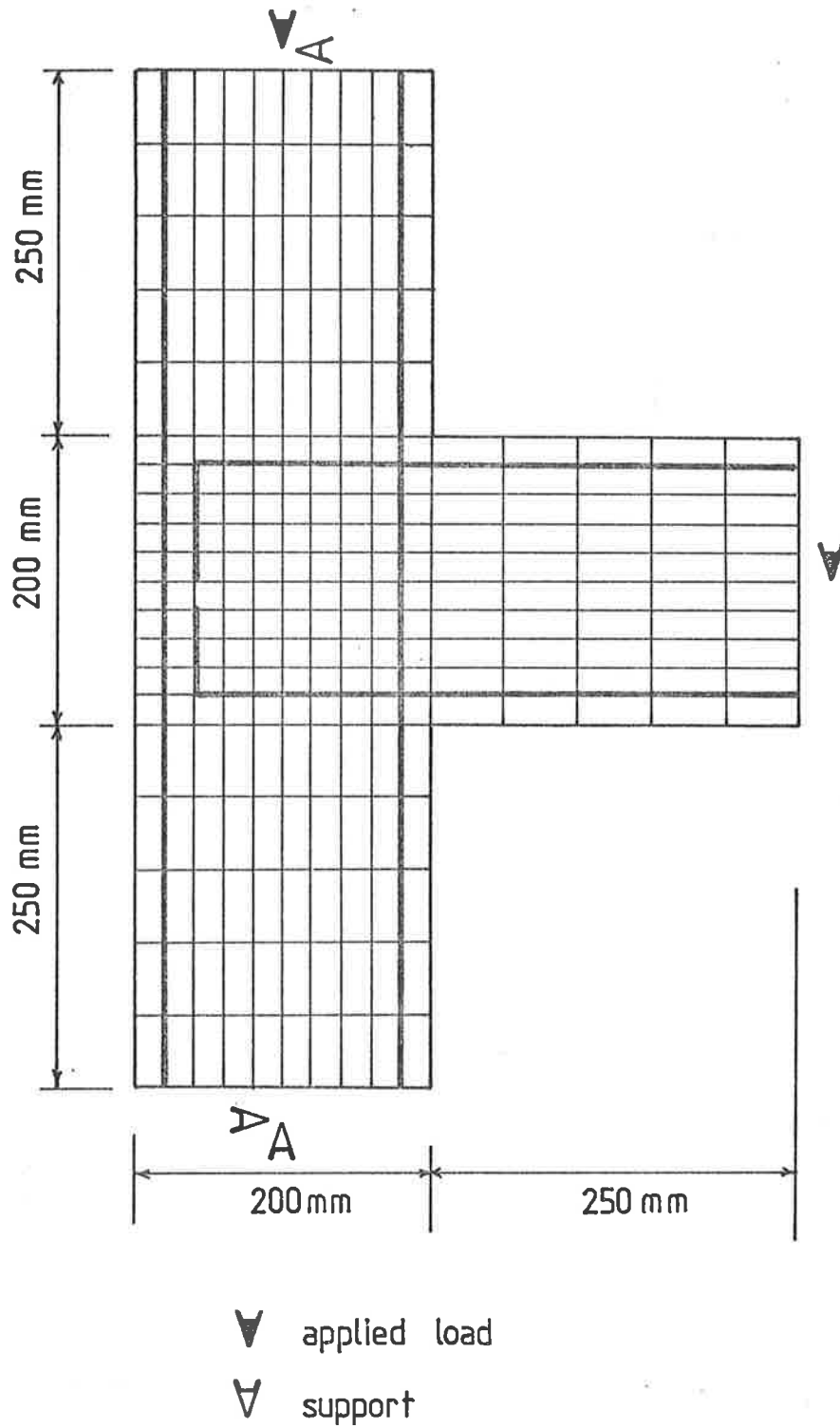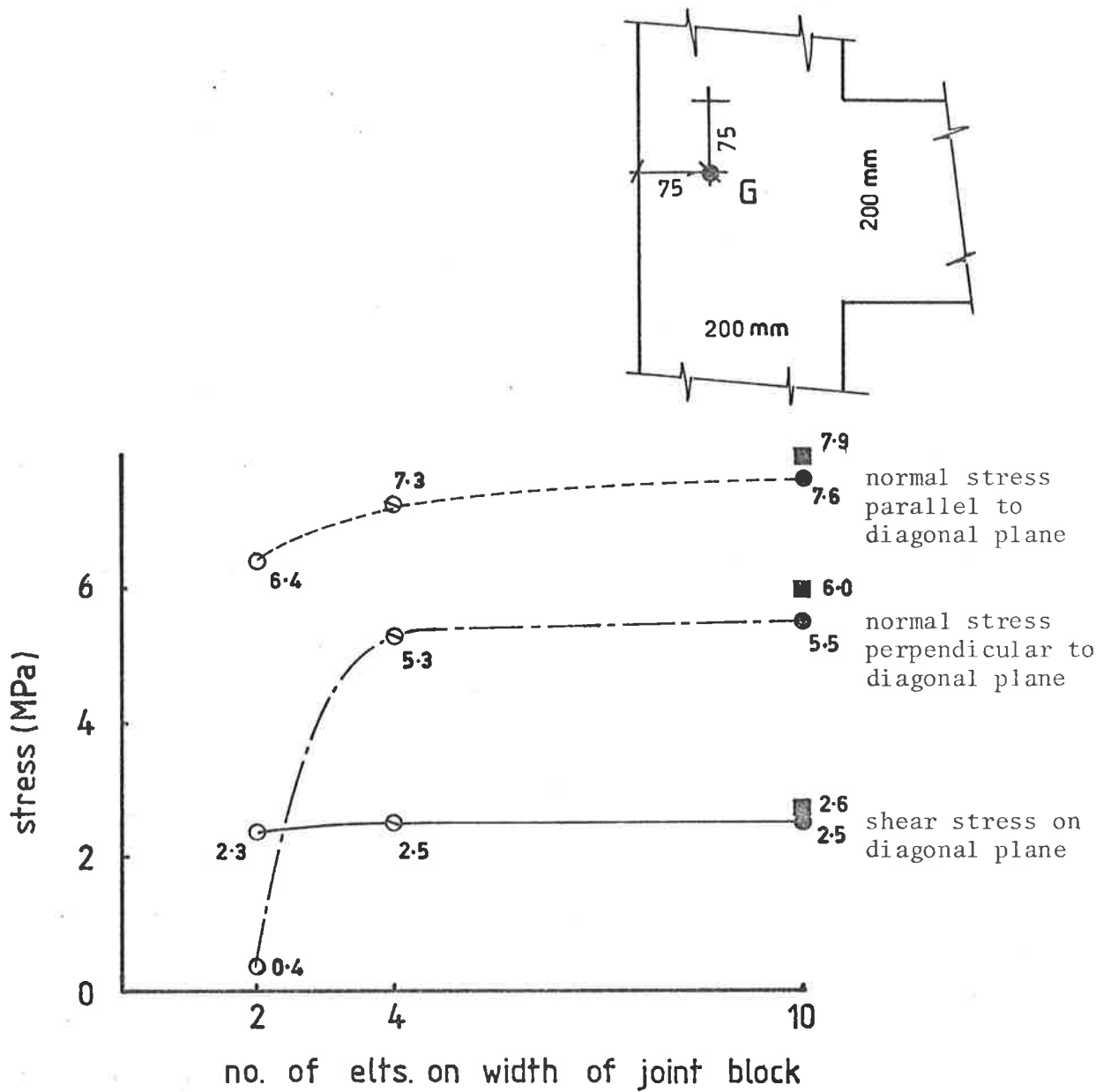
250 mm

200 mm

250 mm

200 mm   250 mm

▼ applied load

∀ support

FIGURE 3.4   The element mesh used in the linear F.E.
analysis. The thick lines indicate one of
the reinforcement patterns used in the analysis.

FIGURE 3.5 The effect of the number and type of elements on stresses in the F.E. model. The stresses are indicated for the point G on the diagonal of the joint block.

tension reinforcement. Further bar elements were used to represent steel ligatures of 6.3 mm diameter placed at 50 mm centres.

3.2.3 Variables used in the Analysis

The computer runs were selected according to the objectives given at the beginning of this section (3.2). The loading distribution was kept within the limits found from the analysis of the typical building frame (Section 3.1). The key parameters for each run are given in Table 3.1.

3.2.4 Results

The results from the computer runs PRG1, PRG2 and PRG3 are shown in Figure 3.6.

The elastic analysis shows the stress on the uncracked primary diagonal of the joint block is parabolic in distribution and is tensile for only the central portion. Compressive stresses occur at the ends of the diagonal which is to be expected for overall equilibrium of the section and joint block. The compressive stresses result from tension and compression forces which act in each member due to the applied bending moment. It was considered unnecessary at this stage to locate the plane on which the tensile stress was largest because it was found automatically in the non-linear F.E. analysis which is discussed in Chapter 4.

Figure 3.6(a) shows the effect of various M/P values on the diagonal tensile stress. An increased axial force (P) results in a reduction of the peak tensile stress. The reduction is caused by a uniform distribution of the column axial load on the cross section. For M/P of 0.2 metres (high column load) the reduction in peak tensile stress due to the column load is approximately one-third of the tensile
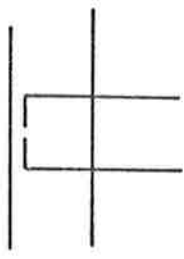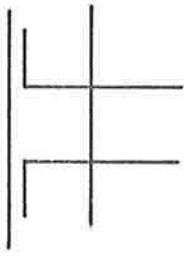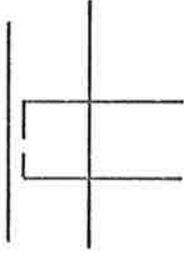
PRG1

M/V = 0.7 metres
M/P = 0.2, 0.6 and 1.0 metres
Beam tension steel = 1.8%
Triangular stress distribution
for moment on end of beam

PRG2

M/V = 0.7 metres
M/P = 0.2, 0.6 and 1.0 metres
Beam tension steel = 1.8%
Triangular stress distribution for
moment on end of beam

PRG3

As for PRG1 but with beam
tension steel = 2.9%.

TABLE 3.1   The variables used in the linear F.E.
parametric study.
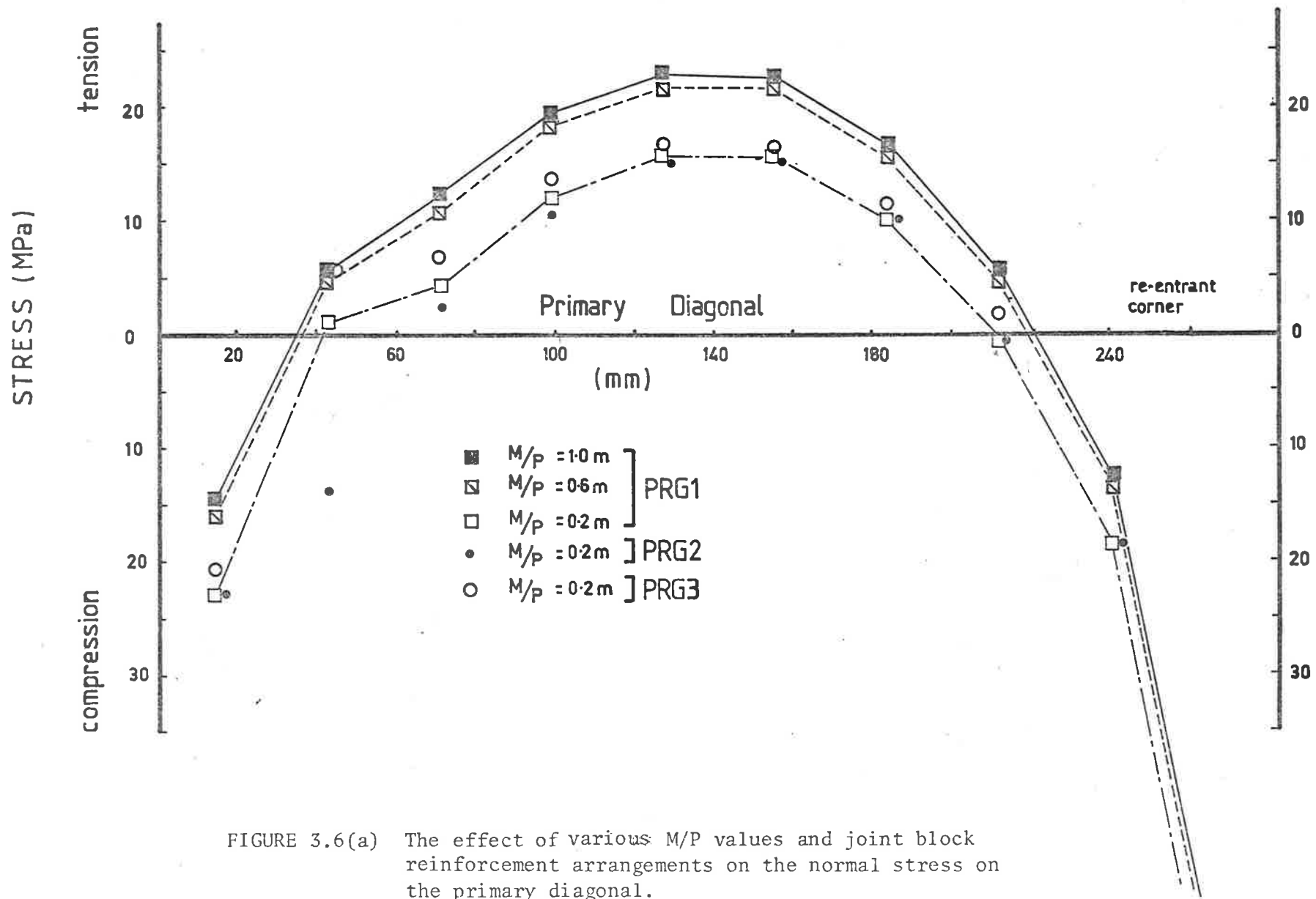
FIGURE 3.6(a)   The effect of various M/P values and joint block
                reinforcement arrangements on the normal stress on
                the primary diagonal.

force scale 1mm = 40N

⊕   tension

⊖   compression

FIGURE 3.6(b) The force in the "steel reinforcement"
elements of the F.E. model (from computer
run PRG1, M/P = 1.0 metres).
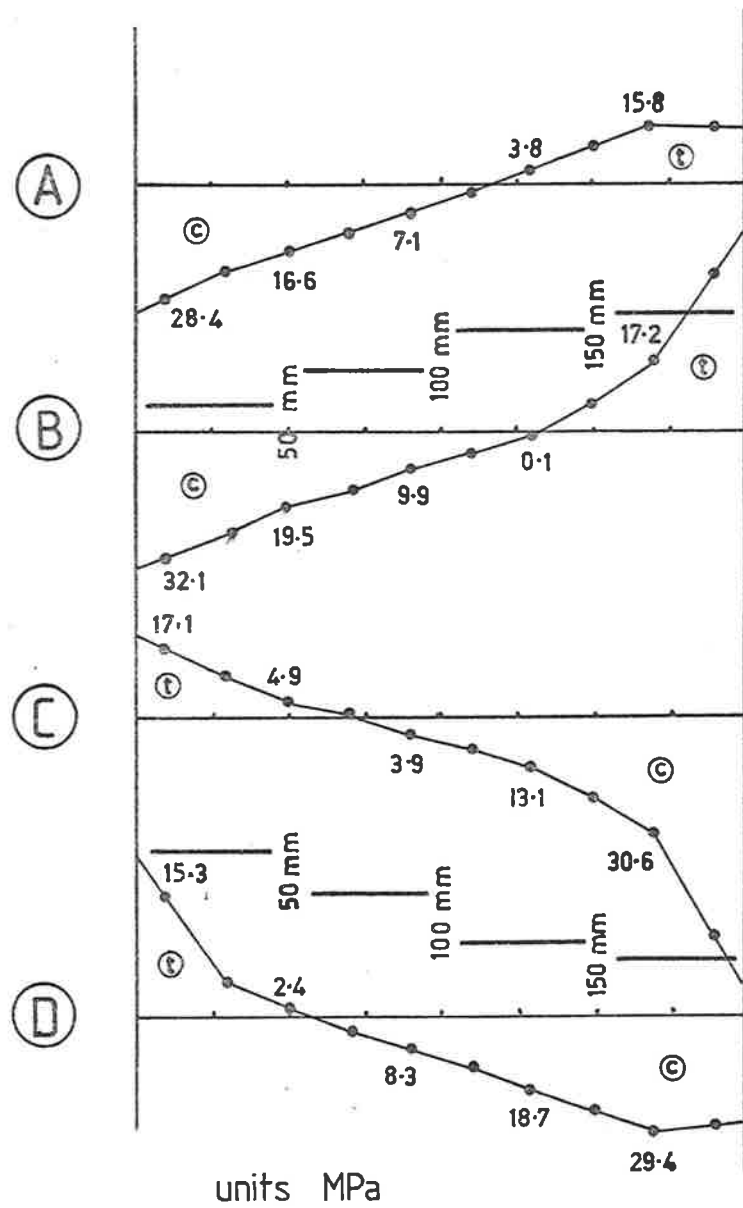
FIG 3.6(c) Patterns of normal stress in the linear F.E. model from computer run PRG1 (M/P = 1.0 metres)

13.4
17.7
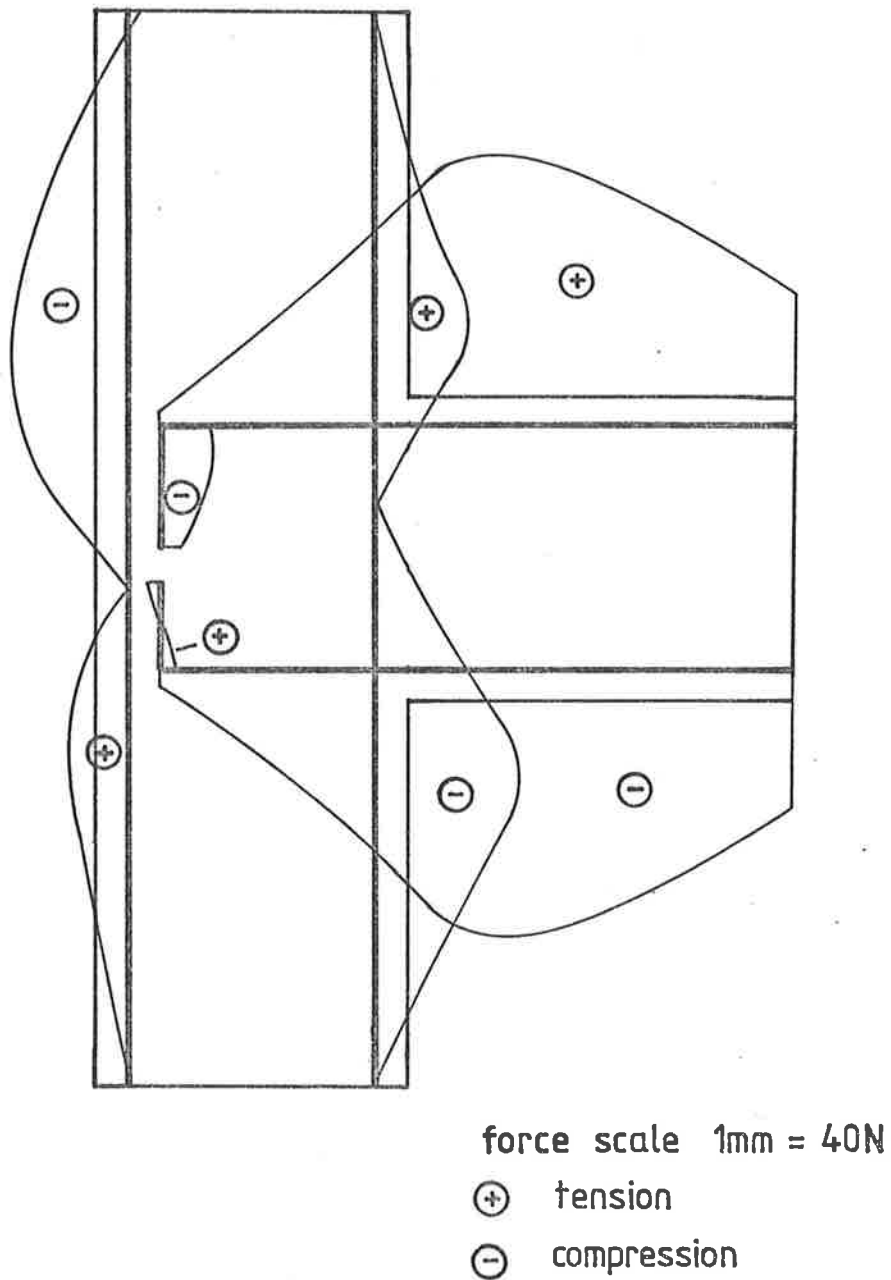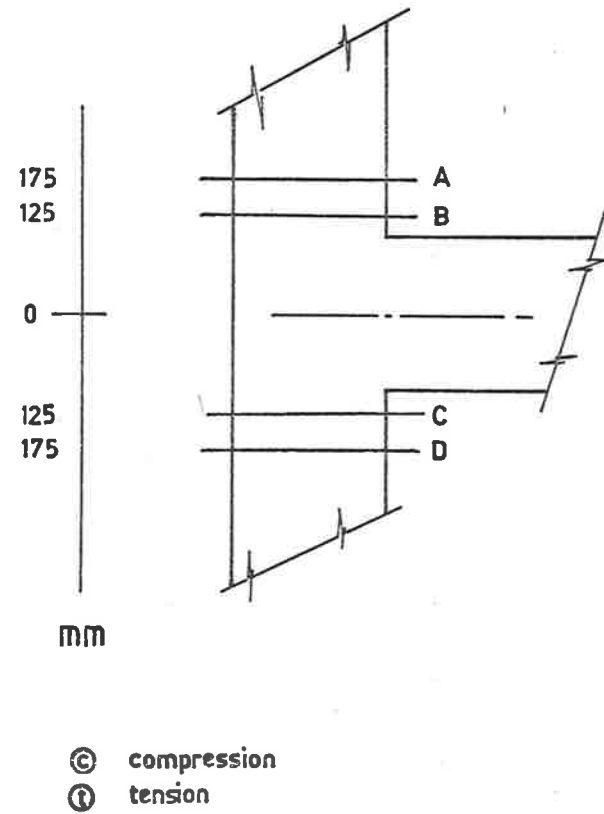20.2
21.3
13.4
16.2
16.2
14.7
13.4
17.7
20.3
21.3
20.9
28.7
29.8
26.2

column c.l.

beam c.l.

units MPa

FIGURE 3.6(d) The shear stress in the joint block elements
adjacent to the beam and column reinforcement.
The load is a moment of 1 KNm applied to the
beam of the T-joint.

3.7
4.3
4.7
4.4
3.7
4.2
4.4
3.9
3.3
4.5
4.9
4.5
3.8
4.9
5.0
4.6

column c.l.

beam c.l.

units MPa

FIGURE 3.6(e) The shear stress distribution in
the joint block elements adjacent to
the beam and column reinforcement.
The load is a force of 1KN on the end
of the beam of the T-joint (350 mm.
lever arm).

stress due to the bending moment alone.

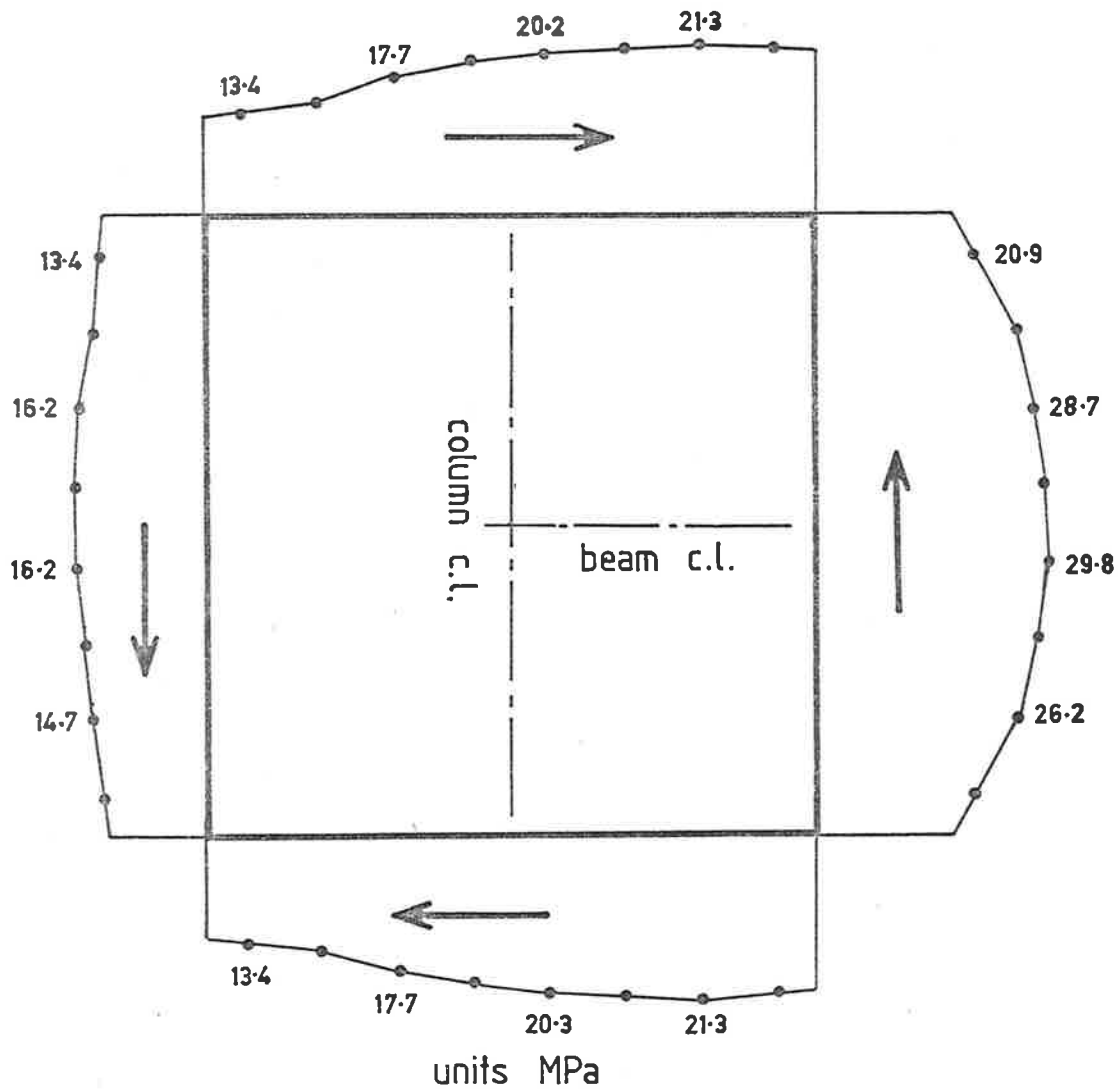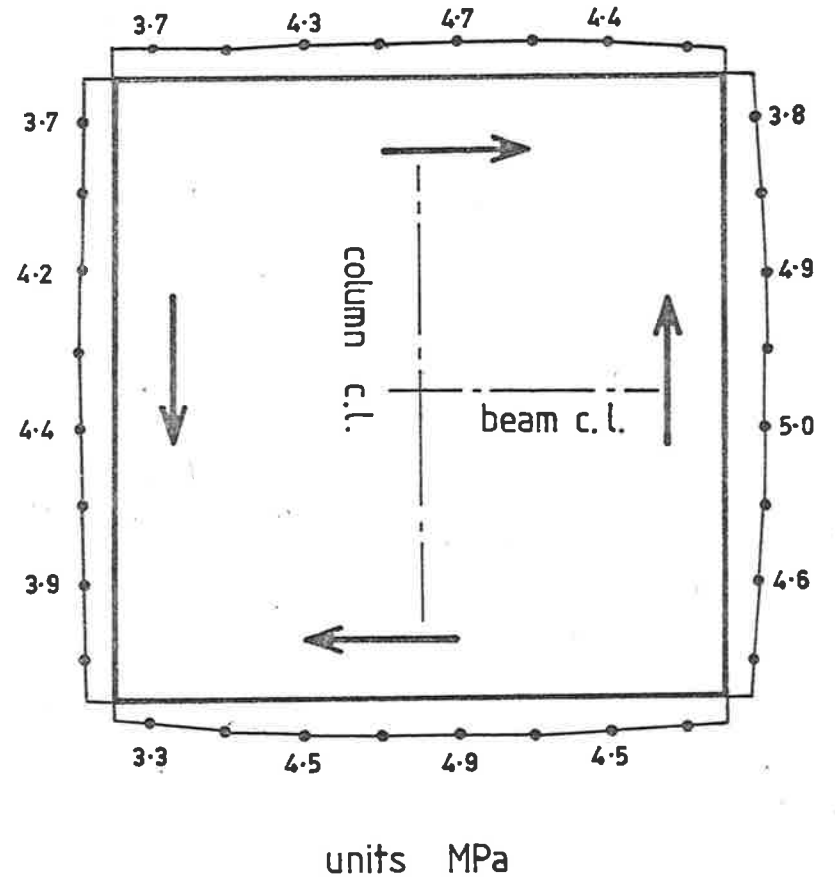Variations in the reinforcement layout and amount produced no significant change in the magnitude or distribution of the stress patterns. This was to some extent expected since the concrete elements in the model behave as if they are uncracked. They are then able to carry unlimited tensile stress in competition with the steel. The significance of the force in the steel elements is further reduced because of the relatively small stiffness of the steel compared with the overall cross section. Compounding this, large radius bends in the steel reinforcement were modelled by connecting two perpendicular bar elements at an element node. This configuration does not model radial stresses or bar bending stiffness which would occur in practice in a large radius bend. The result of this is that the reinforcement after the bend behaves as vertical column reinforcement and not as a continuation of the beam steel. See Figure 3.6(b).

Figure 3.6(d) and (e) show the shear stress patterns in the joint block due to two different load patterns on the joint. These figures show that the shear stresses approximate a parabolic distribution.

The pattern of normal stress in the model around the joint block is affected by the presence of singularities in the stress field caused by the re-entrant corners. Within the limitation of the F.E. model Figure 3.6(c) shows that the peak stress near the re-entrant corners is increased beyond that predicted by a linear distribution. (A similar effect is not observed in the stress patterns in Figure 3.6(d) and (3)). However, despite this effect local to re-entrant corners the general trend and stress pattern within the joint block is illustrated by these analyses.

The shear steel elements used in the F.E. analysis were ineffective because the concrete was able to carry large tensile stresses. The forces which appeared in the shear steel were caused by the Poisson's effect acting on the normal stresses in the beam and columns. The force in the main steel reinforcement in the F.E. model corresponded to the force in the adjacent concrete because of the rigid bonding method used.

Simple beam theory was used to check the normal stresses in the steel and concrete. Large disagreements were found for the concrete and steel elements near the re-entrant corners because of singularities. However, checks on the total shear and moment at various cross-sections found the forces and moments to be in equilibrium with the applied loads.

A limitation of the elastic analysis is its inability to indicate the effect of variation in steel layout, a parameter subsequently shown experimentally to have a marked influence on joint behaviour. Despite this limitation the analysis was considered productive and the results from the F.E. analysis were used to develop the cracking model (see Section 3.4), as a preliminary to a non-linear F.E. program and in the design of the test programme.

3.3 Analysis of Nilsson's Model of Joint Block Cracking

It is an advantage for design engineers to be able to predict the performance of a structure using simplified techniques which do not require large amounts of time or large computers. As noted previously in the literature review, simple models have been developed by Nilsson[3] and Taylor[2] to predict the formation of the crack on the joint block primary diagonal. The prediction of the cracking load is important for both static and fatigue loading.

For static loads and low intensity fatigue loads the appearance
of joint block cracks sometimes violates service requirements. More
importantly, the formation of a crack in some joints results in the
collapse of the joint at a load much lower than that predicted from member
strength calculations. Shear failure of the joint block results unless
the joint block shear forces can be carried by combined action of the
concrete and reinforcement. As has been discussed in Chapter 2, the
reinforcement layout has been shown to have a significant effect on the
joints performance prior to and after the formation of a diagonal crack.

Under fatigue loading,cyclic shear displacements along the
diagonal crack can cause grinding on the crack surface and cracking in
the surrounding concrete. This may lead to a more rapid collapse of the
joint.

An analysis of Nilsson's[3] cracking model showed that it can
generally predict a conservative cracking load and that it should be able
to predict the peak tensile stress on the line of the crack. The
force system used in Nilsson's model is shown in Figure 3.7. Nilsson states
that the crack forms when the concrete tensile strength is equal to the
force in the steel reinforcement at the upper right hand corner of the
joint block. The direction of the crack is perpendicular to the vector
sum of the force in the upper column steel and the beam tension steel.
For a specimen loaded as in Figure 3.7 the crack direction is 29.5°
relative to the column axis. Nilsson showed by an elastic analysis of
the joint block that the tensile stress is distributed parabolically
along the proposed plane of the crack and this has been confirmed by the
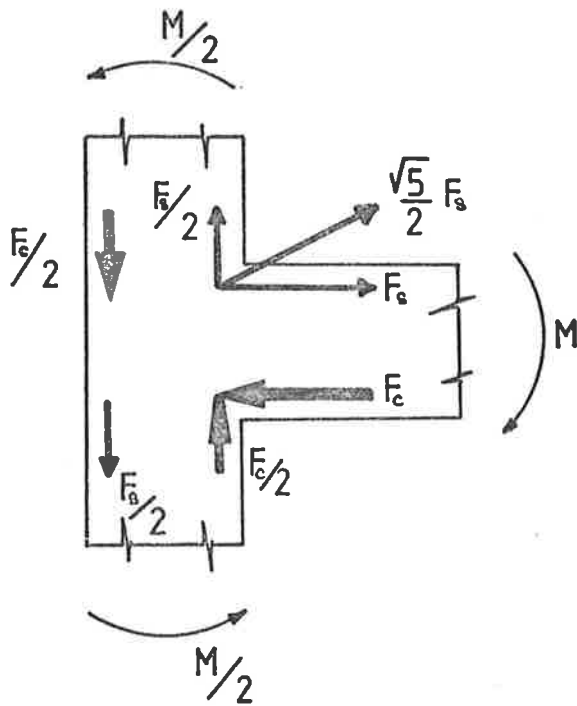author (see Section 3.2). On this basis, the force required to cause the

FIGURE 3.7 The system of forces in
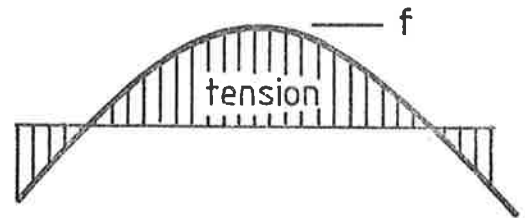Nilsson's model for joint
block cracking.

FIGURE 3.8 The normal stress
distribution on the primary
diagonal as used in Nilsson's
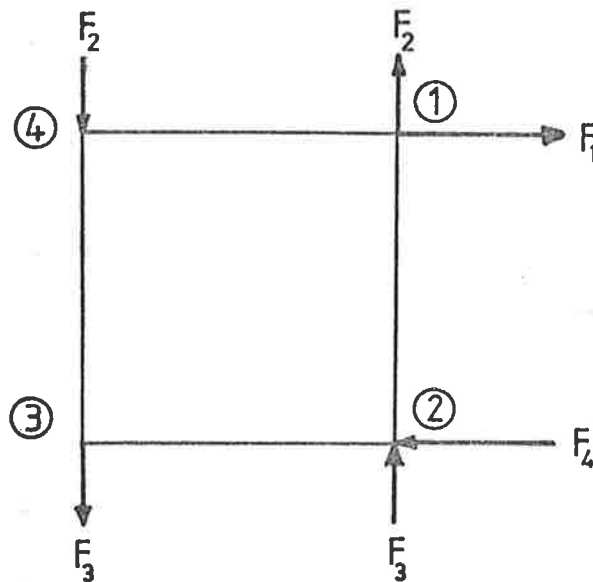model for joint block cracking.

FIGURE 3.9 Forces on the joint block
resulting from moment in the
members of the joint.

crack is found by integrating the tensile stress over the area in tension assuming uniform stress through the thickness of the specimen. (See Figure 3.8) With crack capacity known and hence reinforcement force, the moment of resistance of the joint is the product of the force in the beam reinforcement at the centre of the column with the effective elastic lever arm.

This model makes the following assumptions. The notation is given in Figure 3.9.

(1) The only forces considered to cause cracking are those applied directly to node 1. (This neglects the force applied at node 2 (F_3), which if non-zero has a component perpendicular to the crack).

(2) The direction of cracking is perpendicular to the resolved forces at node 1. (There is no experimental proof of this; the location of the crack appears to be unpredictable).

(3) The forces are only applied at the corners of the joint block. (A later discussion will show that the stress distribution around the joint block is critical in determining the joint block stresses).

If Nilsson's analysis assumes that the column force at node 2 is to be omitted then it is thought that only one half of the force in the beam tension steel should be applied at node 1. Because of the presence of effective tension and compression diagonal "members" in the joint block the shearing force on the joint block is shared between the two members. To maintain consistency, Nilsson's model should use a diagonal

cracking force of $(Fs + Fs)/2\sqrt{2}$ instead of $(Fs/2 + Fs)/\sqrt{2}$. (Fs is shown in Figure 3.7).

Although Nilsson's model appears to have these inconsistencies it still predicted some of his test results very closely. See Table 3.2. The largest error for the compared results was 22 per cent. The load predicted by the model is conservative in all but one case and ignores any reinforcement in the joint block. Experimental evidence shows that many of the practical reinforcement layouts prevent cracking or reduce crack size so that it is not observed until a higher load is reached.

3.4 Development of an Improved Cracking Model

The analysis of Nilsson's model for joint block cracking in Section 3.3 revealed some apparent inconsistencies in the model. Nilsson's model is also restrictive in the type of loads that the model will analyse as it is suitable only for bending moments. The following discussion develops an improved cracking model based on Nilsson's and eliminates the inconsistencies while generalising the load system on the joint. Figure 3.10(a) shows the generalised joint load system used in the development of the model. Figure 3.10(b) shows the forces at the face of the joint block which result from this load distribution.

3.4.1 Force System around the Joint Block

The distribution of forces around the joint block is obviously important. So that the effect of various loads on the joint can be found it is necessary to make some realistic simplifications to the complex stress distribution in the joint. This is assisted by developing a simplified model for the joint block structure.

Forces applied at
shear centres

$*$ indicates the BM at
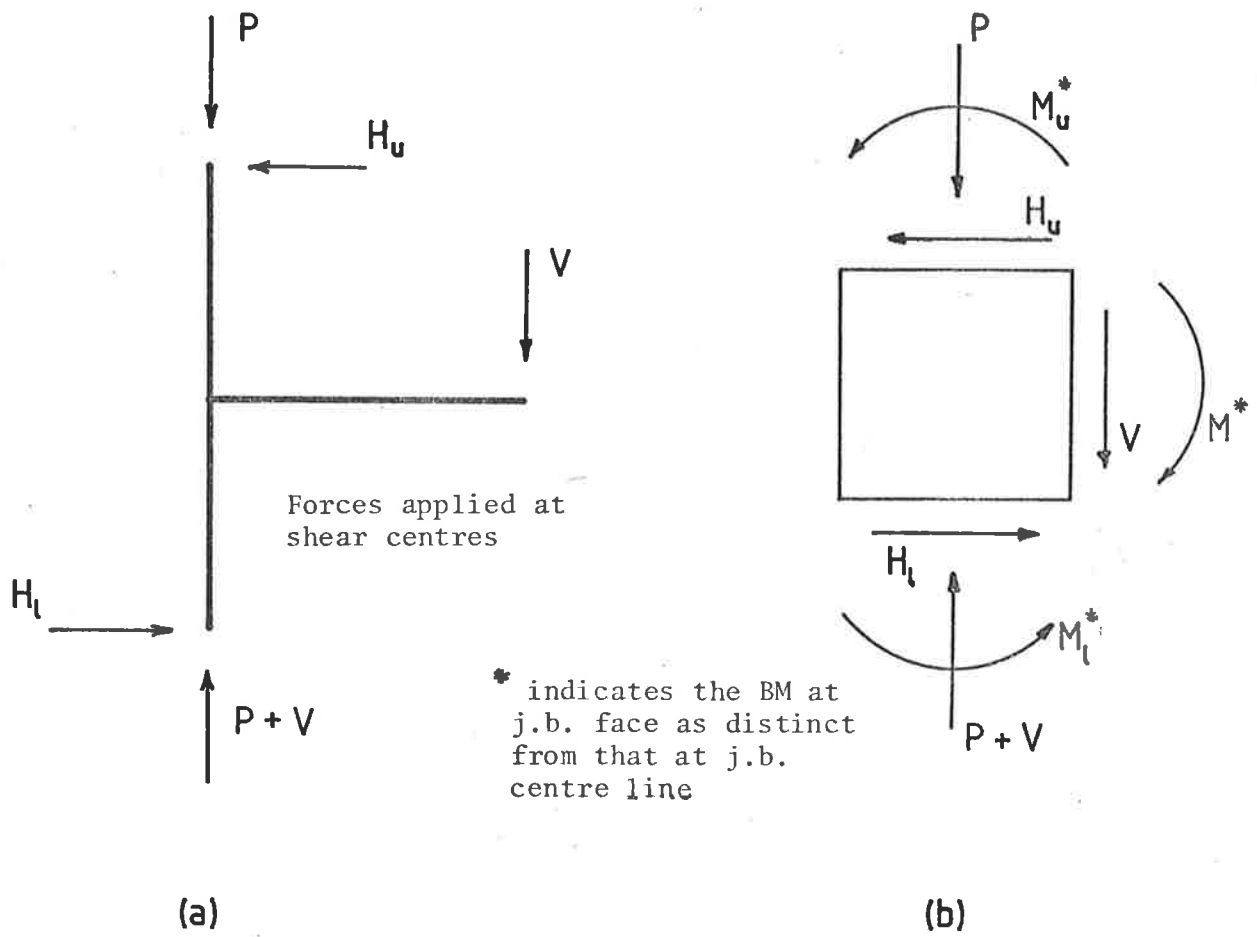j.b. face as distinct
from that at j.b.
centre line

(a)

(b)

FIGURE 3.10   Forces in a real structure.

Consider the joint block to consist of two parts. These are an inner rectangular zone and surrounding 1-dimensional members (See Figure 3.11). The "members" transfer the bending moments in the beam and columns to the shear resisting mechanism of the joint. The connection between the "members" and the inner zone determines the distribution of forces on the inner zone.

Figure 3.12(a) and (c) shows two extreme variations of the stress distribution between the inner zone and surrounding "members". The different distributions may result from changes in the anchorage of the steel reinforcing due to slip and the degradation of the concrete. In an undamaged joint block a distribution as shown in part (a) might be expected. A damaged specimen might have a distribution similar to part (b) or (c).

Consideration of the tensile force on the joint block diagonal resulting from the two force distributions shown in Figure 3.12(a) and (c) shows the importance of using the correct distribution in an analysis. A rigid body analysis of the joint block with the distributed load shown in (a) results in a diagonal force of $(F_1 + F_2)/\sqrt{2}$ while an analysis of the load distribution in (c) gives a diagonal force of $(F_1 + F_2)/2\sqrt{2}$. The diagonal forces differ by a factor of two. A result of this is that the cracking loads for each of the force distributions would differ by a factor of two. The distributed load in (a) gives the lower cracking load. This dependence of cracking load on force distribution raises an important point. Whether the joints shown experimentally to crack at a load very different from that predicted by Nilsson or Taylor have a different stress distribution around the joint than that assumed by the respective models ? This would require a great deal of testing to answer but it is expected
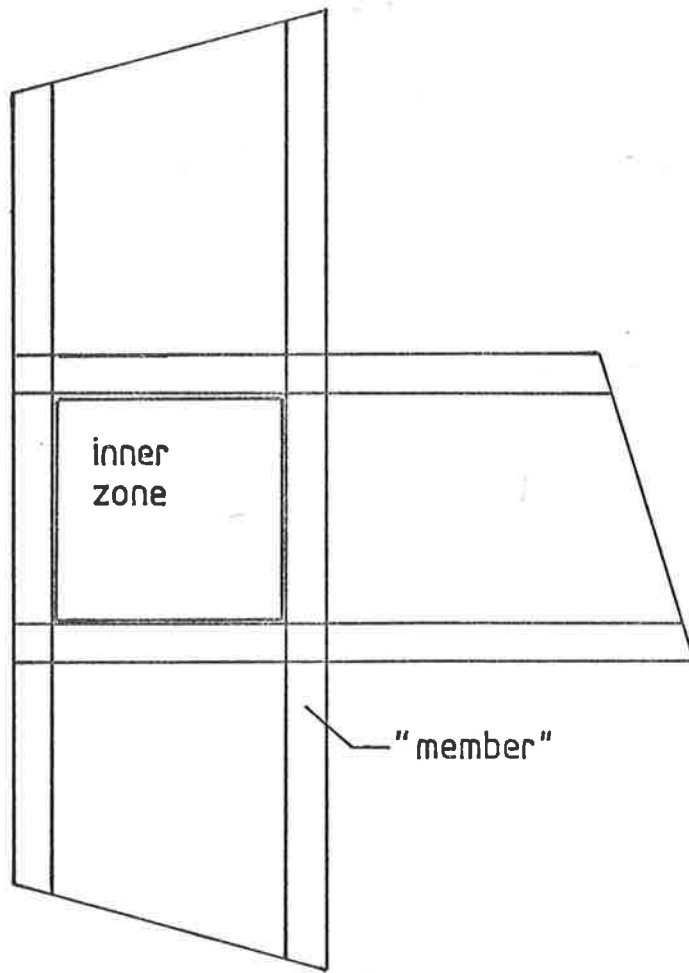
FIGURE 3.11   Structure of improved joint
block model

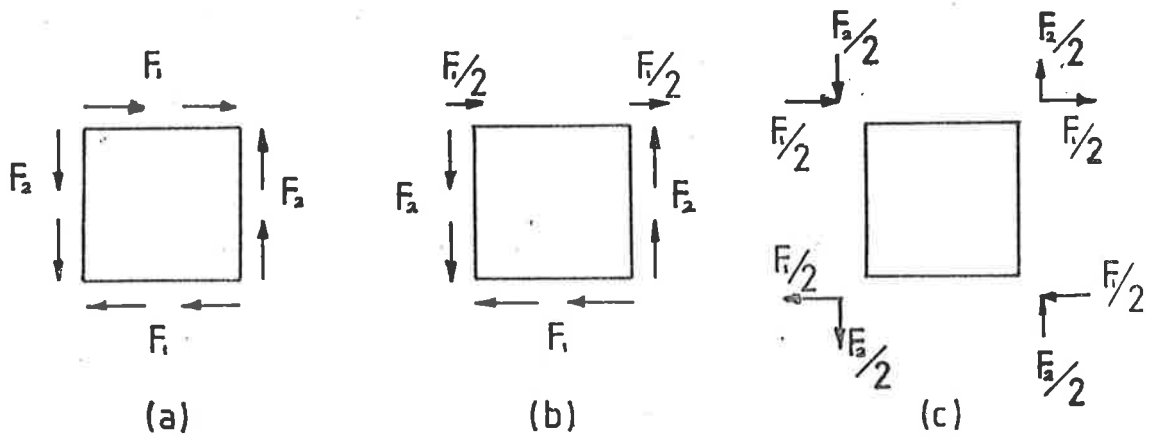(a)   (b)   (c)

FIGURE 3.12   Possible distributions of moment induced shear forces
on the inner zone of the joint block.

that significant changes in the force patterns do occur with increasing load.

3.4.2 Development of an Equation to predict the Peak Tensile Stress on the Primary Diagonal

Taking into account the possible extremes in force distribution already discussed the distribution shown in Figure 3.12(a) is thought to be similar to that in an undamaged joint block. This assumption is based on the linear F.E. analysis discussed in Section 3.2. (see Figure 3.6(b), (d) and (e)). The F.E. analysis also shows that the tensile stress on the primary diagonal is distributed parabolically (see Figure 3.6(a)). The zone in tension on the joint block diagonal corresponds to the inner rectangular zone which carries the major part of the shear force on the joint block. The material in compression corresponds to the "members" which surround the inner zone.

Using the information available from Section 3.4.1 it is possible to relate the forces on the inner zone of the model to the generalised force system in a structure. (see Figures 3.10, 3.11 and 3.12). Thus, assuming the shear forces as shown in Figure 3.12(a), F_1 and F_2 are found from the following equation

$$F_1 = M_b (S_b - D/2)/(S_b.jd) = M_b^*/jd \qquad (1)$$

$$F_2 = M_u (S_u - D/2)/(S_u.jd) + M_\ell (S_\ell - D/2)/(S_\ell.jd) \qquad (2)$$

$$= (M_u^*/jd) + (M_\ell^*/jd)$$

where

"M_b, M_u and M_ℓ" are the moments at the centre of the joint block in the beam, upper column and lower column respectively. "M_b^*, M_u^* and M_ℓ^*" are as above but at the face of the joint block. "S_b, S_u and S_ℓ"

are the shear spans of the beam, upper column and lower column respectively. "jd" is the effective lever arm for the member in question.

The axial force in the column and the shear forces in the upper column and beam produce forces on the diagonals of the joint block. The magnitude of the force is calculated by simple statics to be equal to the force in the beam or column divided by $\sqrt{2}$.

For the purpose of this model, the tensile stress on the joint block diagonal is related to the applied forces by using a modified Nilsson's method (see Figure 3.7 and 3.8). The modified method equates the forces on the inner zone of the joint block to the diagonal cracking force. Using equations (1) and (2), and adding the contribution from the axial and shear forces in the members, the peak tensile stress on the primary diagonal is given by

$$ f = \frac{3}{4.K.D.b} \left[\frac{M_b{}^*}{jd} + \frac{M_u{}^* + M_\ell{}^*}{jd} \right] - \frac{P}{2A_c} - \frac{3H_u}{4A_c} - \frac{3V}{4A_b} \tag{3}$$

where:

"f" is the peak tensile stress on the primary diagonal

"b" is the thickness of the joint block

"D" is the depth of the joint block

"A_b and A_c" are the cross-sectional area of the beam and column respectively

"K" is the fraction of the joint block diagonal in tension

"P" axial force in upper column

"H_u" shear force in upper column

"V" shear force in beam

The results of the linear F.E. analysis and a simple rigid body analysis were used to determine the stress distribution in the joint block for the axial and shear forces in the beam and column. The column axial force P is shown by the linear F.E. analysis to be uniformly distributed on the column cross-sectional area (A_c). A compressive column force gives a diagonal stress of $\frac{P}{2A_c}$.

The shear in the beam and column is shown to be parabolically distributed on the faces of the joint block. Thus the beam shear force (V) would give a parabolic stress distribution on the diagonal with a peak value of $\frac{3V}{4A_b}$ where A_b is the cross-sectional area of the beam. Similarly for the upper column, the peak stress from the column shear force is $\frac{3H_u}{4A_c}$. These forces reduce the effect of the stress due to the moment on the joint block and appear in equation (3) for the peak stress as a negative term.

The equation for peak tensile stress can be used to predict the forces on the joint needed to produce a crack on the primary diagonal once the relevant variables are known. These variables can be determined from the loading conditions, the structure and the material properties. Good estimates of the value of K can be made from the linear F.E. analysis of the joint block. (Typically 0.65). The examples in Appendix A.2 show how the derived equation can be evaluated.

3.4.3 Model Evaluation

Table 3.2 shows the specimen cracking loads predicted by Nilsson's model and the improved model. The improved model computations are given in Appendix A2.1. Nilsson's tests results are for a simple reinforcement layout in which the beam steel was bent out of the joint block (see Figure 2.1). No member axial load was used. A comparison of the results

show that the improved model yields results similar to Nilsson's for this reinforcement layout and joint load distribution. Nilsson's predictions are close to the test results and a marked improvement would not be expected. As noted previously these simple models appear inaccurate for some reinforcement layouts as it ignores any strength from the reinforcement. Further discussion is given in Chapter 6 when the improved model predictions are compared with the author's test results.

MODEL (Brown)	MODEL (Nilsson[3])	TESTED (Nilsson)	F_t
6·3 KNm	6·8 KNm	8·3 KNm	2·1 MPa
7·8	8·7	10·7	2·6
7·2	8·0	6·9	2·4

TABLE 3.2   The moment on the joint needed to cause
diagonal cracking as obtained from simple
models and tests.

4. THE NON-LINEAR FINITE ELEMENT ANALYSIS OF A T-JOINT

It is often not possible to conduct tests on full size structures or specimens and it would be an advantage to be able to accurately predict joint behaviour over the full range of loading with a theoretical model. Previous research[35] has shown that this may be possible with a non-linear finite element (F.E.) analysis. Originally, it was intended to use the F.E. model to predict the test variables which have the greatest effect on performance and then compare the analytical data with that from the tests. Some success was achieved but all the aims were not fulfilled because of limitations of the model.

4.1 The Non-Linear F.E. Program

The finite element computer program was provided by Dr M. Yeo of the Civil Engineering Department of the University of Adelaide. This program is a conventional non-linear finite element program using the initial stiffness method and can handle material non-linearity only. The solution of the initial stiffness equations is carried out by the "front solver" method which economises on computer memory and computing time. A block diagram of the program is given in Figure 4.1.

The program uses 2-dimensional 8 node isoquadrilateral elements in plane strain and 1-dimensional pin ended bar elements to model the structure. The material properties of these elements can be varied to allow for bi-linear stress strain characteristics. Yielding of the material in the 2-dimensional elements is controlled by the Von-Mises yield criteria. In addition, cracking of the material can also be taken into account. (A sub-routine was added to the program by the author to provide a plot of the crack pattern in the specimen after each load or displacement increment).

```
┌─────────────────────────────────────────┐
│     Assemble initial stiffness matrix    │
└─────────────────────────────────────────┘
                      │
┌─────────────────────────────────────────────────────────┐
│ Using initial stiffness matrix determine minimum         │
│ displacement and resulting stress pattern at which       │
│ specimen stiffness changes (in this case due to          │
│ concrete cracking)                                       │
└─────────────────────────────────────────────────────────┘
                      │
┌─────────────────────────────────────────────────────────┐
│ Add displacement increment and any out of balance        │
│ nodal forces                                             │
└─────────────────────────────────────────────────────────┘
                      │
                      ▼
        ┌──────────────────────────────────────┐
        │   Determine stresses at gauss points  │
        └──────────────────────────────────────┘
                      │
      ┌──────────────────────────────────────────────────┐
      │ Check principal stresses at gauss point with the  │
      │ yield - failure criteria of element material      │
      └──────────────────────────────────────────────────┘
                      │
      ┌──────────────────────────────────────────────────┐
      │ Determine a set of out of balance forces to       │
      │ maintain force equilibrium at element nodes and   │
      │ add to next displacement increment analysis.      │
      └──────────────────────────────────────────────────┘
```
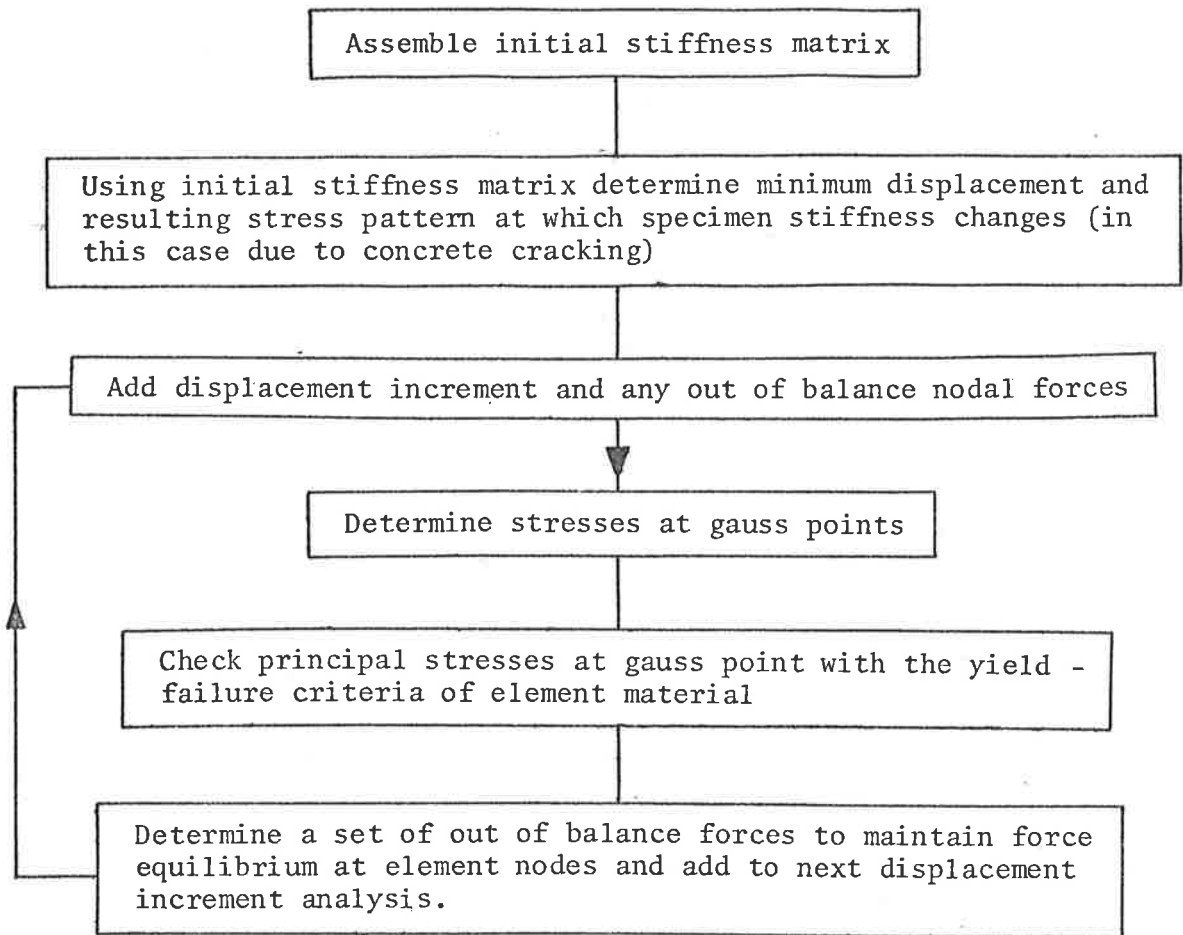
FIGURE 4.1   Block diagram of the non-linear F.E. programme.

At the time of using the program it was still in the process of development and some of the time saving refinements were not installed. So that the analysis methods in the program did not introduce errors the operating conditions were carefully controlled (in particular the load or displacement increment).

4.2 The F.E. Mesh

The steel and concrete in the T-joint was represented in the model by 1-dimensional bar elements and 2-dimensional 8 node isoquadrilateral elements respectively. Because of the relatively good "efficiency" of the isoquadrilateral elements it was possible to reduce the number of elements in the model below those in the linear F.E. model. This decision was guided by the results of the investigation for the linear finite element analysis as discussed in Section 3.2. By using a model with the joint block represented by 16(4 x 4) isoquad elements a similar number of nodal points were obtained as was used in the linear F.E. analysis (i.e. 85 to 121). Some restriction on the number of nodes had to be accepted to yield realistic computer memory requirements and solution times. The mesh chosen was thus a compromise and the program took up 155K of the available 200K on the CYBER 173 at the University of Adelaide.

The mesh layout indicating one of the reinforcement arrangements used is shown in Figure 4.2. The overall dimensions of the mesh are the same as those for the T-joint specimens tested in the manner discussed in Chapter 5; thus allowing the results to be compared.

Because of restrictions on the number of elements it was not possible to provide bends in the steel bar elements of a radius approaching that used in practice. In the model a bend was represented by connecting two perpendicular bar elements at a node. The bond between the steel elements
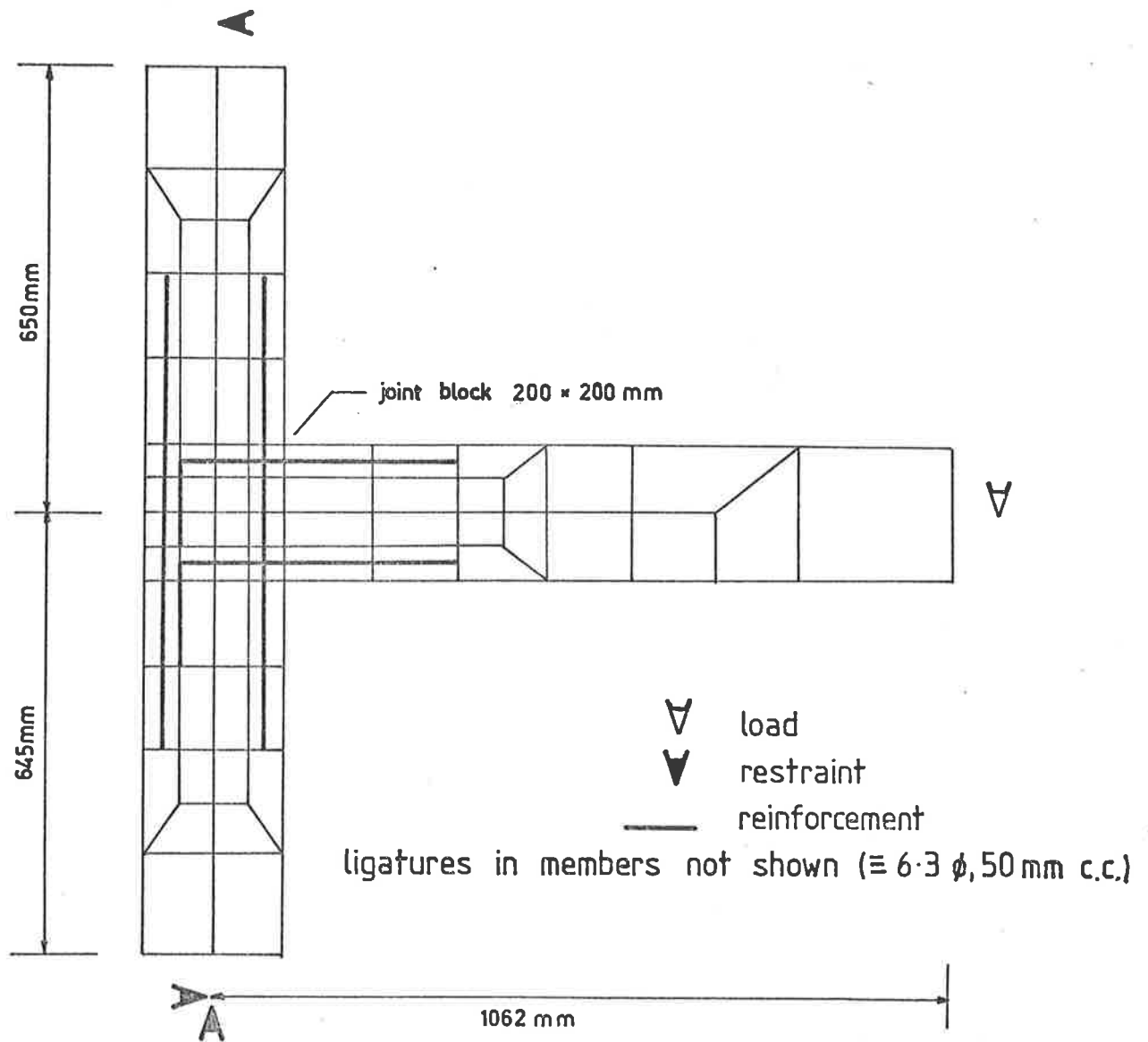
FIGURE 4.2 The element mesh used in the non-linear F.E. model.
The reinforcement pattern shown was used for all but
one computer run as shown in Table 4.1.

and the concrete elements implied that the bond strength of the connection was infinite. The effect of these modelling methods is discussed later.

A total of five element-material types were used in the model to represent different types of concrete and steel elements. Because the loads and restraints were applied as point loads the stresses in the elements around these points became very large. Consequently, to prevent premature failure of the model these elements had much increased failure strengths. Since they were located well away from the area of the joint which fails, strengthening these elements did not affect the final result. The material properties for those elements around the joint block are shown in Figure 4.3. Bi-linear curves were chosen as they were simple in concept but still approached the stress-strain properties of the real material. The material strengths used in the program were found by tests on the material used in the T-joint specimens (see Appendix A.3). These values tended to be close together and a set of representative values were used. The values of Young's modulus and strain hardening modulus were set at typical values for the respective materials. (exceptions to the above were made in the sensitivity analysis - see Table 4.1).

4.3 Results

With any new model or computer program there is a need to check its performance against known data. This was done for the program described in Section 4.1 as no previous checks had been made. Computer runs were made to check the material failure criteria, load distribution types and load-displacement control facilities and were found to be operating correctly. These tests were made on the structure shown in Figure 4.4.

As with this computer program and most other non-linear programs, the successful performance depends on the use of a suitable load or
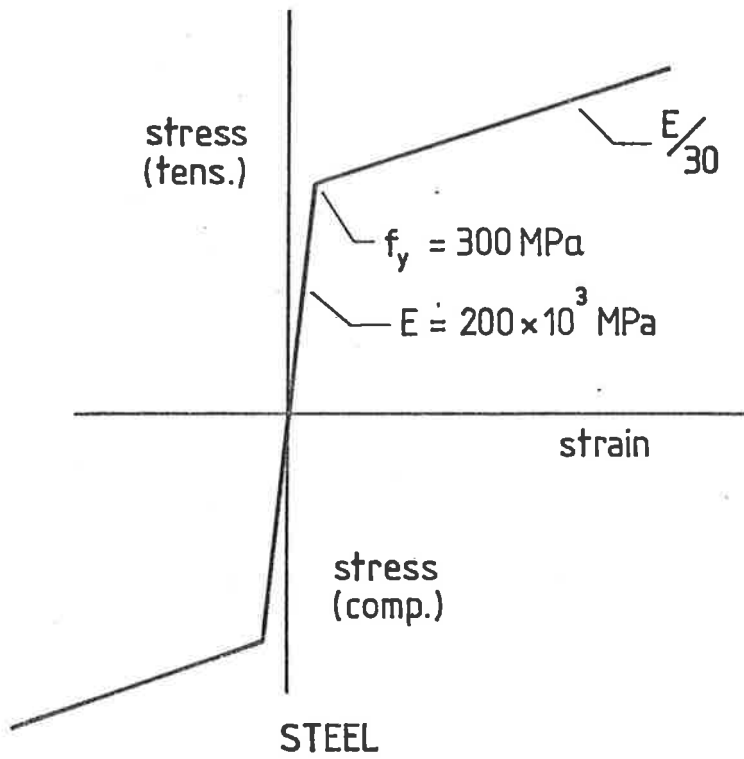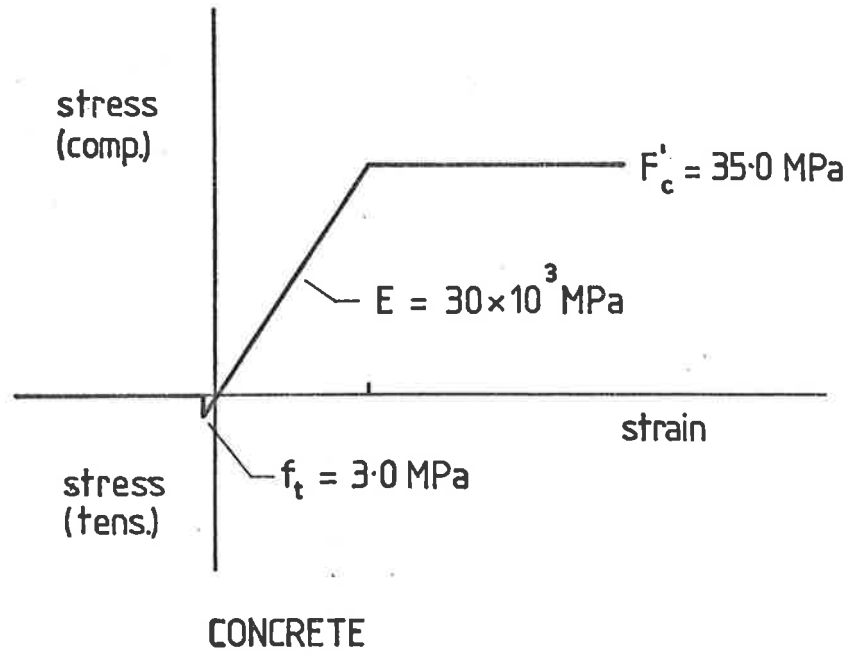
stress
(comp.)

$F'_c = 35.0$ MPa

$E = 30 \times 10^3$ MPa

strain

stress
(tens.)

$f_t = 3.0$ MPa

CONCRETE

stress
(tens.)

$E/30$

$f_y = 300$ MPa

$E \doteq 200 \times 10^3$ MPa

strain

stress
(comp.)

STEEL

FIGURE 4.3   The stress-strain properties of the material
used in the model to predict the test results.

computer run	data
1	disp. inc. = 0·5mm
2	disp. inc. = 0·25mm
3	disp. inc. = 0·05mm
4	disp. inc. = 0·05mm
5	disp inc = 0·25mm steel strain hard.= 0
6	disp inc = 0·25mm f_t = 0·5 MPa

unless indicated otherwise the material properties are as shown in figure 4·3

TABLE 4.1   Data for computer runs.

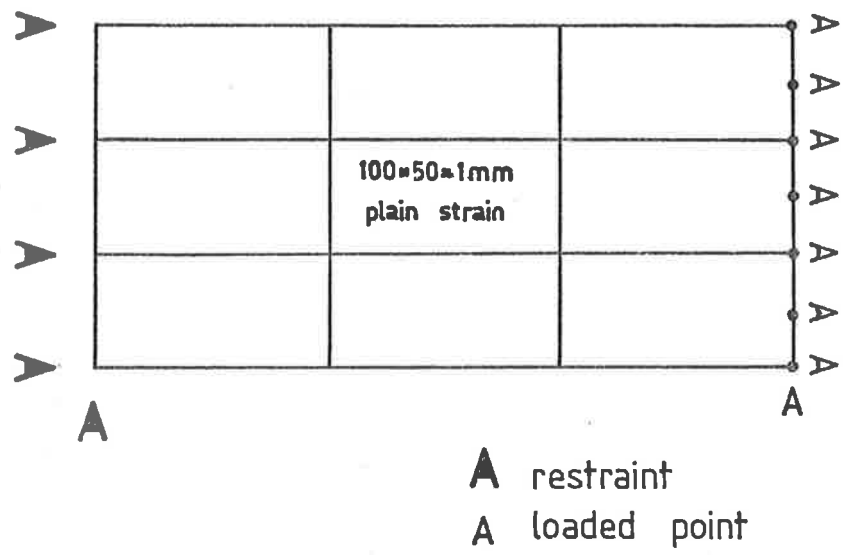100×50×1mm
plain strain

A restraint
A loaded point

FIGURE 4.4   The structure used to check
the operation of the F.E. program

displacement increment. In models which cause large plastic deflections the use of load control can result in large errors unless extremely small increments or a large number of iterations are used. Thus, displacement control was used throughout except for one computer run. This run verified that the model could not be used to check the effect of column load on the crack pattern and the load deflection curve.

Three different displacement increment sizes were used (run 1,2 and 3) to determine the sensitivity of the model to increment size. (See curve a, b and c, Figure 4.5). The results indicated that with a beam displacement increment of 0.05 mm the law of diminishing returns was effective. The 0.05 mm increment was thus considered acceptable and any smaller increment size would have resulted in the already large computing time becoming unrealistic. In order to reduce the computing time some of the evaluation runs were made with a 0.25 mm beam displacement increment.

Run number 3 was also used to predict the performance of the specimen types (1), (2) and (4) as used in the tests. (See Section 5.1). The model characteristics used in run 3 are given in Table 4.1. Figure 4.5 shows the load-deflection plot for this run (curve C). The load-deflection curve for specimen 8 (type 2) is also shown on this figure. A comparison of the 2 load-deflection curves shows that the model closely predicts the performance of the specimen in the elastic and plastic range. Until the specimen becomes plastic the 2 curves are almost identical. The difference in the yield load and plastic portion of the curves possibly results from the use of a deflection increment which is too large.

All of the runs discussed previously were for a reinforcement arrangement with the beam steel bent into the joint block. Computer run 4 was used to predict the experimental load-deflection curve of specimen 10 in which
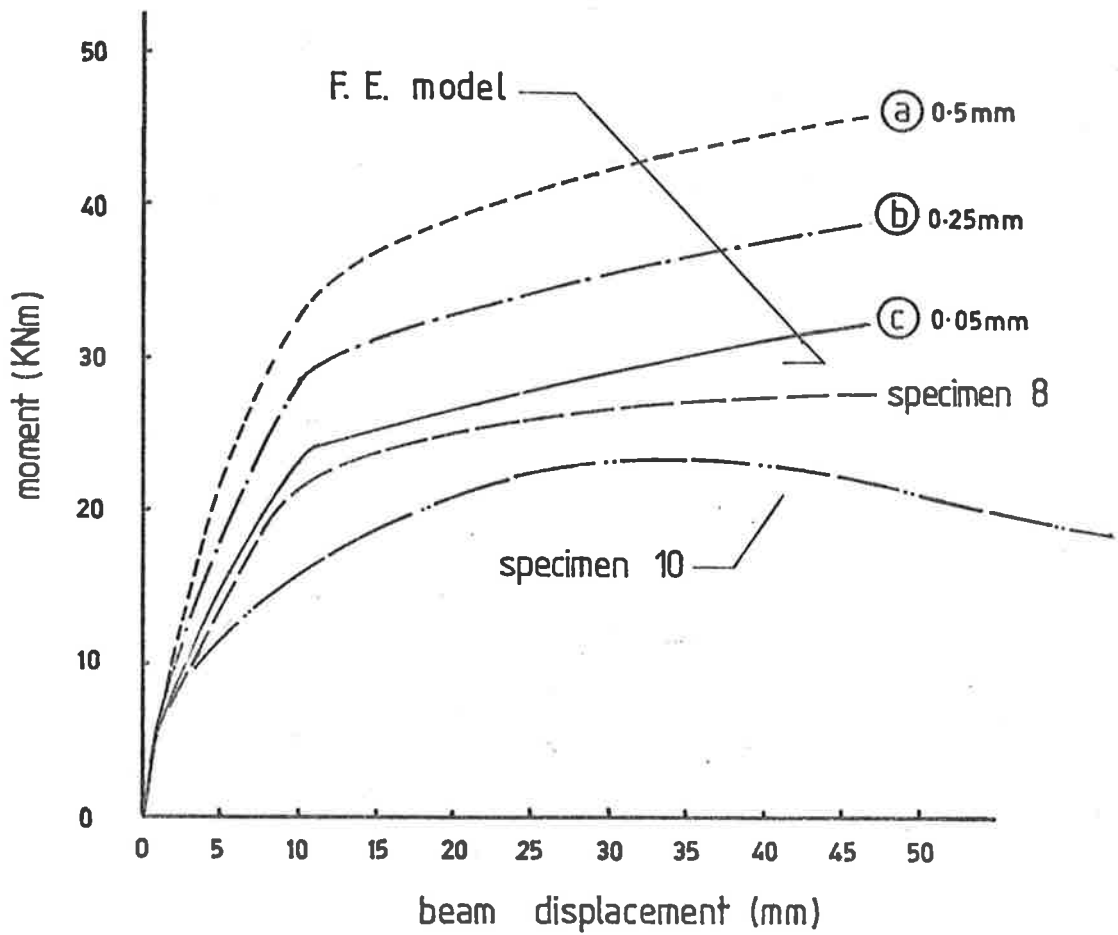
FIGURE 4.5   The effect of beam displacement increment
             size on the ability of the F.E. model to
             predict the load-deflection curve of a
             T-joint specimen.

the beam steel was bent out of the joint block. (Joints with this type of reinforcement arrangement had been found by testing to be weaker. See Section 5.4). However, the load deflection curve obtained from the F.E. model was the same as that obtained when the beam steel in the model was bent into the joint block (curve C in Figure 4.5). Although it cannot be determined from the results this is considered to occur because the model is not able to predict collapse within the joint block of the specimen. Assuming that the model could only fail in the beam (as for the superior test specimens) the predictions are thus independent of the reinforcement arrangement in the joint block. The inability to indicate the failure within the joint block is considered to be caused by the method used to model the steel to concrete bonding which does not allow slip to occur.

In order to determine the significance of the choice of some of the material properties a sensitivity analysis was conducted. This involved variations in the tensile strength of the concrete and the strain hardening modulus of the steel reinforcement. These computer runs were made with a larger displacement increment (0.25 mm) to reduce the computing time required. Although the results cannot be compared directly to those made with the 0.05 mm displacement increment they do show the effect of the variations by comparing the results with those from computer run 2.

Computer run 5 was the same as run 2 except that the strain hardening modulus in the steel was reduced to zero. As would be expected, there was no change in the elastic portion of the load-deflection curve and the plastic portion differed in that the strain hardening was almost zero (see Figure 4.6 curve d).

The effect on the model of a different concrete tensile strength was found from run number 6 in which the concrete tensile strength was set at
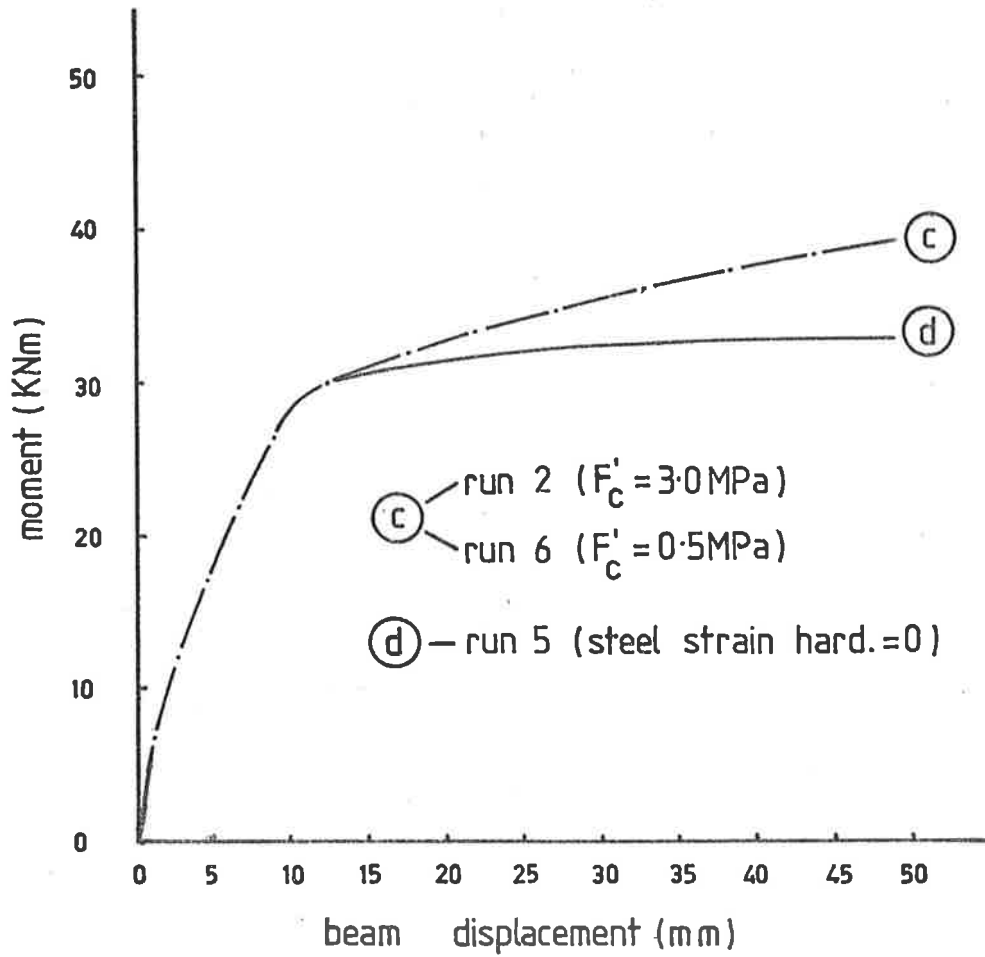
FIGURE 4.6   The results of the sensitivity analysis on the F.E. model to determine the effect of different material properties on the load-deflection curve.

0.5 MPa. As seen in Figure 4.6 the overall results are the same as those obtained for concrete tensile strengths of 3.0 MPa. The finite element model thus appears insensitive to concrete cracking.

The F.E. modelling has shown that it is possible to predict the experimental behaviour of the T-joint for at least some situations. The closeness of the theoretical and test results indicates the usefulness of the model in these instances. Further comparison of the results from the model and the tests is given in Section 6.2. With further development of the model to allow for bond slip and geometric non-linearity greater success would be achieved.

5. EXPERIMENTAL RESEARCH

The test programme was planned to evaluate the fatigue performance of the T-joint under conditions similar to those occurring during cyclonic wind loading. The experimental and analytical research programmes were also planned so that they would complement each other. These aims were aided by a survey of the literature on T-joint tests under static and seismic loading. (See Chapter 2). The fatigue performance of the joint components was also included in the survey. Results of the survey indicated that the T-joint performance is controlled by a large number of inter-dependant loading and joint configuration parameters.

So that the overall pattern of the joint performance could be established by a limited number of tests, rationalisation of the parameters was needed. This was achieved by investigating only those parameters which were shown in the earlier static[1]-[6] seismic[8]-[12] and fatigue[18]-[29] tests to have the greatest effect. Initially, the parameters chosen for testing were the magnitude of the M/P ratio, and the magnitude of the fatigue load. The type of joint used is currently used in practice. The choice of the variables used in these tests (Series 1) is discussed further in Section 5.1.1. After 7 specimens had been tested it became obvious that specimens of this type were not likely to fail in fatigue until the number of load cycles has greatly exceeded the low cycle fatigue limit taken as 10,000 cycles. The figure of 10,000 cycles being taken as that likely to give protection against cyclonic loading and is currently adopted in the Darwin Building Regulations[36]. As there were no fatigue failures recorded for the Series 1 specimens the effect of the test variables on fatigue life was

not observed. As it was considered important to verify the effect
of the performance parameters a second series of specimens were tested
(Series 2). The test variables used for the second series were the
M/P ratio and the reinforcement in the specimen. Further discussion is
given in Section 5.1.2. on the choice of the test variables.

For practical considerations half-scale specimens were used in the
experimental programme. This raised the problem of scale effects both
in modelling reinforced concrete and ensuring that the applied test
loads were representative of those on a full scale structure. Further
discussion on these matters is given in Section 5.2, but clearly the
testing rig had to be designed and built to reduce these problems.
The subsequent performance of the rig in the tests justified the
considerable time taken for development.

5.1 Testing Programme

5.1.1 Series 1 Tests

The linear computer model discussed in Section 3.2 had
indicated the performance of the T-joint might be related to the
distribution of forces applied to the joint block. This series of tests
was planned to determine if and what effect load variations have on
the low cycle fatigue life of a T-joint. Specimens were tested under
fatigue load and static load. The static tests provided a standard so
that comparisons could be made with the earlier static tests[1]-[3] and
between the static and fatigue performance of the joint. To reduce the
parameters involved only one type of reinforcement layout was used in
the Series 1 specimens although two types of reinforcing steel were used.

Test Variables

A total of nine specimens were originally planned for the first
series. The loading conditions for each specimen are given in Table 5.1.

	SPECIMEN	TYPE	S/F	M/P (metres)	L%	F'$_c$ (MPa)	F$_t$ (MPa)	F$_y$ (MPa)
Series 1	1	1	S	1.83	–	36.2	2.7	303
	2	2	F	1.83	100	33.7	2.9	300
	3	2	F	1.83	85	32.7	2.3	300
	4	2	F	0.14	100	33.8	2.9	300
	5	2	S	0.14	–	35.6	3.1	300
	6	2	F	1.83	70	NOT	TESTED	300
	7	2	F	0.14	85	NOT	TESTED	300
	8	2	S	1.83	–	35.9	2.8	300
	9	2	S	0.14	–	35.7	3.1	300
Series 2	10	3	S	1.83	–	36.1	2.8	303
	11	3	F	1.83	100	30.8	2.8	303
	12	4	S	1.83	–	33.2	2.4	303
	13	4	F	1.83	100	33.6	2.8	303
	14	4	S	0.14	–	34.2	2.6	303
	15	4	F	0.14	100	36.9	3.2	303

"Type"   Specimen as shown in Figures 5.2 and 5.3

"S/F"   Static or fatigue loading

"L%"   Magnitude of fatigue load as a percentage of the test yield load.

"F'$_c$"   Compressive strength of concrete.

"F$_t$"   Tensile strength of concrete.

"F$_y$"   Yield strength of main reinforcement.

TABLE 5.1   Test Variables.

Not all of the planned tests were carried out because of the absence of failure even under the most severe test loading conditions.

The load cases were selected to answer the following questions

(1) What is the effect of different M/P values on the static and fatigue performance of a joint ?

(2) What is the effect of different magnitudes of fatigue load (sometimes referred to as load range or stress range) on the fatigue life of a joint ?

(3) What is the load-deflection or deflection-time curve of a commonly used joint under static and fatigue loads ?

The values of M/P, M/V and load range used in the tests were based on the results of previous tests (See Chapter 2) and the results of the analysis of a typical building frame which is discussed in Section 3.1. The M/P values of 0.14 and 1.83 metres represent extreme values and are due to combinations of the wind load (WL), self weight (DL) and live load (LL). The value of 1.83 metres was considered realistic as the upper limit for the tests as the difference in the column stress for M/P of 1.83 metres and infinity is small in comparison to that due to M/P of 0.14 metres. The M/V (of 1.06 metres) and the M/P values are within the range of values given in the AS1480[34] concrete code.

As discussed previously in Chapter 2, research has shown that there is a large increase in the number of cycles to failure for concrete as the applied load is reduced to 60-70 per cent of the static collapse load. This is sometimes regarded as a fatigue limit[21][22]. The peak values of the sinusoidal fatigue load selected for the Series 1 tests

were 100, 85 and 70 per cent of the static yield load. (Such high intensity loads, outside the normal design range, could well be applied to a structure under extreme cyclone loading). These loads provided points on the S/N curve between static yield and the fatigue limit. The minimum value of applied load within each cycle for all tests was that due to the D.L. of the rig and specimen supported on the lower connection.

As discussed previously in Section 2.3, it has been shown that the frequency of loading and stress range are significant in controlling the life of plain concrete in fatigue. The effect of stress rate was not identified under fatigue loading although it has been shown to affect the static strength of plain concrete cylinders. It is possible that these three parameters would have an effect on reinforced concrete similar to that on unreinforced concrete. As it was not possible to keep two of these variables constant and vary the third when using a sinusoidal loading pattern it was necessary to examine the loading on a real structure to decide on which parameters to vary.

Assuming a certain "type" of cyclone occurs, the peak load value and the frequency of loading on the building will depend on the cyclone. The stress rate will depend more on the stiffness of the building than the other two variables do. Because of this it was decided that the loading in these tests should be of a fixed frequency and variable amplitude. A frequency of 0.5 Hz was used as it was considered to be within the range of the gust period of a cyclonic wind storm and enabled the tests to be completed in a reasonable amount of time.

The previous discussion outlines the processes used to select the test parameters and their values. The testing procedures used to obtain the desired parameter values given in Table 5.1 are discussed in Section 5.3.4.

Specimens

The dimensions and reinforcement for the Series 1 specimens are shown in Figures 5.1 and 5.2 respectively. All of the specimens were of the same overall dimensions and were loaded at the same points on the members. The specimen cross-section was 200 mm (D) by 125 mm (b) and the beam and column steel percentages were 1.8 and 3.6 per cent respectively. Reinforcement types 1 and 2 differ only in the type of steel and the bond length used. Plain round structural grade bars were used in specimens of type 1 and deformed structural grade bars in specimens of type 2.

To prevent a shear failure of the members in the specimen 6.3 mm diameter hard drawn wire ligatures were placed at 50 mm centres. No ligatures were located in the joint block and for type 2 specimens the first ligatures were located 20-40 mm from the face of the joint block. Connection of the specimen to the testing rig and machine were made by threaded extensions on the column reinforcing and by casting bolts into the upper face of the beam. Two of the specimens (8 and 9) contained 8 pairs of electrical resistance strain (ERS) gauges which were located on the steel reinforcement as shown in Figure 5.4. The ERS gauges were wired in series so that any bending stress in the steel would be cancelled. Readings taken from the gauges during the tests did not provide any useful quantitative information. However, they did show that loss of bond occurred on the column bars where they passed through the joint block. The ERS gauge readings show this occurred at joint moments as low as 9.7 KNm which is approximately one-third of the yield load for the joint.

The reinforcement arrangement in Figure 5.2 was used in the Series 1 specimens because it had been shown to have superior static and seismic performance[3]. This reinforcement layout also had the following advantages;
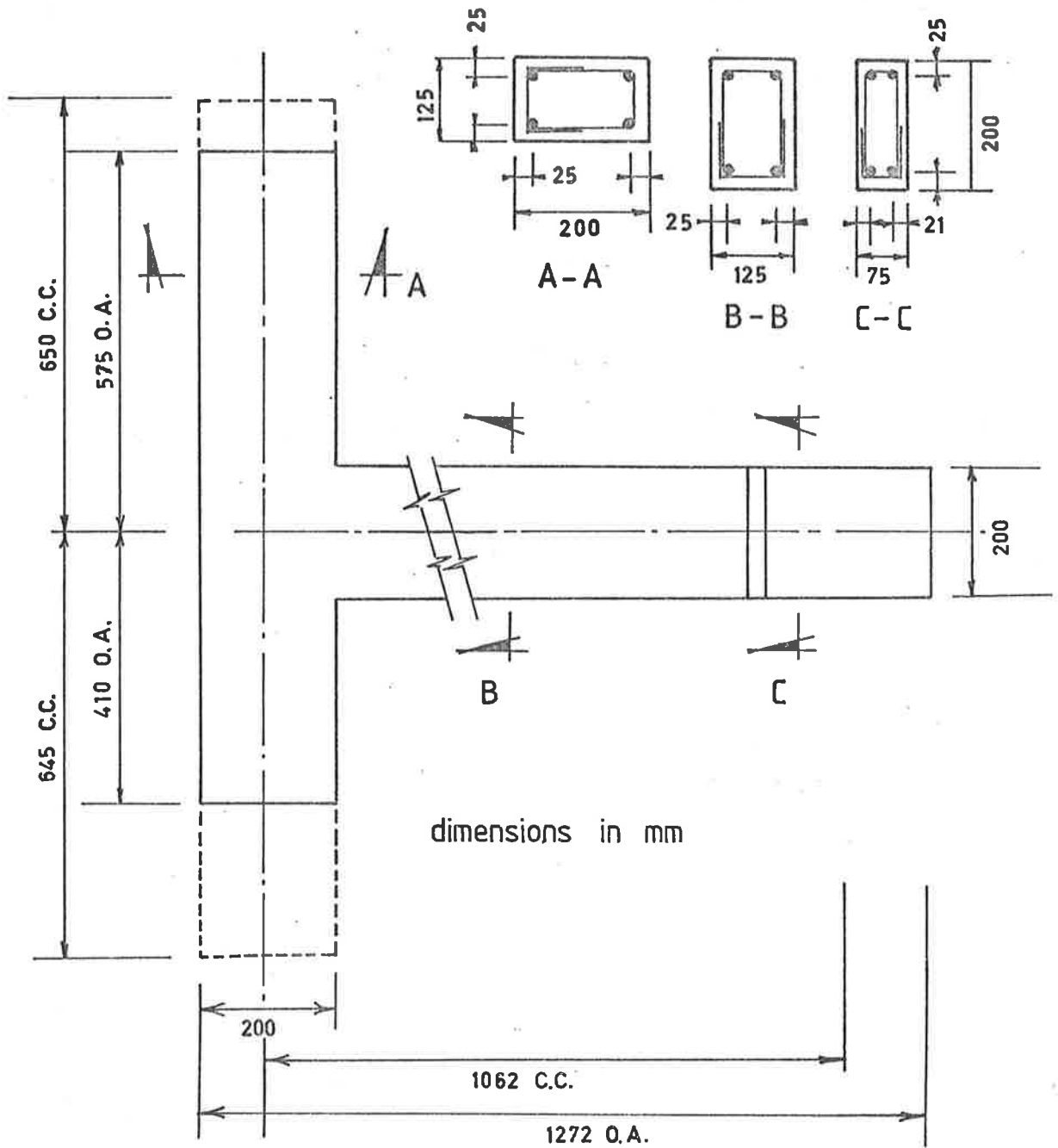
dimensions in mm

N.B. Dimensions marked C.C. indicate the lengths between connection
     points for testing rig. The dotted outline indicates
     the effective length of specimen when connected to
     testing rig.
     Dimensions marked O.A. indicate the actual dimensions
     of the reinforced concrete.

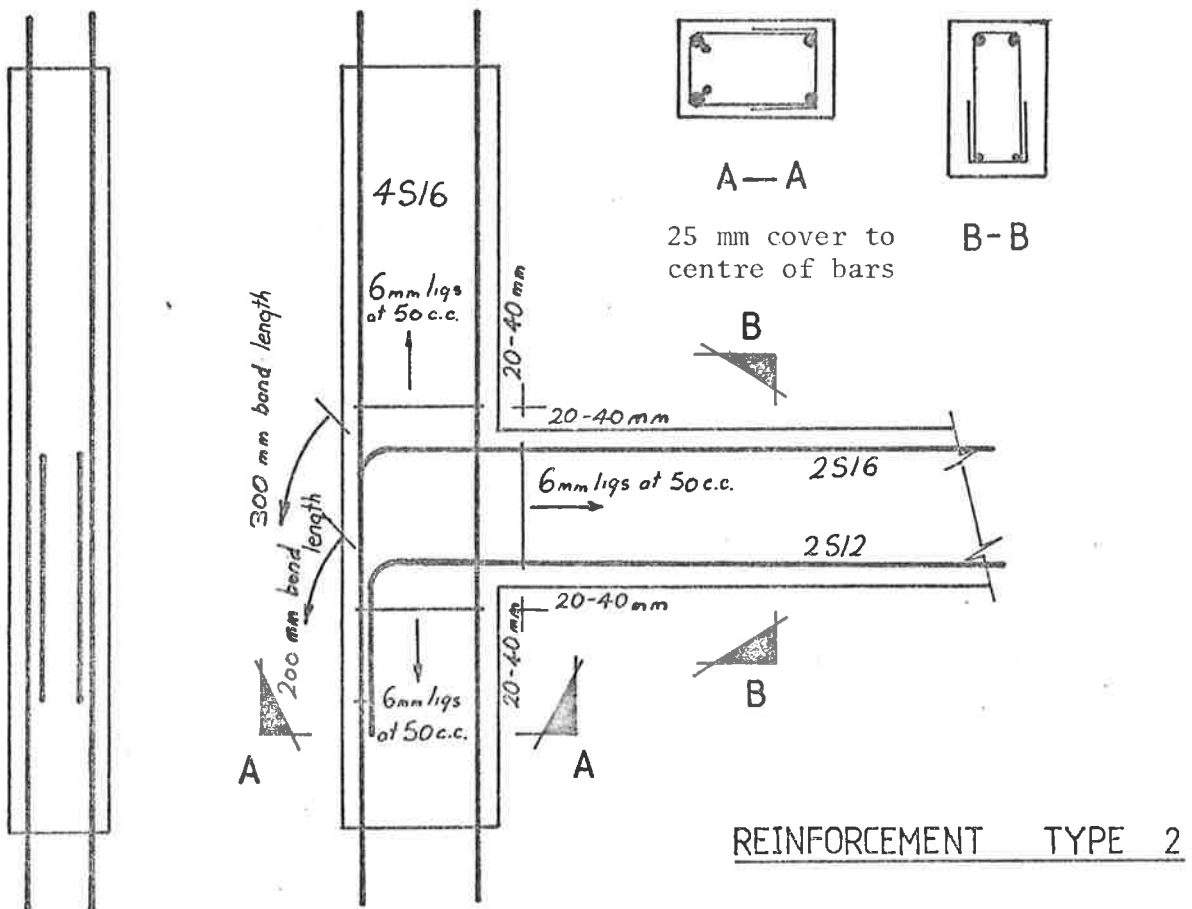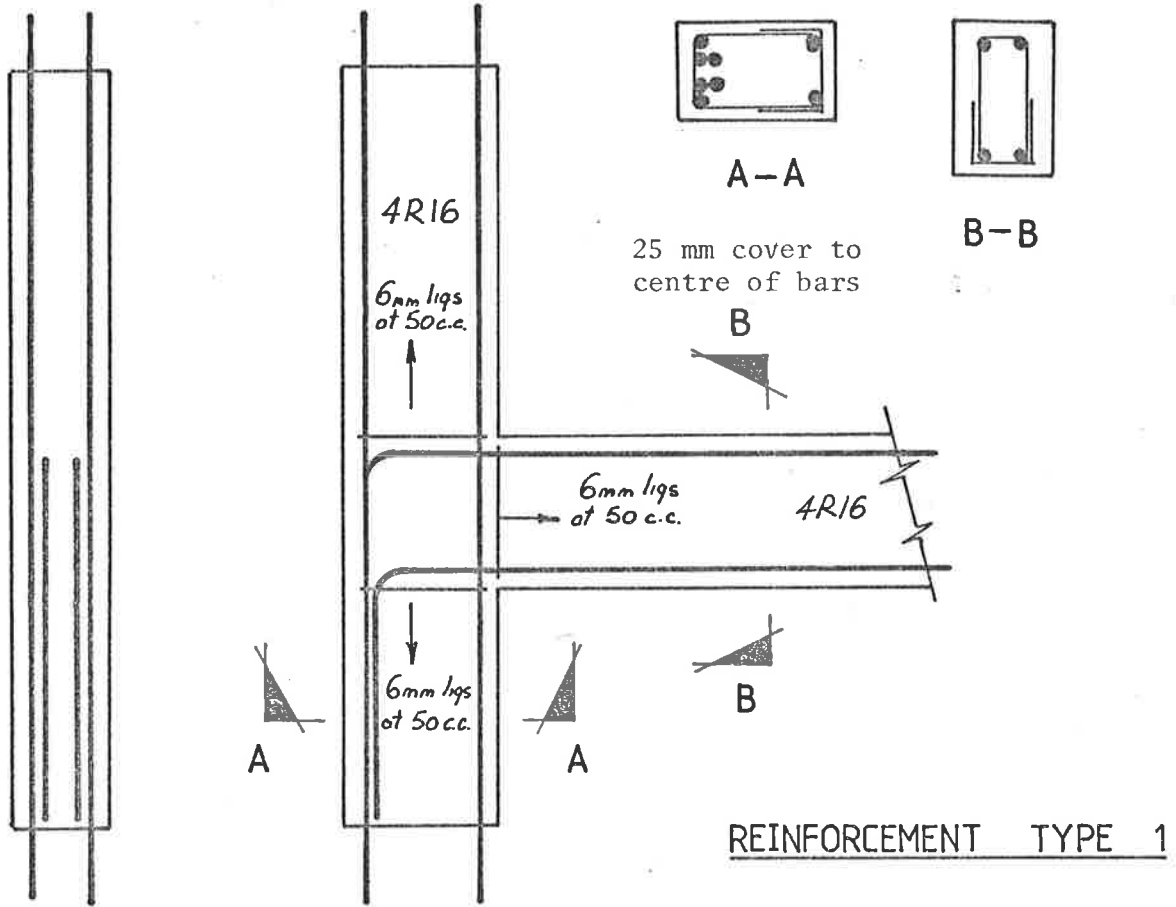FIGURE 5.1   T-joint specimen dimensions.

A—A

25 mm cover to
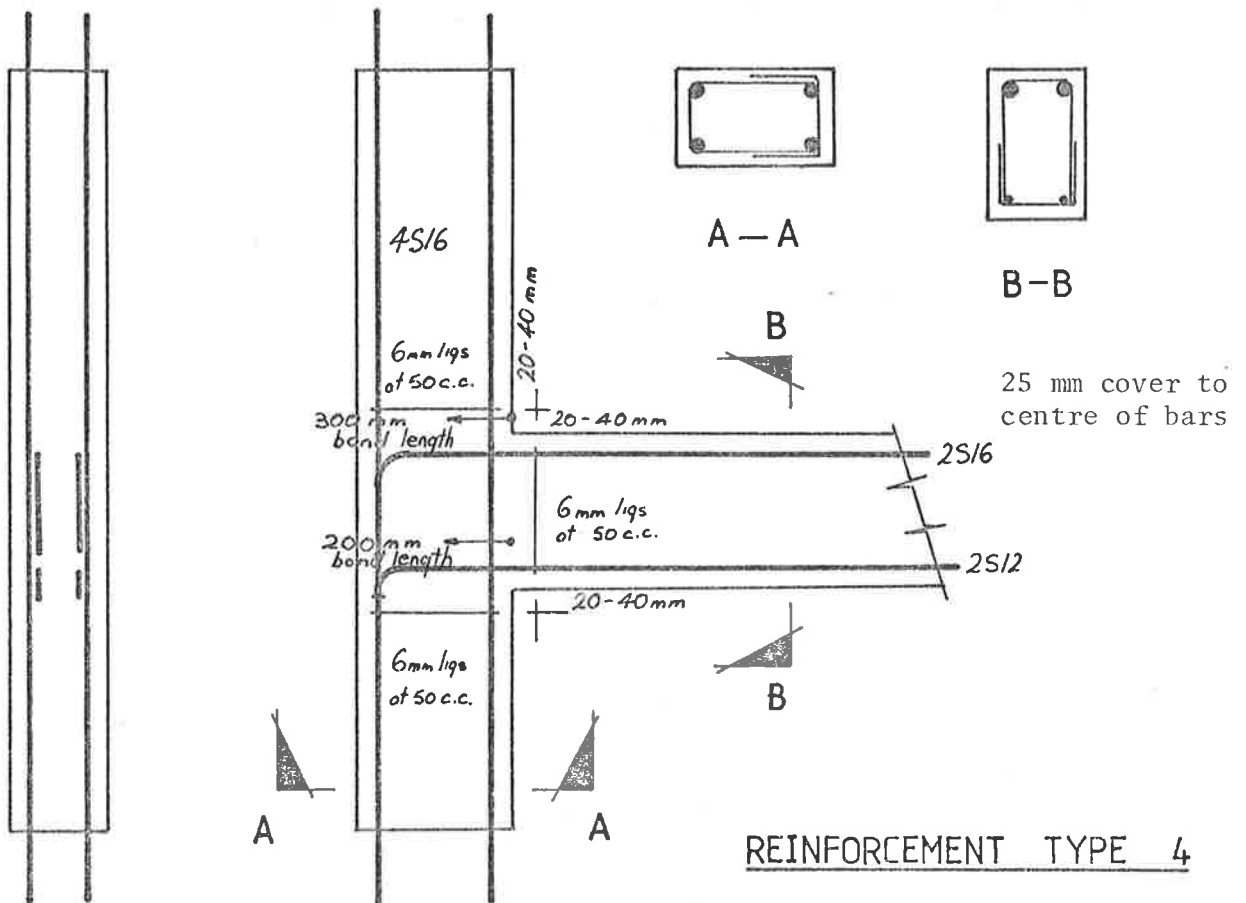centre of bars

B—B

4R16

6mm ligs
at 50 c.c.

6mm ligs
at 50 c.c.

6mm ligs
at 50 c.c.

4R16

B

B

A   A

REINFORCEMENT   TYPE   1

A—A

25 mm cover to
centre of bars

B-B

4S16

6mm ligs
at 50 c.c.

20-40 mm

20-40 mm

300 mm bond length

200 mm bond length

6mm ligs at 50 c.c.

2S16

2S12

20-40 mm

20-40 mm

6mm ligs
at 50 c.c.

B

B

A   A

REINFORCEMENT   TYPE   2

FIGURE 5.2   Series 1 specimens.

REINFORCEMENT TYPE 3

25 mm cover to centre of bars

REINFORCEMENT TYPE 4

25 mm cover to centre of bars
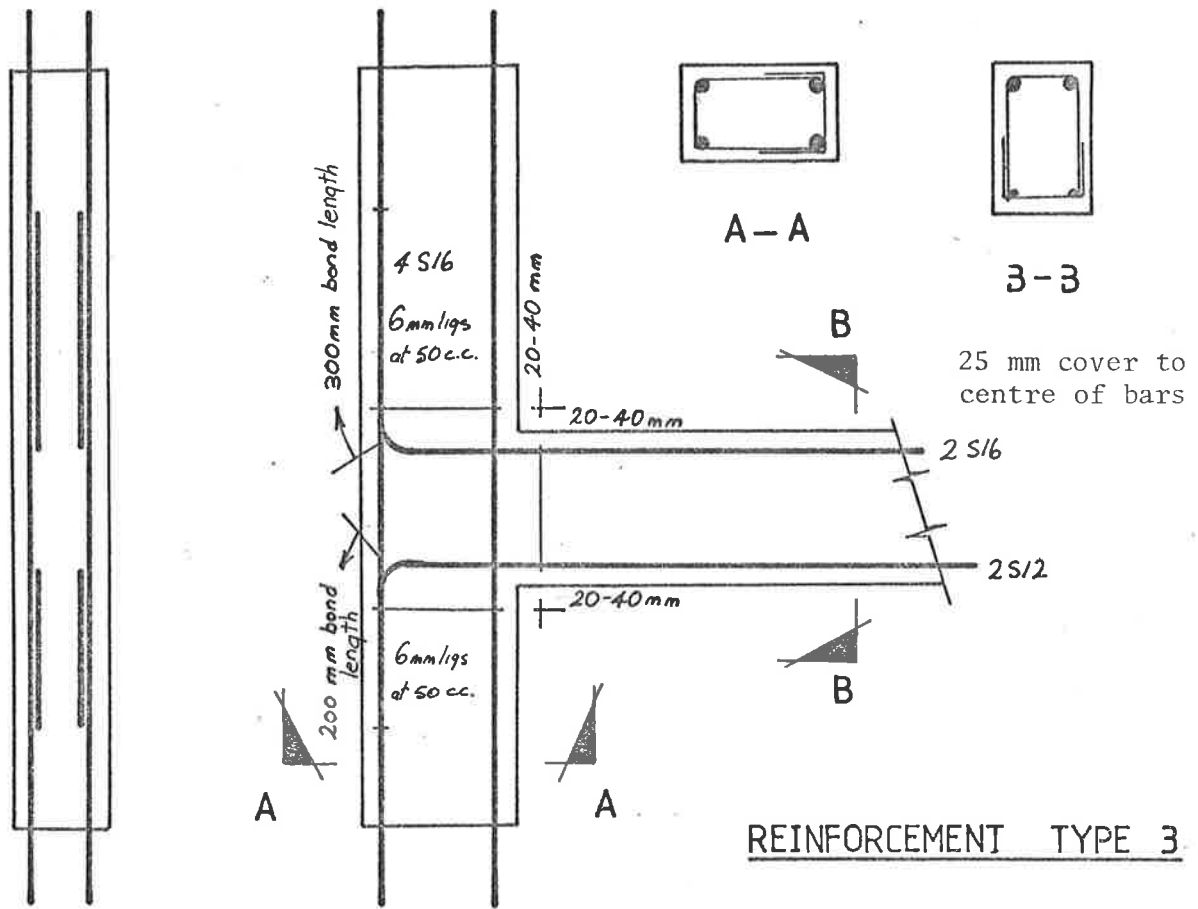
FIGURE 5.3.   Series 2 specimens.

1. Large arrows indicate direction of applied bending moment

2. Notation indicates number of gauge pair and the reinforcing bar to which it is attached.

dimensions in mm
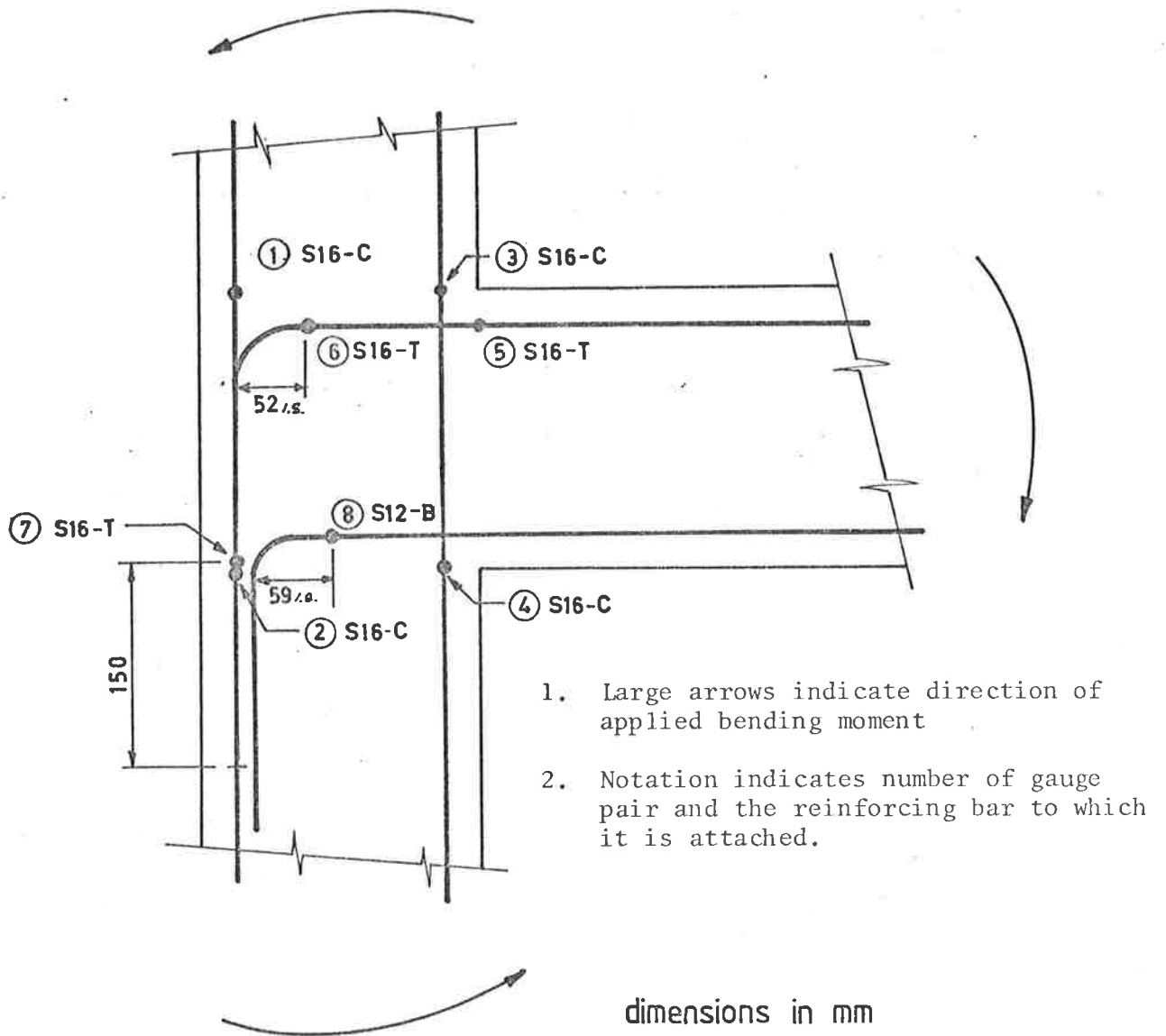
FIGURE 5.4   The E.R.S. gauge locations in specimen 8 and 9.

(1) it was similar to joints currently used in Australia,

(2) it was possible to compare the performance of the joint

with that predicted by the model for joint block

cracking and the F.E. models,

(3) it was simple to construct and is easily adaptable.

The following discussion enlarges on these points.

As noted previously in Chapter 2, the joints which have the
beam steel bent into the joint block have superior performance compared
to the joints which have the beam steel bent out of the joint block.
This is because the radial forces at the bend in the tension steel act
directly against the diagonal compression strut in the joint block.
Research[3] has shown that the difference in the static strength
efficiency of the two joint types is as great as 85 per cent. Because
of the poor static performance of the joint with the beam steel bent out
of the joint block it was considered to be not worthwhile to use it
for a full scale performance study. With the scale of specimen tested
it was not possible to bend both the beam tension and compression steel
into the joint block as they would have interfered with the column steel.
The lower beam steel was bent into the lower column. The difference in
performance because of this was considered to be small as the concrete
carries the major proportion of the compressive force in the beam. No
test evidence was available to confirm this.

Park and Paulay[9] have shown that the effectiveness of the bond
on the reinforcement is important in controlling joint performance. The
joints which had the larger or more effective bond lengths had better
performance. The current Australian concrete structures code AS1480
suggests the calculated bond length to begin from the inner face of the
column. Park and Paulay[9] consider that this may be inadequate where
the depth of the column cross-section and the column axial load are

small. Thus, it was decided to design the Series 1 specimens with the bond length provided from the bend in the reinforcement as suggested by Park and Paulay.

The beam steel was positioned inside the column steel because it is common practice. This arrangement is considered by Taylor[2] to reduce the risk of a bearing failure under the bend in the beam tension steel because of the lateral confinement given by the column bars.

In Australia shear steel is rarely used in the joint block because of economic limitations and it has not been a code requirement. Because of this, the test specimens were only reinforced against shear failure in the members. The extent of the shear steel is shown in Figure 5.2. Furthermore, it was considered that if the fatigue performance of the joint was not satisfactory, then methods other than shear steel in the joint block could be used to improve the performance.

Structural grade (230 MPa minimum yield) deformed bar was used for specimens 2-9 (Type 2). The deformed bar has better anchorage than the plain round bar and it is normally used in practice. Only Specimen 1 contained plain round bar and since the full AS1480[34] code bond length could not be provided on the beam tension bars because of the short length of the lower column its use was discontinued.

As noted in Chapter 2, high bond stresses occur on the column bars where they pass through the joint block because of the rapid change in bar force in this region. Because the joint block in the test specimens was only 200 mm deep it was not possible to provide the full AS1480[34] bond length of 292 mm on the deformed column bars within the joint block.

The plain round column bars required 584 mm for full anchorage within the joint block. Although the AS1480 code does not require that the full bond length is provided within the joint block it could be

considered an advantage so that bond slip in the joint block is minimised or prevented.

Table 5.1 indicates the test variables and Table 5.2 in Section 5.4 indicates the variables and results of the tests.

5.1.2   Series 2 Tests

During the testing of the Series 1 specimens it became apparent that the specimens were performing better than would be required under non-reversing wind induced fatigue loads. A specimen tested with a peak cyclic load of 100 per cent of its yield load had not failed when the test was stopped at 46287 cycles. Although the Series 1 tests had shown that a joint could be built to withstand the loading conditions used in the tests the effect of the test variable (load variations) on failure had not been observed since no specimen actually collapsed. This is discussed in more detail in Section 5.3.4.

Another series of six tests was devised specifically to demonstrate the effect of selected variables. The test variables were chosen so that the Series 2 tests would supplement the results of Series 1. Reinforcement layout, bond length and load distribution were chosen as the test variables. Specimen types 3 and 4 as shown in Figure 5.3 were used for specimens 10 and 11, and 12-15 respectively.

As noted previously, those joints with the beam tension steel bent out of the joint block have inferior static and seismic performance. This layout was selected for specimens 10 and 11 so that a comparison could be made with the Series 1 specimens. For specimens 10 and 11 the bond length used to anchor the beam steel was provided from the bend in the steel as in specimen 2-9. The only difference between specimens 10 and 11, and specimens 2-9 was whether this anchorage was within or outside the joint block (see Figure 5.2 and 5.3). Specimens 12-15 were designed to show the effect of reduced bond length on the beam steel when compared

with the performance of specimens 2-9 in Series 1. The tests on
specimens 12-15 were also designed to show how the load distribution
affects the joints performance. Two M/P values were used to do this
and were the same values used in the Series 1 tests (0.14 and 1.83
metres). It was expected that the low M/P would result in improved
performance. This effect had been predicted by the improved cracking
model and linear F.E. analysis (discussed in Chapter 3), and had been
shown in tests by Nilsson[3]. Of the six specimens in the Series 2 tests,
three were used for static tests and three for fatigue tests. Table 5.2
shows the test variables and results.

5.2   The Testing Rig

In many testing programmes the equipment or rig used to test
the specimens is not the subject of significant investigation and design.
This is because suitable equipment exists, is of minor proportions or
its design does not significantly affect the test results. During the
planning of this research programme it became obvious that a testing rig
would have to be developed as nothing suitable was available.

A joint is only a very small part of a total structure and if its
performance is to be investigated in a realistic manner the loading
method (test rig and applied forces) must be able to represent the
rest of the structure. An INSTRON 1280 Dynamic Testing Machine was used
to apply both the static and cyclic load to the specimen. The testing
rig was fitted to the INSTRON to distribute the single point load to
the loaded points of the specimen. (See Figures 5.9). Because the
testing rig acted integrally with the specimen its operation was an
important part of the programme. Thus a detailed description of the rig
design and layout have been included in the thesis.

The INSTRON testing machine is capable of operating in
displacement, load or strain control. The dynamic operation of the

machine can be varied in frequency, waveform and amplitude. An X-Y plotter incorporated in the machine provides plots which have ordinates of displacement, load, strain or time. The number of load cycles is recorded on a counter in the control panel which will also stop the machine at a preset number of cycles. For this research programme the machine was fitted with a 200 kN load cell. (With the appropriate load cell fitted the machine is capable of 1000 kN static load or 500 kN dynamic load). The machine actuator (ram) is capable of 75 mm displacement in tension or compression. Only the compressive mode was used in these tests.

5.2.1 Testing Requirements and Rig Layout

An investigation was conducted to determine the testing rig requirements. The following points were found to be important.

(1) The rig must be able to produce a bending moment and shear force in the joint beam and a compressive axial load in the column. It must be possible to vary the magnitude of these three forces independently so that the force distribution is typical of that in a full size structure. The ability to apply these loads in two opposite directions or be readily modified to do it would be an advantage.

(2) The rig must have sufficient static and fatigue strength to complete the test programme.

(3) The stiffness of the rig must be such that rig deflections are small.

(4) The rig and specimen should constitute a statically determinate structure.

(5) The dimensions of the rig and specimen are sufficient so that scale effects do not occur.

(6) The rig and specimen must fit in the INSTRON testing machine.

(7)   The rig must allow unobstructed vision and access
to the joint block of the specimen.

The photographs and drawings in Figures 5.5 and 5.6 show the
rig used which satisfied the requirements. The testing rig consisted
of two fully welded box beams 350 mm deep by 75 mm wide. These were
connected by the rigid joints at D and C with High Strength Friction
Grip Bolts (H.S.F.G.). The rig and specimen were connected at A and
B through SKF spherical self-aligning bearings. (see Figure 5.6)
Connection to the testing machine load cell and actuator were made using
the connections marked D and E in Figure 5.6 .   Both of these
connections contained spherical bearings and did not transmit moments.
The connection used at E is one of a pair built at the University of
Adelaide and designed by Dr K. E. Moxham for another testing programme.
It has a designed static strength of 500 kN and contains a SKF 60 mm
spherical bearing. The load was applied to the end of the beam of the
specimen through connections B, C and the inter-connecting link-arms
which could be moved parallel to the beam axis. Transverse shafts in
connections B and C supported the spherical bearings in the link-
arms. Bolts were cast into the concrete specimen to secure it to
connection B . During the tests the link-arms were initially located
perpendicular to the beam so that only shear forces were applied to the
beam .   During the test, beam rotations meant that an axial force
component was introduced into the beam. However, these angle changes
were such that this component was small. Connection A provided the
transverse restraint to the top of the column to resist the moment in
the upper column. A 200 kN capacity hydraulic jack in connection A
was used to load the specimen column in compression independantly of the
load from the testing machine (see Figure 5.5 (c)). The oil supply to
the jack was controlled using a hydraulic pump mounted away from the rig
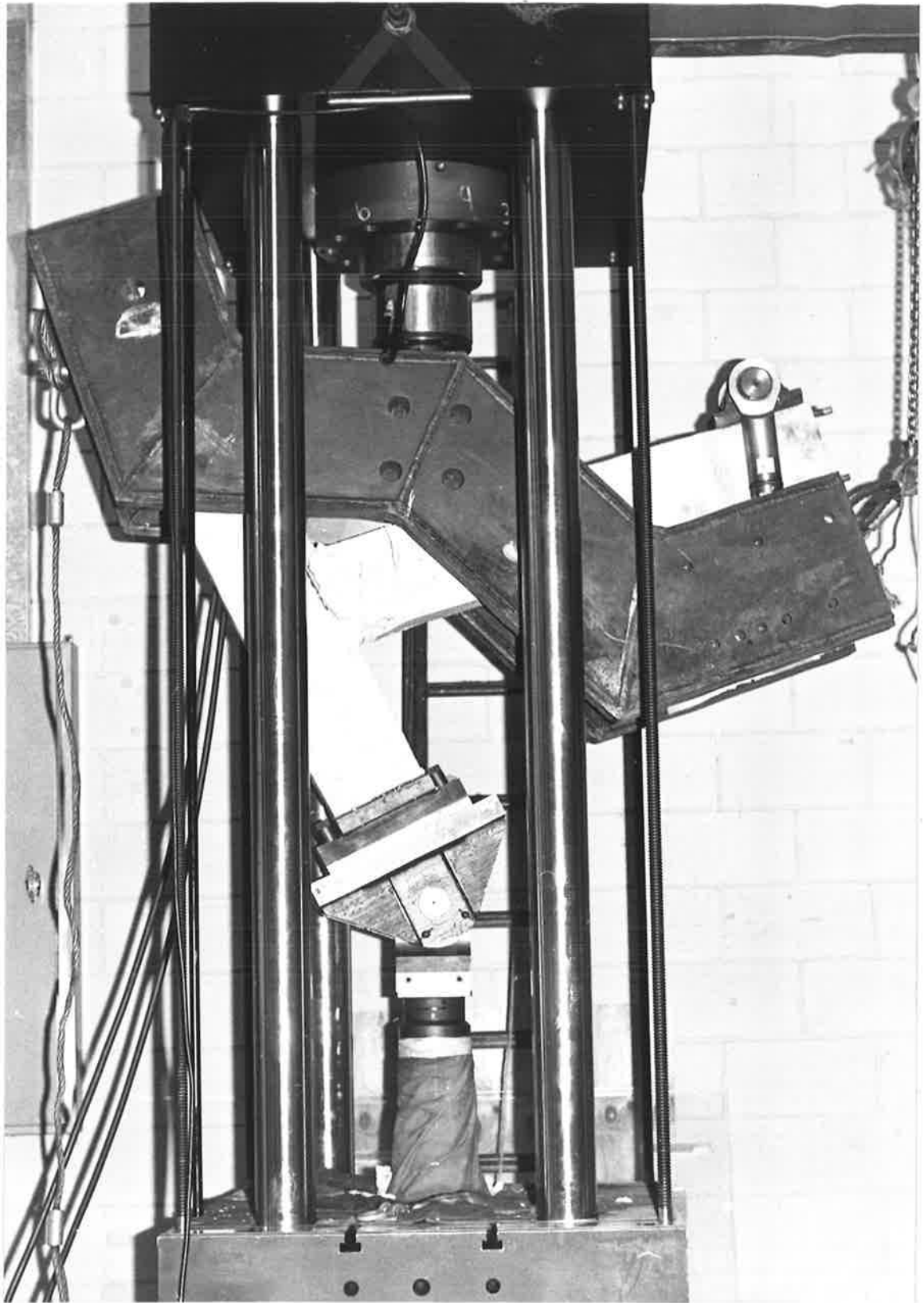
FIGURE 5.5(a)   Testing Rig and Specimen in
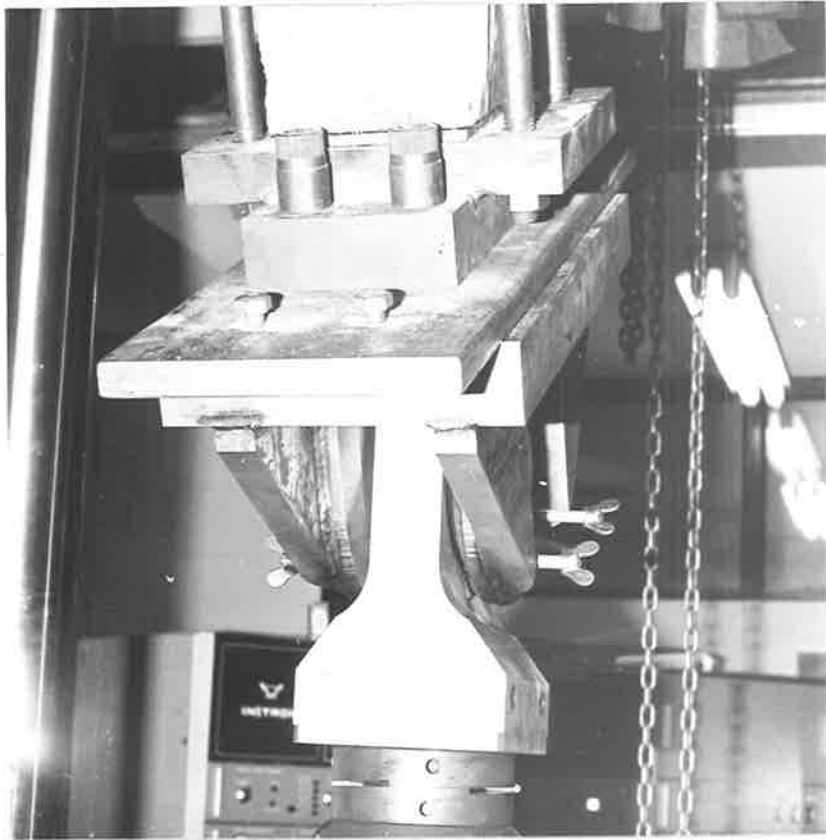   Instron Testing Machine.

FIGURE 5.5(b)   View of the connection (E) between the testing machine actuator and the lower column of the specimen.
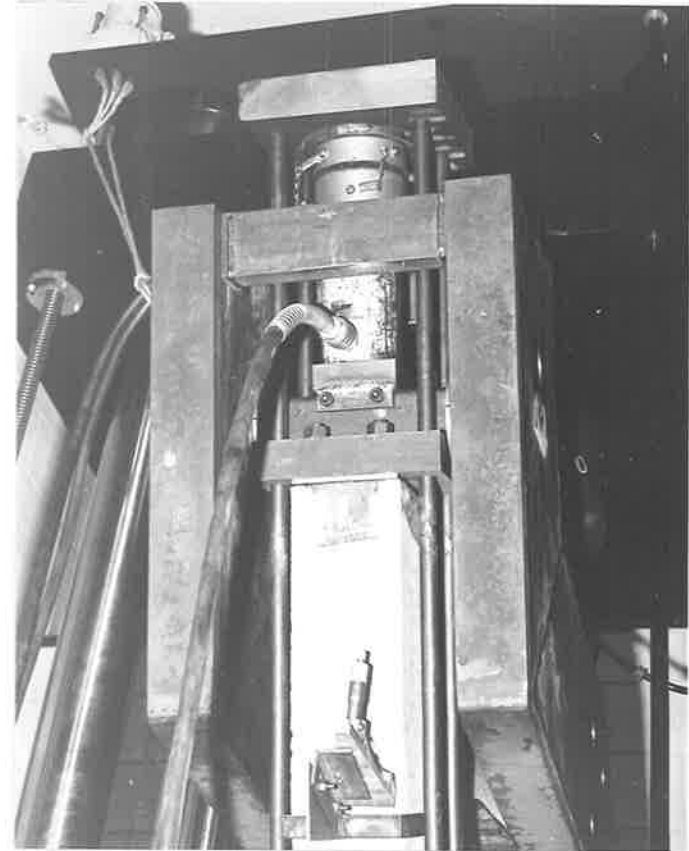

FIGURE 5.5(c)   View of the connection (A) between the upper column and the testing rig showing the hydraulic ram and fittings used to apply the axial load to the column of the specimen.
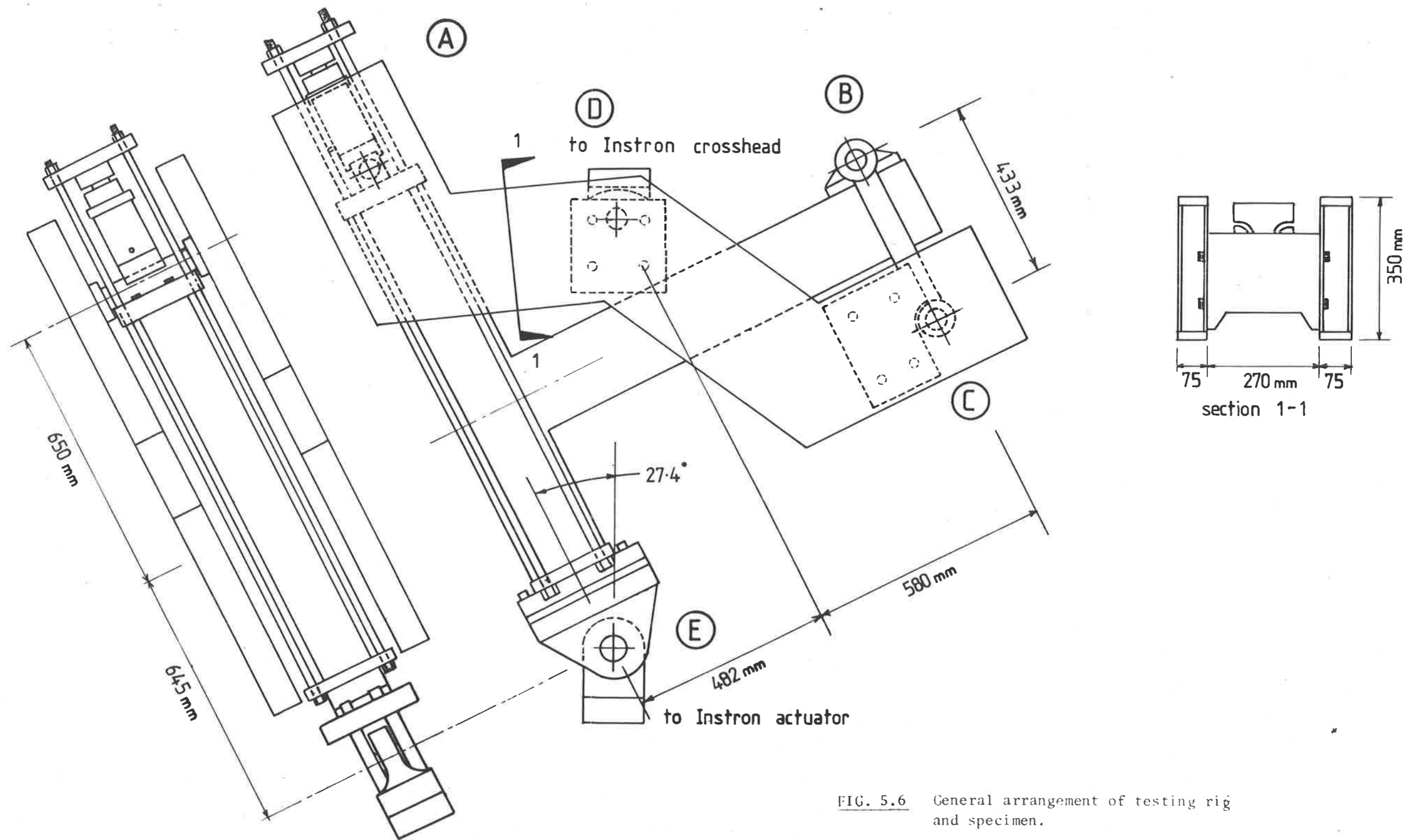
to Instron crosshead

to Instron actuator

27·4°

650 mm

645 mm

433 mm

580 mm

482 mm

Ⓐ Ⓑ Ⓒ Ⓓ Ⓔ

1

1

section 1-1

350 mm

75   270 mm   75

FIG. 5.6   General arrangement of testing rig and specimen.

The connection between the specimen and rig at A was made using a transverse shaft on spherical bearings in the box beams.

The position of connections B and C could be varied by using different bolt holes (see Figure 5.5 (a)) to give variations in the M/P and M/V ratios as shown in Figure 5.7. The ratios shown neglect the effect of specimen self-weight and column precompression. During this programme the link-arms were used in position 2. Figure 5.9 shows the member forces and reactions for this layout with unit applied compressive load. The self-weight of the rig and specimen was 6.2 KN which was approximately 15 per cent of the load required to cause yielding of the beam in the specimen. Figure 5.8 shows the joint block forces due to the self-weight of the rig and specimen supported on the lower connection. The self-weight was accounted for during testing and evaluation of the results by referring to the total moment on the specimen.

The test specimen was made as large as possible to avoid scale effects. Large connections on the rig reduced the length available for the specimen members. This was overcome at the lower connection E by ensuring that the connection between the concrete specimen and the end plate of connection E was rigid. The effective length of the column was that between the bearings of connections A and E . The minimum ℓ/d ratio for the upper and lower column was 3.23 (645/200). Such a value was considered representative of a full size specimen.

5.2.2 Design

To enable the rig to be used for tests on different specimens it was assumed that the strongest specimen would have a member cross-section 200 mm by 125 mm with an S20 steel bar in each corner. The calculated strength of such a specimen was increased by a factor of 2 to
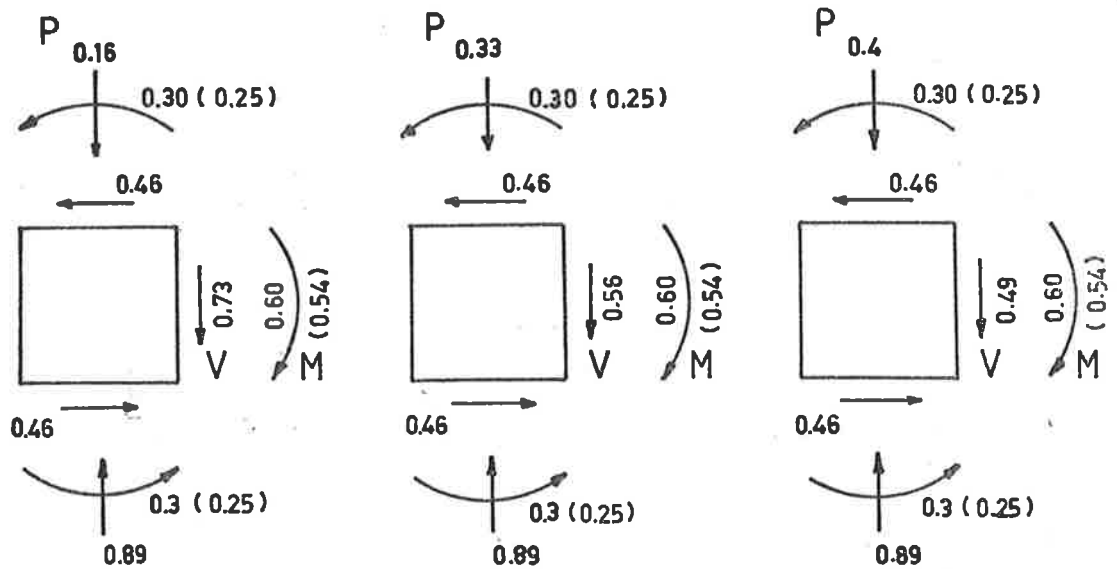
M/V 0.82 m	M/V 1.06 m	M/V 1.22 m
M/P 3.78 m	M/P 1.83 m	M/P 1.50 m
position 1	position 2	position 3

● all forces in KN or KNm

1. The above forces (KN, KNm) result from a 1 KN load applied to the testing rig.

2. DL of rig and specimen is neglected and no column pre-stress is applied

3. Positions 1,2,3 refer to the adjustable beam length - Position 2 used throughout.

4. All forces shown occur at centre of joint except for moments in parentheses which occur at face of joint block.

FIGURE 5.7 Joint Block Force Distribution due to 1 KN Load applied to Test Rig.

P - (KN)
V - (KN)
M - (KNm)

at jnt. blk. C_L   at jnt. blk. face
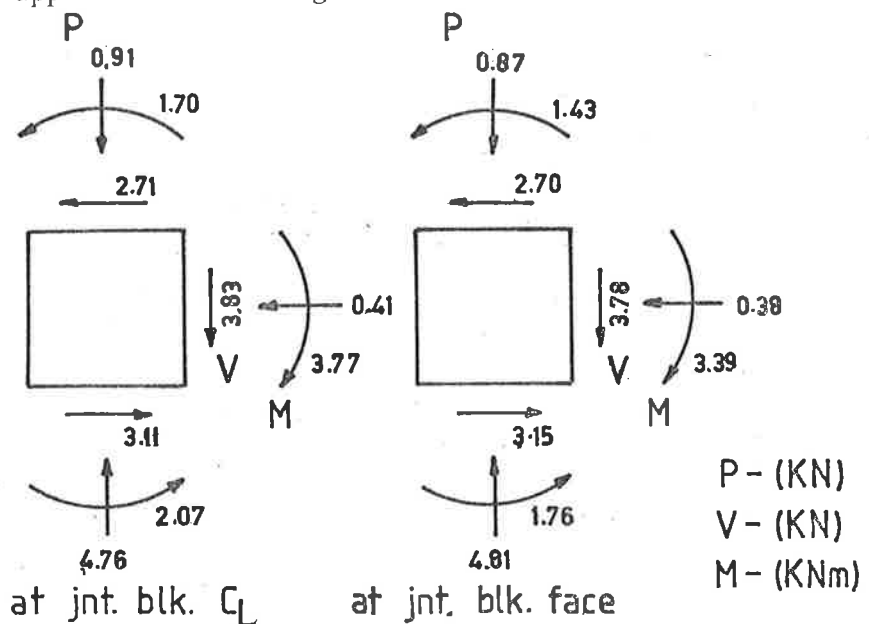
FIGURE 5.8 Joint Block Forces due to deadload of Rig and Specimen.

Column pre-stressing force

0.32P$_m$

P$_m$ Load applied by testing machine

0.46P$_m$
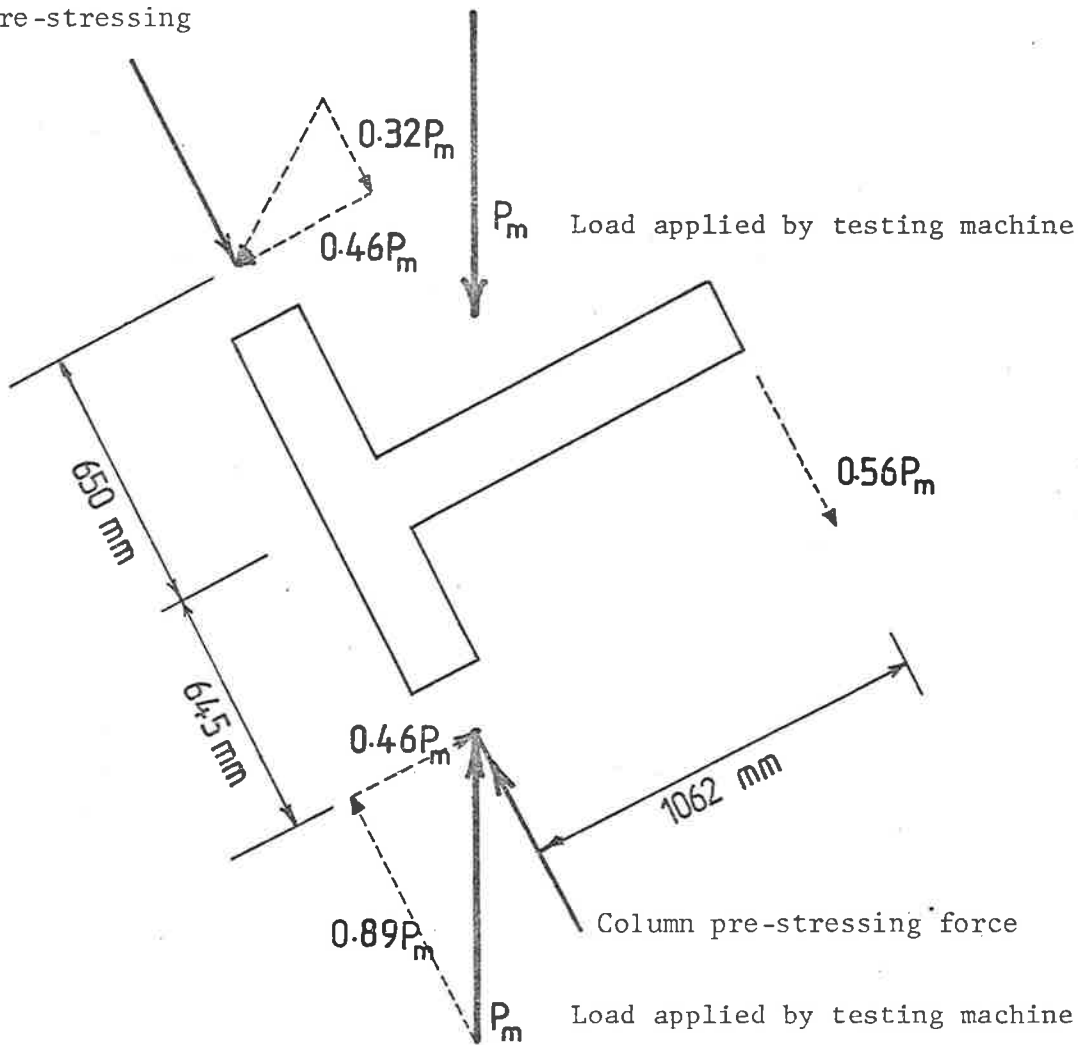
Components of load applied by testing machine.

650 mm

64.5 mm

0.56P$_m$

Loads applied to the testing rig or directly to the specimen

0.46P$_m$

1062 mm

Column pre-stressing force

0.89P$_m$

P$_m$ Load applied by testing machine

FIGURE 5.9   The member forces and reactions in the specimen and testing rig due only to applied loads.

determine the design load for the rig and corresponds to a 60 KN load on the INSTRON. A fatigue life of 10^6 cycles at the design load was considered to provide the rig with an adequate life to complete the planned test programme. The design of the rig was carried out using accepted simple structural theory and design techniques.

The Side Beams were designed using simple beam theory to calculate the maximum shear force and bending moment. Allowance was made for the warping stresses due to the induced torsion. To simplify the analysis of the warping stresses the box beams were considered to be one half their actual length with one fixed and one pinned end support. The maximum normal stresses were limited to one-third of the steel yield stress of 250 MPa. Full depth fully welded stiffeners were provided at all corners to carry the out of balance forces and to increase the rigidity of the section. A design check showed that the expected beam centre span deflection would be 1 mm for the design load. Using AS1250[37] SAA-Steel Structures Code as a guide for design all of the welds were made as full strength butt welds. Lateral buckling of the beams was not considered to be critical because of the rigidity of the box beams and the connections between them. The use of simple beam theory, although not exact on a beam of this shape, was considered adequate because of the limit on applied stress.

The Connections were designed using simple beam theory supplemented where possible by a mechanistic assessment of expected structural behaviour. Because of the large forces on the rig and its required fatigue life some of the bearing shafts and housings were designed in a high tensile alloy steel (X4150) which has good ductility and fatigue properties. The dimensions of the shafts were selected by simple beam theory. Because

the ℓ/d ratios of the shafts were small the shaft bending stresses found by simple bending theory were conservative but the sizes so selected gave satisfactory performance. Because of a need to have a very rigid structure all bolts between the box beams and fabricated connections were H.S.F.G. bolts which were designed to function below their slip load.

5.2.3 Fabrication

All fabrication was carried out in the University of Adelaide Civil Engineering Department Workshop. The large butt welds used in the rig could have caused large welding distortions but this was minimised by using good welding practice. Any small distortions which occurred were subsequently removed by the machining of contact faces on the beams and connections. Prior to machining, all parts of the rig were heat treated to reduce residual stresses and improve fatigue performance. Under test conditions the rig gave excellent performance and satisfied all of the requirements listed previously. At the end of the test programme the rig had withstood the static design load and had sustained 0.5×10^6 cycles at 0.6 of the design load with no indication of distress or failure.

5.3 Equipment Preparation and Testing Procedures

5.3.1 Specimen Construction and Preparation

Figure 5.10 shows the formwork used to cast the specimens of Series 1 and 2. By casting the specimens on the flat, vibration of the concrete was much easier and sedimentation was minimised. The surface of the formwork was coated with epoxy resin to ensure a smooth finish on the specimen, a long life for the formwork and to allow easy stripping.
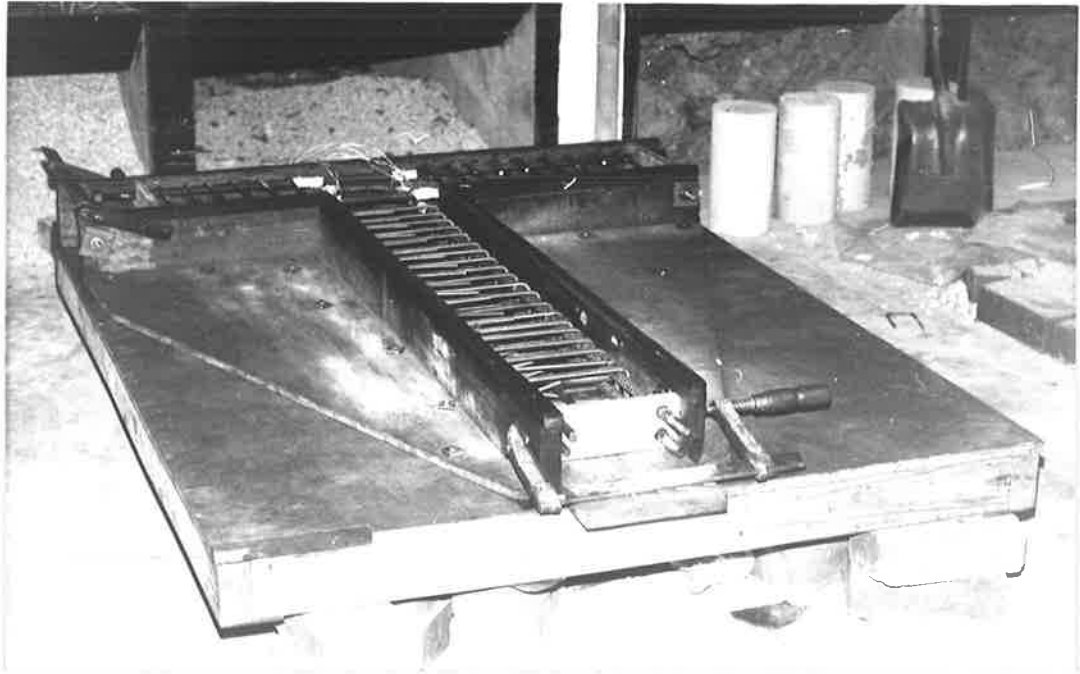
FIGURE 5.10   An overall view of the formwork and reinforcement
              used for the preparation of the T-joint specimens.

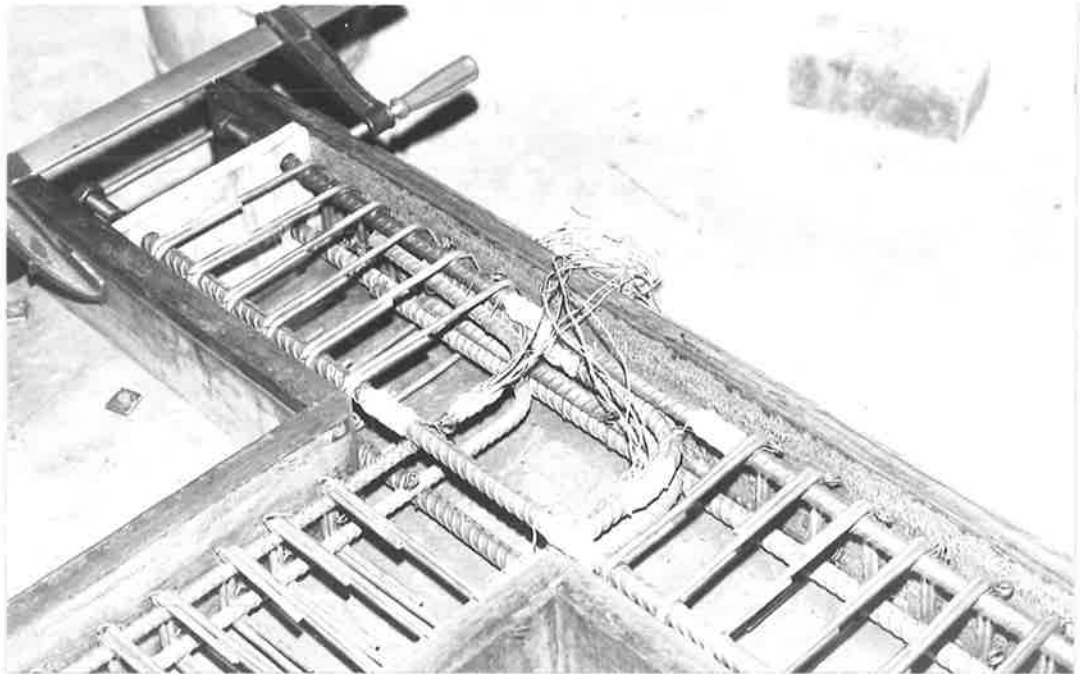FIGURE 5.11   A close up view of the reinforcement prior to
              pouring the concrete. The water proofed gauges used
              only in specimens 8 and 9 can be seen attached to
              the steel in the joint block zone.

Figure 5.11 shows the reinforcing in the formwork prior to pouring the concrete. The waterproofed ERS gauges used only in specimens 8 and 9 can be seen attached to the reinforcing. All bends in the reinforcing were cold formed to specifications given in the AS1480[34] code. Any oil on the reinforcing was removed by acetone prior to pouring the concrete. Where the cover on the main steel bars was reduced to less than 15 mm (at connection C on the beam) it was considered necessary to use ligatures with increased bond length. The concrete used was a 4 : 2 : 1 mix which consisted of 20 mm and 10 mm quartzite aggregate, ovendried Noarlunga sand and Normal Portland Cement. The water cement ratio of 0.58 was selected by trial to provide good workability and a target compressive cylinder strength of 35 MPa. Two batches of concrete were required for pouring the specimen and the 150 mm diameter test cylinders. The first batch was used to fill the part of the specimen near the joint block as well as 6 No 150 mm diameter test cylinders. The second mix was used to fill the remainder of the specimen and 2 additional test cylinders. These were used to monitor the mix variations but were not used to determine the strength of the concrete in the joint itself. The additional test cylinders were a precautionary measure as the specimens were designed to fail in the zone filled by the first batch of concrete.

Twenty four hours after pouring, the specimens were stripped and placed in a fog room for 7 days. After removal from the fog room, the specimens were stored at room temperature in the laboratory until required for testing. Prior to testing, the end faces of the columns were prepared by attaching a 6 mm thick steel bearing plate. The plate was bedded-in with epoxy resin and care was taken to ensure that the surface of the plate was perpendicular to the axis of the column.

This provided a good bearing surface between the specimen and the rig.

5.3.2 Loading Rig and Specimen into Testing Machine

The weight and size of the rig and specimen made their combined movement difficult so the rig was kept attached to the INSTRON testing machine between tests. When a specimen was to be tested it was lifted into place using a gantry crane and a block and tackle. Before the connecting bolts on the specimen were fully tightened the alignment of the specimen was checked to ensure the member axes were concentric with the connections. This was done so that the correct loading would be applied to the specimen under test.

5.3.3 Instrumentation of Specimen

The instrumentation discussed below was used in the test programme.

(1)   The load-deflection or deflection-time curve of the loading machine actuator was recorded by an X-Y plotter incorporated in the INSTRON control panel.

(2)   The member rotations were measured by inclinometers attached to the members at a length $D/2$ from the face of the joint block. (see Figure 5.12).

(3)   Deflections of the end of the members were measured by dial gauges. This was only used for specimen 8 and subsequently discontinued as it did not prove to be of any value.

(4)   Axial strains in the reinforcement in specimens 8 and 9 were measured by ERS gauges attached to the reinforcement. As noted previously the information obtained from the ERS gauges was of little value.
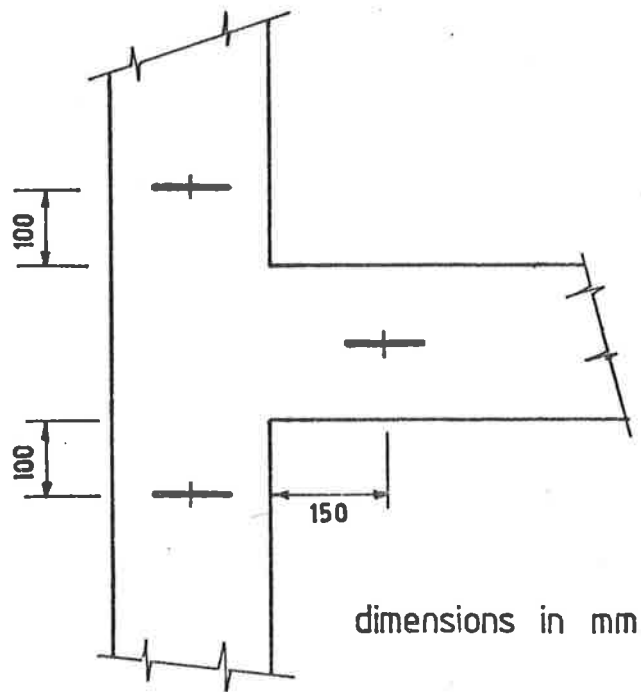
FIGURE 5.12 The location of the inclinometers used to determine the change in the joint "angles".
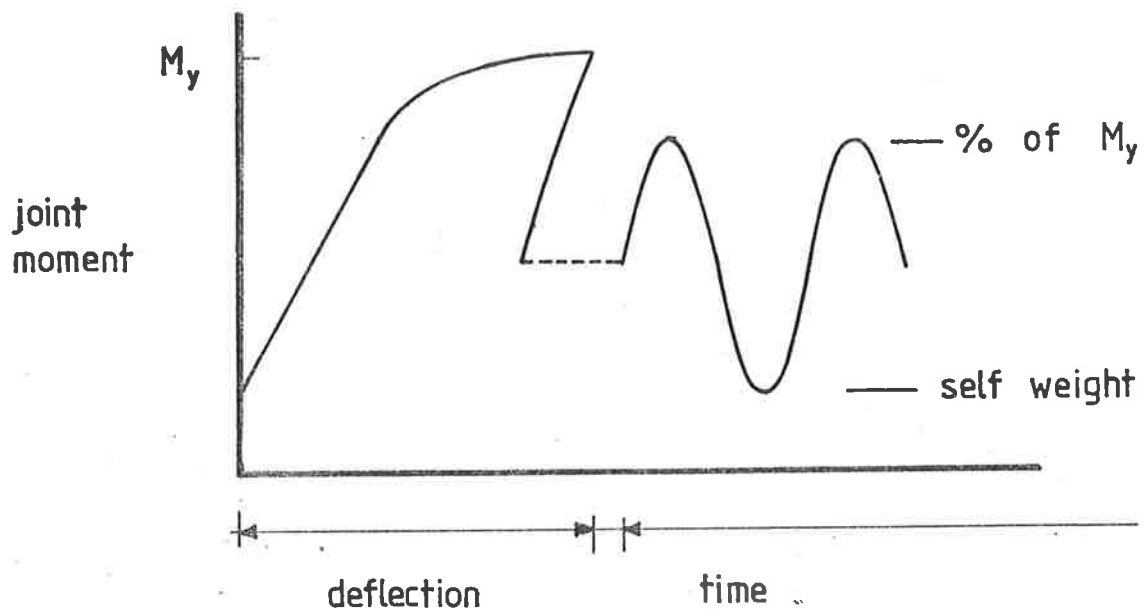

FIGURE 5.13 The load pattern used to determine the fatigue life of a T-joint specimen.

(5) Crack patterns were recorded by photographing the
specimens at various stages of loading.

5.3.4. Testing Procedures

Testing procedures were selected so the loading would be similar
to that occurring in a real structure. The discussion in Section 5.1
describes the variables modelled by the specimen loads.

(1) Prior to testing the T-joint specimens the material
properties of both the steel and concrete were determined.
The 150 mm diameter concrete cylinders poured with each T-joint
specimen were used to determine the compressive ($F'c$) and tensile (Ft)
strength of the concrete in the T-joint specimen. The compression tests
on the cylinders were conducted according to AS1012[38] and were
carried out in the 1000 KN AVERY testing machine at the University. A
spherical head was used on the lower platten to avoid any eccentric
loading due to misalignment of the end faces of the cylinders. Plywood
was used on the upper face of the cylinder to prevent any effect from
the irregularities of the trowelled surface. The Brazilian tests were
conducted in the same machine as the compression tests in the manner
prescribed by AS1012[39]. A rig was used to locate the hardwood packing
strips on each of the loaded edges.

The yield or proof stress of the steel reinforcing was determined
by tensile tests conducted according to AS1302[40] and AS1303[41].
Two specimens were tested from each batch of steel and the average of
the two values taken.

A detailed list of the material strengths is given in Appendix A.3.
The averaged material failure stresses for each T-joint specimen are
included in Table 5.1 in Section 5.1.

(2) The following procedures were used to test the T-joint
specimens. The self-weight of the rig and specimen was calculated to
be 6.2 KN. Before the tests began this was estimated to be 10-20 per
cent of the joint yield strength. To account for the self-weight the
testing machine load reading was set to zero while the rig and specimen
were supported from the load cell on the cross-head. After the specimen
was connected to the machine actuator (Connection E) a 6.2 KN compressive
load was applied. The rig and specimen were then considered to be
supported vertically only on the lower connection E. Structural analysis
of the rig and specimen in this condition determined the load distribution
due to the self-weight (see Figure 5.8). By re-setting the machine load
reading to zero, the load applied during the test could be read directly
from the control panel. The forces in the specimen at any time were
found by combining those due to the applied machine load and self-weight
(see Figures 5.7, 5.8 and 5.9).

After the adjustment for self-weight the column pre-stress was
applied as required but only to those specimens tested with a low M/P
ratio. A compressive column load of 175 KN was applied by the
hydraulic jack mounted on top of the specimen column. (see Figure 5.5 (c)).
The column load was maintained at this value throughout the test to give
the desired M/P at the expected yield load of the specimen. The yield
load was found from the early tests which did not use the column pre-stress.
Those specimens which were tested with the high M/P ratio did not require
setting of the jack to apply additional axial load.

For the pure static tests the specimens were loaded in compression
with 2 KN load increments until yielding occurred. The testing machine
control was changed from load to displacement when the specimen yielded.
The specimen was then displaced by 3.5 mm increments of the machine

actuator. Instrument readings were made after each load or displacement
increment. The inclinometers were removed when damage to the instruments
was likely. Displacement of the specimen continued until the limit of
the actuator travel was reached. This usually occurred at an effective
actuator displacement of approximately 60 mm .

For the fatigue tests the specimens were loaded by the machine
as shown in Figure 5.13. This mono-directional cyclic load had a peak
cyclic value of a set percentage of the yield load of the specimen. The
minimum cyclic value of load was that due to the self-weight of the rig
and specimen supported on the actuator.

To be able to load the specimen to a percentage of its yield load
it was necessary to know the yield load accurately. An error of 5 per
cent was considered the maximum permissible. Brooks and Hirst[7] had
tested a series of L-joints with a particular reinforcement layout and
found that the S/N curve is extremely flat. If the same situation applies
for the T-joints, large errors could have been produced in the S/N
curves because of the error in the applied loads. Several methods were
considered to determine the yield load of the specimen.

Following Brooks and Hirst the method used to determine the yield
load of the specimen was to statically yield each fatigue specimen before
the fatigue load was applied. This was carried out with the testing
machine in load control. As was also found for the pure static tests,
this was unsuitable as it sometimes resulted in large unpredictable
deflections at yield before the machine could be placed in displacement
control. The deflection of the specimen prior to the fatigue load being
applied is given in Table 5.2. The significance of the plastic
displacement is discussed later in this section. The Type 3 specimens
(10 and 11), which had the beam tension steel bent out of the joint block,

did not exhibit a well defined yield point but did have a peak load. (see Figure 5.15). Because of the absence of a distinct yield load the fatigue specimen was tested at 100 per cent of the peak load.

The static yielding method was used to determine the yield load of the specimen as it was accurate and made no assumptions about failure modes. Overloading of a specimen prior to a fatigue test could improve fatigue life, depending on the nature of any locked-in stressed induced and the subsequent fatigue failure mechanism. Alternatively, it could induce initial damage and hence reduce fatigue life below that of a virgin specimen.

Only 1 of the Series 2 specimens failed in fatigue and in order to investigate this further some additional tests were conducted to show the significance of the damage done to the specimen by the initial static yielding. Specimen 13 was damaged in the joint block and beam during the static yielding and collapsed after 1665 load cycles. Specimen 15, nominally the same as 13, was tested initially with a high column pre-stress and was only damaged in the beam during the static yielding. When subjected to 111451 load cycles no additional damage was observed except for a hairline diagonal crack in the joint block. At this stage it was tested as Specimen 13. The only difference being, that unlike Specimen 13 it was not substantially damaged within the joint block; only a hairline crack being visible under load. An additional 7948 load cycles were applied and collapse had not occurred when the test was halted. Comparing the behaviour of Specimens 13 and 15 indicates that the damage done to the specimen by the static yielding could be equivalent to many thousands of cycles of the yield load. Ideally, this yielding procedure requires further experimental investigation but this was not possible in the time available.

The alternative method considered for determining the yield load of the specimen for the fatigue tests was to factor the yield load from the pure static test. The factors required would be obtained from the relative strengths of the concrete test cylinders. This method was considered unsatisfactory because it implied that all the specimens would yield at the same location and that the yield load is related to the compressive strength of the concrete which is not always true.

In retrospect, perhaps conventional fatigue testing procedures should have been used with a very large number of tests applying absolute loads, not values relative to yield. This implies a larger scatter of experimental results but the results can be operated on statistically. However, such a programme requires a correspondingly longer period of time for testing.

The fatigue loading on a specimen was continued until the specimen collapsed or a pre-determined number of cycles was attained. The minimum number of load cycles at which a test was halted was set at 40,000. This figure was well outside the low cycle fatigue range considered to extend to 10,000 cycles. A deflection versus log-cycle plot for the most severely fatigue-loaded specimen (2) in Series 1 predicted its life to be greater than 0.5×10^6 cycles (see Figure 5.14). Not all of the Series 1 fatigue tests were conducted as the initial fatigue tests indicated that the Type 2 specimen had a fatigue life outside the range of interest.

The loading procedures described above were considered to be generally representative with what occurs in a real structure. However,
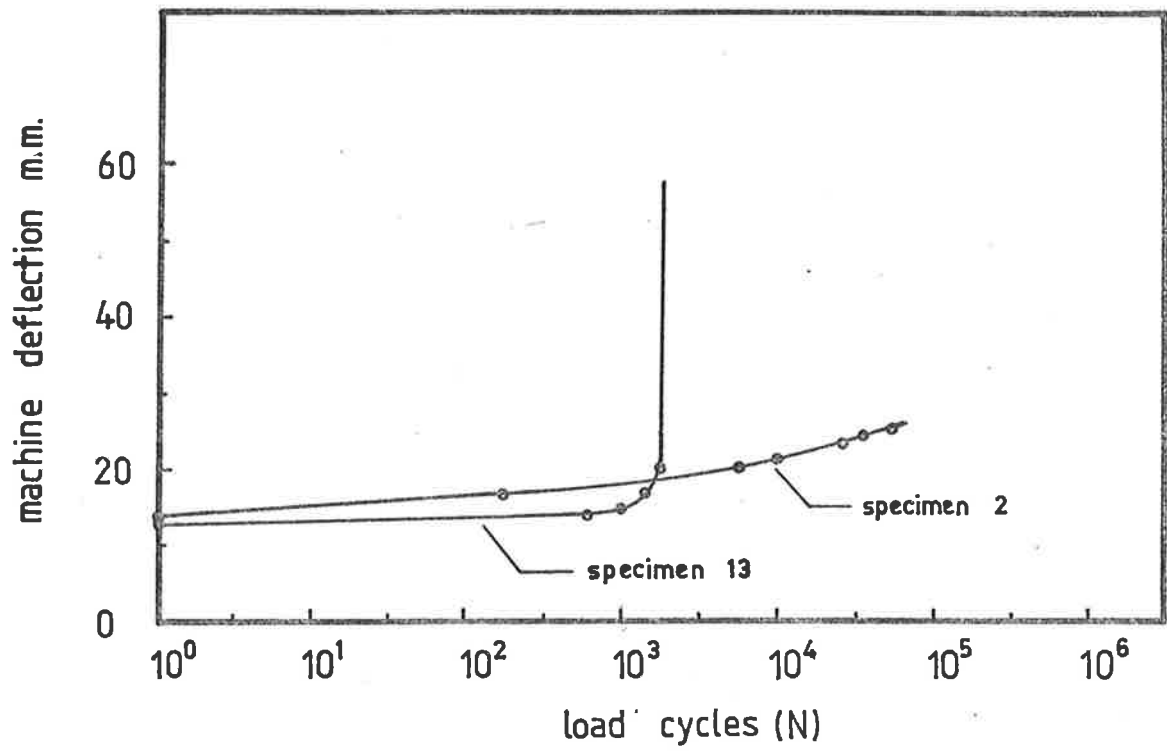
FIGURE 5.14   The effect of reinforcement layout on the
number of cycles to failure.

an obvious discrepancy is the method used to determine the yield
load of the specimens tested in fatigue. The effect of this on the
results of the Series 1 tests was irrelevant because no fatigue
failures occurred. The effect of the static yielding on the results
of the Series 2 tests has been discussed previously and shown to be
a decrease of thousands of cycles in the fatigue life of one particular
type of specimen.

5.4   Test Results

A total of 13 T-joint specimens were tested for this research
programme. The tests were made with both static (7 tests) and
fatigue (6 tests) loads according to the procedures discussed in
Section 5.3.4. Table 5.2 contains the numerical test data for each
of the specimens. Excluding Specimen 9, only one of the statically
tested specimens collapsed (Specimen 10) although the rest (Specimens
1, 5, 8, 12 and 14) underwent large deflections by hinging of the
beam. (The failure of Specimen 9 was influenced by an initial
application of the load in the reverse direction because of a machine
malfunction. The effect of this is discussed in Chapter 6). Those
specimens of Series 1 (Type 2) which were tested in fatigue (Specimens
2, 3 and 4) did not collapse even though subjected to at least 40,000
cycles of the yield load. The fatigue performance of the Series 2
specimens (Types 3 and 4) varied between collapse of the joint block
after 38 load cycles (Specimen 11) to no collapse after 111,000 load
cycles (Specimen 15).

The joint moment-machine deflection curves obtained from the
static load tests on the T-joint specimens are shown in Figure 5.15.

| | SPECIMEN | | M/P | S/F | L% | Θ_{cr} | My | Myp | M_u | Static Disp | Cycles | Failure |
	No.	Type	(metres)				(KNm)	(KNm)	(KNm)	(mm)		
Series 1	1	1	1.83	S	–	–	25.7	16.8	31.8	–	–	Beam hinging
	2	2	1.83	F	100	–	24.6	16.7	–	13.8	46287	No collapse
	3	2	1.83	F	85	>0.45 >0.32	24.6	16.7	–	17.1	114754	No collapse
	4	2	0.14	F	100	>0.42 >0.39	24.6	16.7	–	12.8	156985	No collapse
	5	2	0.14	S	–	–	22.8	16.8	>39.1	–	–	Beam hinging
	6	2	1.83	F	70	N O T T E S T E D						
	7	2	0.14	F	85	N O T T E S T E D						
Series 2	8	2	1.83	S	–	0.38 0.32	22.8	16.8	37.1	–	–	Beam hinging
	9	2	0.14	S	–	1.62 1.62	–	16.8	36.6	–	–	Joint collapse
	10	3	1.83	S	–	>0.14 >0.12	23.0	17.0	23.0	–	–	Joint collapse
	11	3	1.83	F	100	0.19 0.19	21.5	16.7	–	11.6	38	Joint collapse
	12	4	1.83	S	–	0.20 0.18	24.0	16.7	>41.6	–	–	Beam hinging
	13	4	1.83	F	100	0.34 0.32	25.2	16.8	–	13.1	1665	Bond failure in joint
	14	4	0.14	S	–	–	23.6	16.9	>37.3	–	–	Beam hinging
	15	4	0.14	F	100	–	24.0	17.0	–	12.4	111451	No collapse

"Type" Type of specimen as shown in Figures 5.2 and 5.3.

"S/F" Static or fatigue test.

"L%" The peak value of the fatigue load as a percentage of the test yield load of the specimen.

"Θ_{cr}" The deformation of the upper and lower angles of the joint when the diagonal crack formed in the joint block.

"M_y" Yield load of specimen (tested).

"M_{yp}" Predicted flexural strength of beam (AS1480).

"Static Disp" The maximum displacement of machine actuator prior to commencing fatigue loading.

"M_u" Maximum load attained in test (> indicates maximum strength of specimen not reached)

"Cycles" Number of load cycles applied to specimen.

TABLE 5.2 Results for Series 1 and Series 2 Tests.
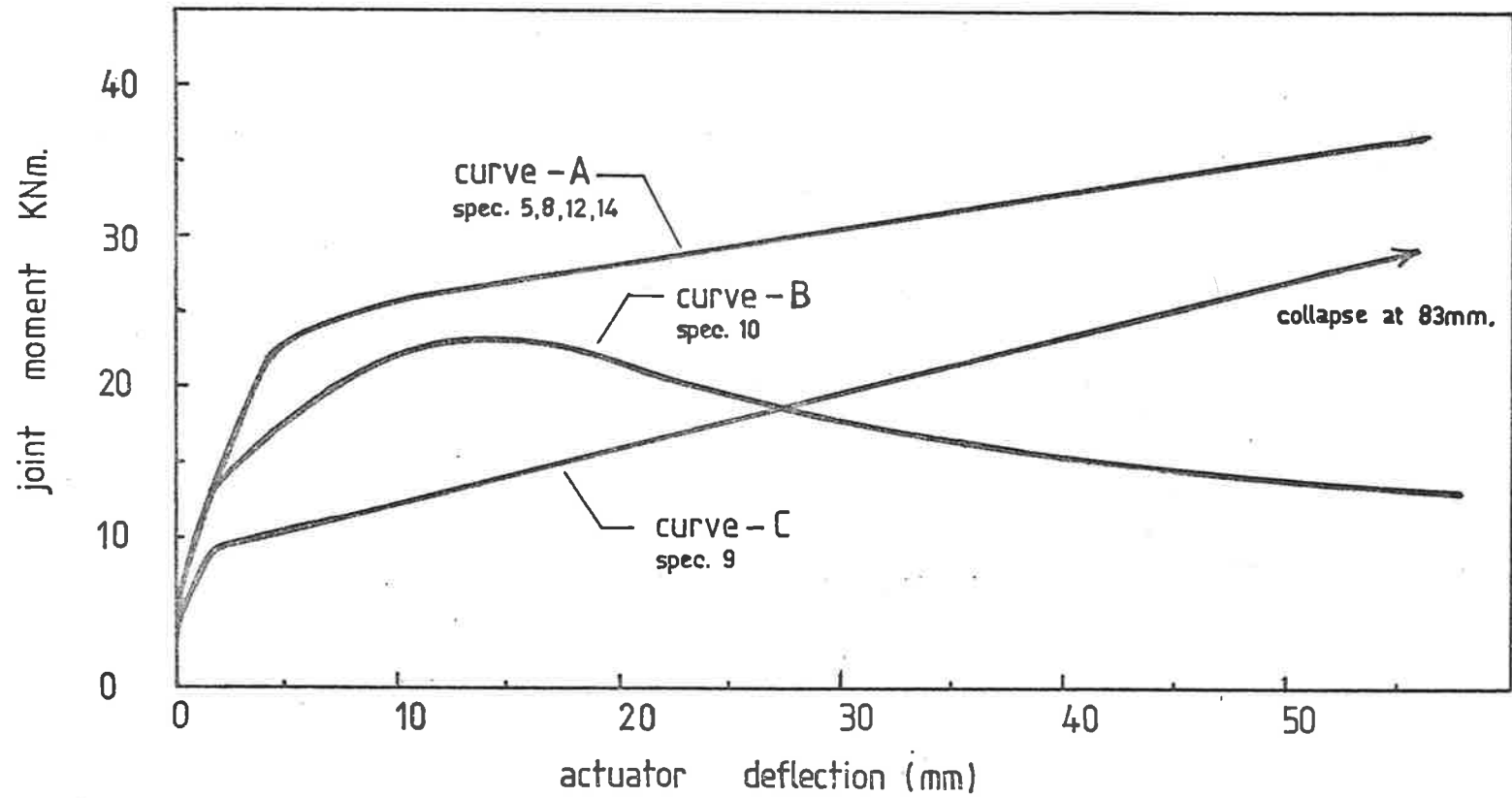
FIG 5.15   Static load versus deflection (machine actuator) for Series 1 and 2 specimens.

Only three different types of curve were obtained; these resulted from specimens with different reinforcement and loading. Curve C was produced by Specimen 9 after the initial loading in tension. Specimens of Type 2 and 4 produced Curve A irrespective of the M/P ratio used in the test. Curve A has the characteristics of ideal elastic-plastic behaviour. The strain hardening of the specimens which occurred during the plastic deflection resulted in a specimen stiffness of 0.05 of the average initial stiffness. Curve B is non-linear and has no distinct elastic-plastic yield point.

Figure 5.16 shows the change in joint angle during loading as calculated from the inclinometer readings. As would be expected the shape of the curve is the same as the initial portion of the moment-deflection curve (see Figure 5.15) for the same specimen.

Specimens 1, 5 and 8 of Series 1 were tested statically and with different magnitudes of compressive load in the column. (Specimen 1 and 8 had no column pre-stress, Specimen 5 had 175 KN). The reinforcement arrangement was similar for all specimens (Types 1 and 2) as shown in Figure 5.2. The specimens failed at high loads by hinging of the beam (see Figure 5.17 (1), (5) and (8)). The moment-deflection curve obtained from the tests on Specimens 5 and 8 is Curve A in Figure 5.15 which shows that even at very large beam deflections the high loads were sustained. The moment-deflection curve for Specimen 1 is not shown as the graph plotter was inoperative in the early part of the test. Although Specimen 1 had a yield moment equal to Specimens 5 and 8 it exhibited negligible strain hardening after an initial increase in strength.
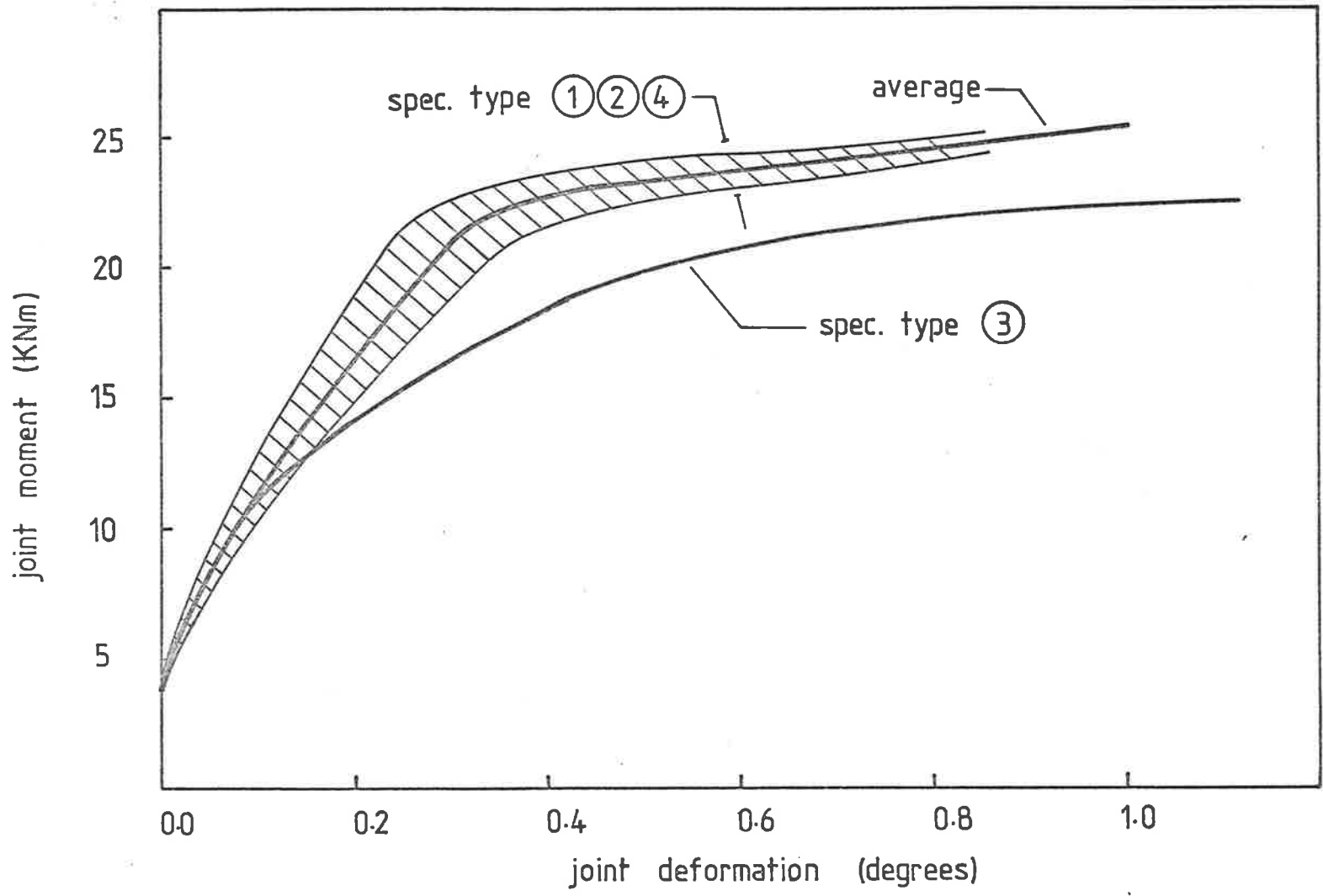
FIG 5.16   Static load versus joint deformation (angle change) for Series 1 and 2 specimens.
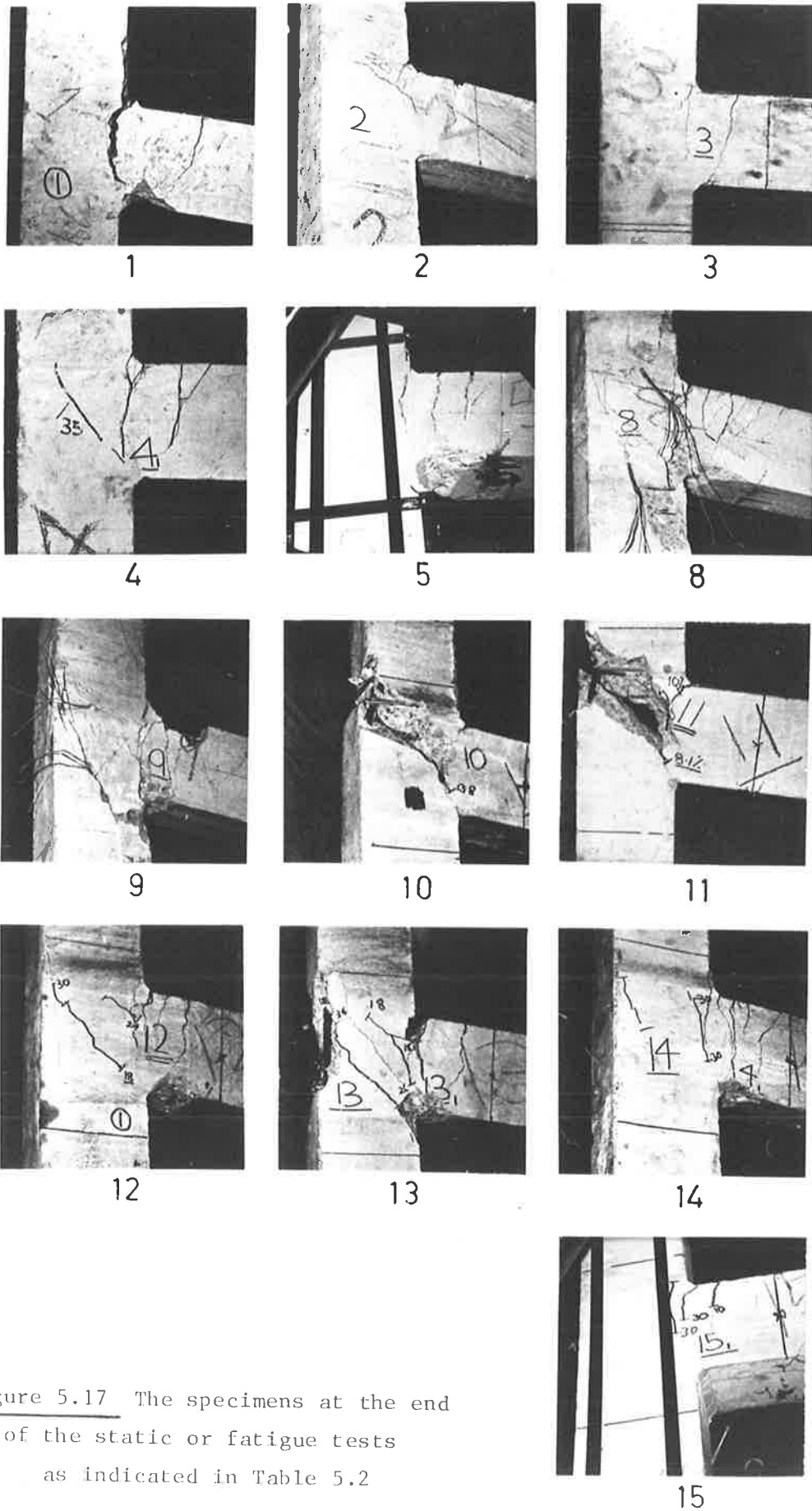
Figure 5.17 The specimens at the end
of the static or fatigue tests
as indicated in Table 5.2

The first flexural cracks in the beam were observed at joint moments as low as 6 KNm. Further cracks formed in the joint block along the interfaces with the upper column and the beam, on the primary diagonal and near the outer column bars. There was some difference in the crack patterns and resistance to cracking on the primary diagonal in each of the specimens. Specimen 5 sustained a diagonal crack of very small width and this was high in the joint block. The crack remained small in width throughout the test. This crack was possibly caused by flexural stresses in the adjacent members rather than tensile stresses on the primary diagonal. Specimens 1 and 8 both sustained cracks on the primary diagonal of the joint block. The photographs (Figure 5.17 (1), (5) and (8)) indicate a difference in the severity of the cracks in Specimen 8 with those of Specimens 1 and 5 at the conclusion of the test. (Some of the cracks in the Specimens 1 and 5 are not visible in the photographs). The greatly increased cracking in Specimen 8 occurred with the movement of the machine actuator from 58.5 mm to 67.5 mm . There was a corresponding 14 per cent drop in the load. Specimen 1 also lost strength (10 per cent) at a similar deflection.

Specimen 9 (Type 2) was tested statically without any column pre-stress. The reinforcement arrangement was that shown in Figure 5.2 and is the same as that used in the above tests. As noted previously, this specimen was initially loaded in tension and not in compression as was the case for all other specimens. The tensile load caused beam hinging and a hairline crack on the primary diagonal. (see Figure 5.18 (a)). When the load was re-applied in compression the specimen exhibited elastic behaviour but with increased load became plastic.

FIGURE 5.18(a) Specimen 9 after the testing machine malfunction caused the load to be applied in the reverse direction.

FIGURE 5.18(b) Specimen 9 after collapse at 83 mm actuator deflection.

(See Curve C, Figure 5.15). At 18.1 KNm joint moment a hairline diagonal crack formed low in the joint block. With increased load the joint block began to break up. Collapse of the joint block occurred at a moment of 36.6 KN (83 mm actuator displacement) with a shearing displacement of 15 mm on the diagonal crack. (see Figure 5.17 (9) and 5.18 (b)). Splitting also occurred on the rear face of the joint block.

Specimens 10 (Type 3), 12 and 14 (Type 4) were tested statically. Table 5.2 indicates the numerical test results. The specimens contained two different reinforcement arrangements and the effect of the magnitude of the column load was also tested on one of the arrangements. Only Specimen 10 collapsed under load (beam steel bent out of the joint block). Large flexural cracks did not form in the beam as the yield load of the beam was not reached. A 1 mm wide crack formed on the primary diagonal at 13.2 KNm load. After the crack formed the load-deflection curve became non-linear. The static load-deflection curve (B) is shown in Figure 5.15. A comparison of the curves A, B and C, Figure 5.15 shows that the Type 3 joint

(1)   has low stiffness prior to the peak load

(2)   has a low peak load

(3)   has a short yield plateau

(4)   loses strength after the peak load is reached.

The loss of strength was associated with a 15 mm shearing displacement along the diagonal crack in the joint block. (see Figure 5.17 (10)).

This displacement caused a crank to form in the outer column bars where they crossed the diagonal crack. Because of this, the concrete surrounding this area spalled. The first ligature in the upper column had begun to "unwind" due to the shear force in the column bars. This ligature had partially restrained the deformation of the column steel and limited the extent of damage in the column (see Figure 5.19). During the collapse (shearing displacement) of the specimen a large volume of concrete around the diagonal crack disintegrated.

Specimens 12 and 14 (beam steel bent into joint block - short bond lengths - two different column loads) suffered little damage to the joint block as the failure was due to beam hinging. The amount of cracking in the joint block of specimen 12 (low column pre-stress) was slightly greater than that in Specimen 14 (high column load). Specimen 12 cracked on the primary diagonal and on the rear face of the joint block (see Figure 5.17 (12)). Specimen 14 cracked near the outer column bars for the full depth of the joint block but the crack line was not fully inked-in and is not visible in Figure 5.17 (14)).

Specimens 2, 3 and 4 (Type 2) of Series 1 were tested in fatigue as shown in Figure 5.13 after the initial static yielding (actuator displacements of 13.8, 17.1 and 12.8 mm respectively). These specimens had the beam steel bent into the joint block, long bond lengths, different column loads and different magnitudes of fatigue loading. (see Table 5.2). The damage to the specimens due to the static loading was similar to that sustained by the Specimens 1, 5 and 8 in the early part of the loading. Specimen 2 did not crack on the primary diagonal until the fatigue load had been applied (less than 10,000 cycles). Specimen 3 cracked when the yield load was applied and Specimen 4 cracked during the subsequent

plastic deflection. Cracking also occurred in the beam and on the interfaces of the joint block and the members. The cracking was not always the same on the opposite faces of the joint block but because the widths of the cracks were small this was not considered important. Under fatigue loading none of the specimens collapsed and the increase in visual damage was small. The difference in the performance of the specimens was small considering the difference in the magnitude and distribution of the applied load and the difference in the number of load cycles.

Specimens 11 (Type 3), 13 and 15 (Type 4) were tested in fatigue after the initial static yielding. (11.6, 13.1 and 12.4 mm actuator displacement respectively). See Figure 5.3 and Table 5.2 for the reinforcement arrangement and test details. The collapse mechanism of Specimen 11 under fatigue load was the same as that for Specimen 10 under static loading. (see Figure 5.17 (11) and 5.19). Specimen 11 sustained 38 load cycles before collapsing completely but the joint had begun to collapse on the application of the first load cycle. Under the initial static loading, the performance of Specimen 13 was the same as Specimen 12. After 300 load cycles the diagonal joint block crack had extended. The collapse of the specimen occurred at 1665 load cycles by beam flexure (see Figure 5.14, Section 5.3). This was due to loss of bond on the beam tension steel which had been pulled through the concrete (see Figures 5.17 (13) and 5.20). When Specimen 15 was yielded the only cracks which formed were in the beam hinge. A diagonal joint block crack did not form until 76,000 load cycles had been applied. The crack was only visible when the specimen was loaded and did not cause a
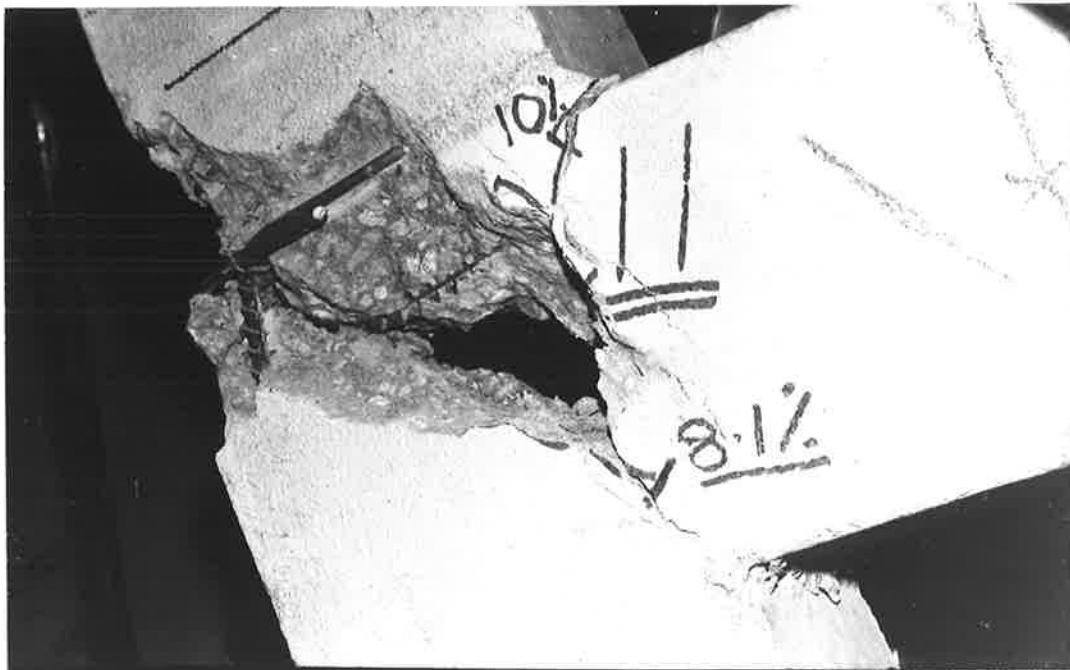
FIGURE 5.19 Specimen 11 after collapsing due to joint block shearing. The appearance of specimen 10 after it collapsed was identical to this.
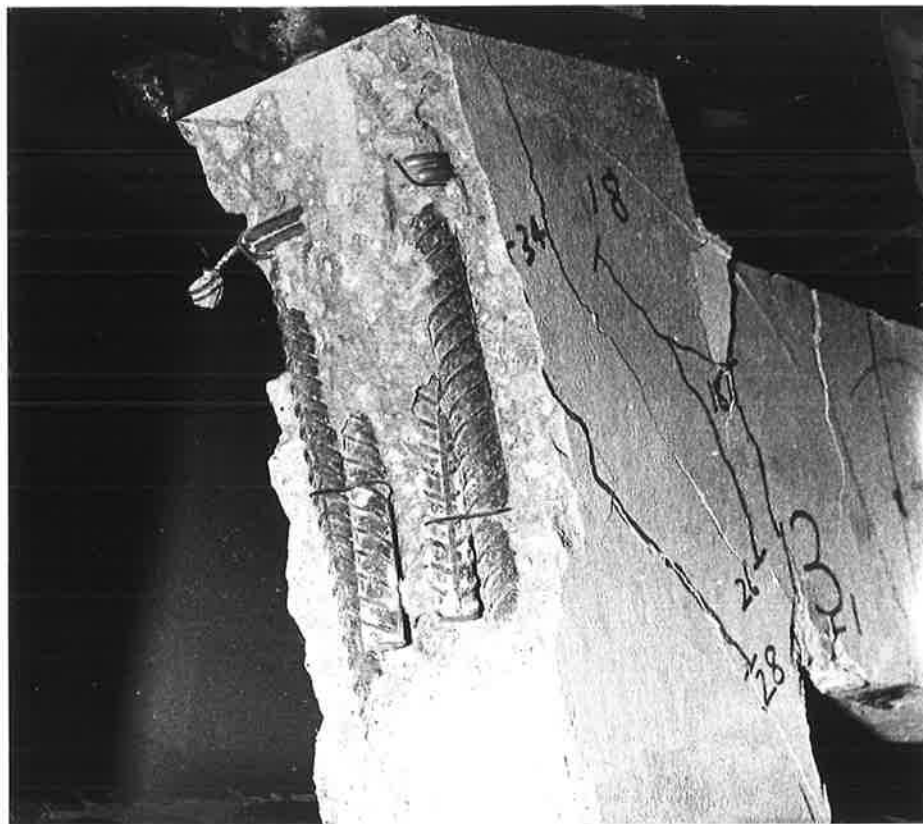
FIGURE 5.20 Specimen 13 after bond failure on the beam steel

change in stiffness. After the specimen had deflected 4 mm in the first 50 cycles the deflection remained constant. When the column pre-stress was removed after 111451 load cycles the total damage to the specimen was minimal. (see Figure 5.17 (15)). As noted previously, collapse did not occur even after a further 7948 load cycles without column pre-stress.

From the results of Specimens (1-15) it is possible to identify four areas in the joint in which cracking occurred (see Figure 5.21).

(1) Area 1, consists of a length D of the beam near the joint block. The cracks in this zone were due to beam flexure and became very large. (see Figure 5.17 (8)).

(2) Area 2, extends along the line of the beam tensile reinforcement and inner column reinforcement where it passes through the joint block. The cracks in this zone were generally parallel to the reinforcement but sometimes formed at 45 degrees to the reinforcement in the corner of the joint block. (see Figure 5.17 (2) and (12)).
These cracks were due to flexure of the beam and upper column.

(3) Area 3, surrounds the joint block primary diagonal. Cracks in this zone were due to the tensile stresses produced by the shearing forces on the joint block. (see Figure 5.17 (10)).

(4) Area 4, surrounds the outer column bars where they pass through the joint block. Cracking in this sometimes resulted in the concrete spalling. (see
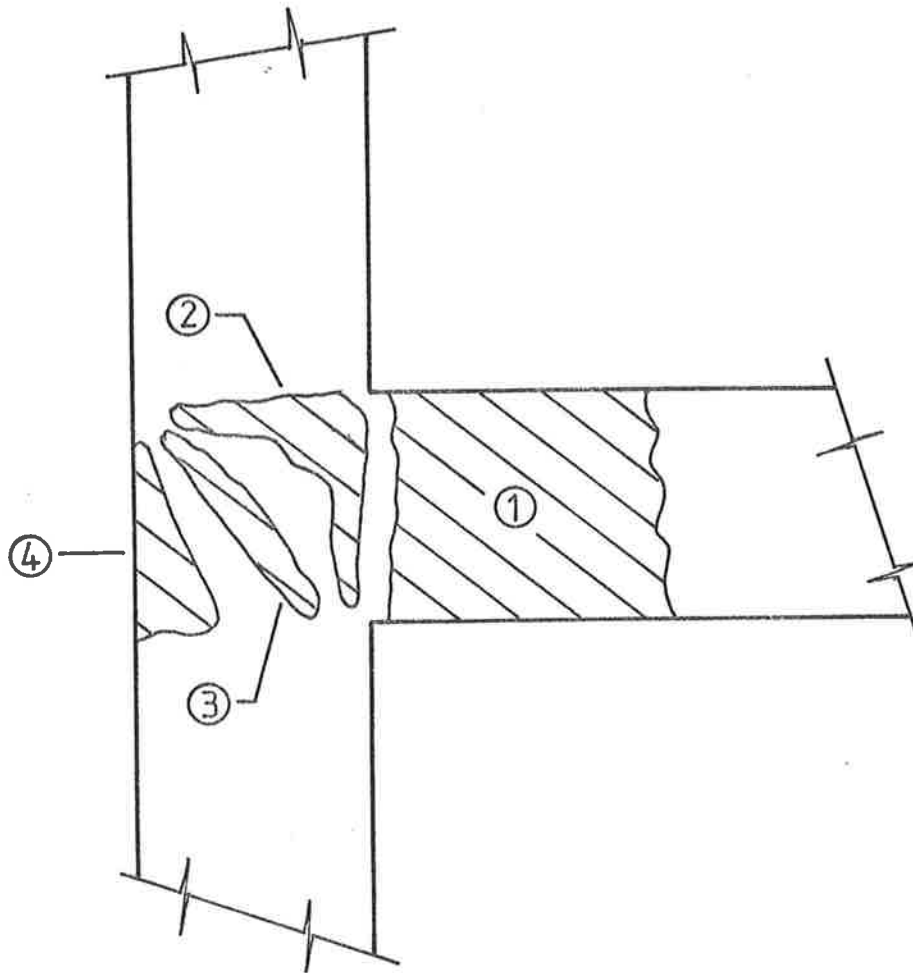
FIGURE 5.21. The areas of the joint in which cracking occurred during the tests.

Figure 5.20). The cracks were due to high

bond stresses on the reinforcement or cranking

of the column bars.

The photographs (Figure 5.17) taken at the end of the tests described
in Table 5.2 indicate the extent of the major cracks. Some of the cracks
were small in width and were not inked-in and they are not visible on
the photographs. It is evident that within each of the four areas of
cracking the size and significance of the cracks varied. In some of
the specimens the diagonal joint block crack extended outside of the
Area (3) indicated and in others it was difficult to distinguish between
cracks in Areas (2) and (3), and, (3) and (4). Formation of a crack in
any of the areas did not necessarily result in collapse of the joint.
The results show that the crack formation and significance is related
to the reinforcement layout and load distribution.

The failure modes of the joint types can be summarised as;

(1) Specimens of Type 1 and 2 failed by beam hinging
    under static load and no failures were recorded
    under fatigue loads.

(2) Specimens of Type 3 collapsed by shearing of
    the joint block under static and fatigue load.

(3) Specimens of Type 4 failed by beam hinging under
    static load and by failure of the steel bond under
    fatigue load with a large M/P value. No failures
    were recorded for specimens tested in fatigue with
    a small M/P value.

The tests on the T-joint specimens have shown that under static
loads specimens of Type 1, 2 and 4 are satisfactory and Type 3 specimens

are not (see Figure 5.15 curves A and B). The fatigue tests show that

joints of Type 2 have excellent high load fatigue performance, Type 3

is unacceptable and the use of a Type 4 joint would depend on the

magnitude of the column load .

6.   DISCUSSION OF RESULTS

The initial aim of this research programme was to determine the effect of variations of the column axial load and magnitude of the fatigue load on the performance of a T-joint containing a reinforcement arrangement commonly used in practice. This was expanded to include different reinforcement arrangements. The following discusses the main findings of the experimental and theoretical aspects of the project.

6.1 Experimental Results

The performance of the joint (Type 2 reinforcement layout) initially chosen for test evaluation, which is representative of joints commonly used in service, was found to be completely satisfactory for the applied loading conditions. All fatigue tested specimens of this type sustained at least 40,000 cycles of the yield load. No effect was observed in the fatigue life with variations of the M/P ratio or reduction in the magnitude of the applied load. This occurred because no fatigue failures were recorded for this reinforcement arrangement, even with the most severe loading conditions. Also, as the damage was mainly in the beam hinge, formed during the initial static yielding, the column load had little effect on performance of the specimen.

Increased resistance to cracking on the primary diagonal was observed in Specimen 5 but it is not possible to say that this was due to the action of the column load because another specimen with a large column load showed no such increased resistance and only a small number of specimens were tested. However, at deflections greater than 58.5 mm some effect was observed. (Minor loss of strength in Specimens 1 and 8 which were tested without any column pre-stress). As the effect was

relatively small (maximum loss of strength equal to 15 per cent),
and the rotation of the hinge well outside the limits of operation
under fatigue loading (the maximum beam rotation in the specimen
estimated as 10.5°) it is considered that the column load has little
effect on the performance of an undamaged specimen of this type under
static or fatigue loading. However, this may not be the case for a
joint in which considerable damage has occurred previously.

The yield strength of the joint was found to be 1.4 times the
ultimate strength of the beam in the joint as given by the AS1480[34]
code. This occurred because of the factors of safety used in the code,
the complex mechanism operating in the beam hinge at the face of the
joint block and the bending moment at the beam hinge is less than that
at the centre of the joint block.

The combined static and fatigue tests show that the Type 2
joint is suitable for use under fatigue loads as used in the tests.
Also, when subjected to static overload, the strain hardening properties
result in increased strength.

The effect of the magnitude of the column load on the performance
of Type 4 specimens was found to be large. The presence of the effect
was also found to be dependant on the type of loading applied to the
joint. This was shown when the performances of Specimens 12-15 (Type 4)
were compared. Under static loading with high column load no cracks
formed on the diagonal of the joint block, although there were minor
cracks in other areas in the joint block. With no column load minor
cracks appeared on the diagonal of the joint block. However, the effect
was considered to be small, as the load-deflection curve was the same
and collapse did not occur. This effect had been predicted by the

theoretical joint models which showed that increased column load reduced the peak tensile stress on the joint block diagonal.

Under fatigue loading the increased column load prevented the bond failure on the beam steel. Bond failure occurred in the specimen with the low column load after relatively few (1665) cycles compared to the number of load cycles applied to the other specimens (111451). Also, the specimen tested with the large column load did not crack on the joint block diagonal until 76,000 load cycles had been applied. A crack was observed in the specimen with low column load during the initial static loading. The column load is considered to affect the performance of the joint in two ways. These being,

(1) The increased column load reduces the tensile stress on the primary diagonal,

(2) The compressive stress in the column increases the bond strength on the beam tensile reinforcement where it enters the column.

For this type of reinforcement arrangement the latter appears to be the most important.

The compressive load in the column can be resolved into components which are parallel and perpendicular to the primary diagonal crack in the joint block. The component parallel to the crack will increase the sliding force along the crack. A greatly simplified rigid body analysis of the joint block shows that when a bending moment and column load are applied the sliding force is zero on the plane of maximum tensile stress. When the crack is not on the plane of maximum tensile stress the analysis shows the effective sliding force may be in a positive or negative direction (not yet observed in practice).

The component of the column force which is perpendicular to the crack acts to constrain it. Thus, by effectively reducing the width of the crack, the sliding resistance along the crack due to the interlocking of the angular interface is increased and the risk of shearing is reduced.

The arrangement of the reinforcement has been shown to have a large effect on the overall performance of the joint tested with fatigue or static loads. The test results confirm the effect of bending the beam steel into or out of the joint block as noted by Nilsson[3] and Park[9]. When the beam tension steel is bent out of the joint block (Type 3) the joint has poor static and fatigue performance. This is because the radial forces in the beam tension steel do not act against the diagonal compressive strut on the primary diagonal of the joint block. The force in the compressive strut is only resisted by the keying action of the outer column bars and the shear strength of the concrete in the joint block. When the sliding resistance on the diagonal crack is exceeded the outer column bars are unable to resist the force in the diagonal strut and shearing occurs. This failure mode is suppressed when the beam tension steel is bent into the joint block as the radial forces in the bend in the tensile steel act directly against the diagonal compression strut.

When Specimen 9 was initially yielded in tension due to the machine malfunction, the joint block did not collapse although the performance of Specimens 10 and 11 (discussed above) indicate that it was likely. Damage was confined to a hairline crack on the diagonal of the joint block and large flexural cracks in the beam hinge. It is considered that a shear failure of the joint block did not occur because,

(1) the flexural strength of the beam in the
specimen was less when loaded in this direction
and the beam yielded before shear failure occurred,

(2) compared to Specimens 10 and 11 there was a
greater amount of steel in the rear face of the
column to act as a key to increase the sliding
resistance on the crack.

The effect of bond length variations depended on the type of
loading applied to the joint. Where the bond length on the beam steel
was provided from the face of the column the Specimens (Type 4) were
found to be,

(1) satisfactory for static loading,

(2) satisfactory for only a limited number of
load cycles when no column load was applied
(this will require further testing to determine
an S/N curve),

(3) satisfactory for at least 100,000 load
cycles when an M/P ratio of 0.14 metres is used.

By providing the same bond length (AS1480 code value) from the bend in
the steel it was shown that the joints (Type 2) performed satisfactorily
under static and fatigue load without any column pre-stress. It is
considered that where the compressive axial load in the column is not
always large in magnitude, that extra bond length should be provided by
beginning the code bond length from the bend in the steel.

As discussed previously, the malfunction of the testing machine
during the testing of Specimen 9 resulted in the joint performing in a
manner which would have otherwise not have been observed. When reloaded

in compression, Specimen 9 collapsed due to shear failure of the joint block at a very large deformation (approximately 160 mm beam deflection). Also, the load-deflection curve obtained for the compressive loading indicated the joint was much softer than if only loaded in compression. The results of the tests on Specimen 9 indicate that there is a need to study the effect of at least a few cycles of reversed load on the fatigue performance of a joint. Normally, in a cyclone, the loading direction changes when the eye of the cyclone passes the structure. From the limited experience of these tests, reversed loading would result in a reduced fatigue life. Information from the fatigue test on Specimen 15 indicated the importance of the damage suffered by the specimen prior to the application of the fatigue load. Specimen 15 was able to sustain an additional 7948 cycles without the column pre-stress and did not collapse, although Specimen 13 collapsed after 1665 cycles. As noted previously, this damage sustained by Specimem 13 during the initial yielding greatly reduced the fatigue life.

The results of the tests on Specimen 15 indicate that there is a need to determine the damage sustained by the joints under dead load and live load prior to the action of the cyclonic or fatigue loads.

6.2   Comparison of Model Predictions and Test Results

In previous discussion (Sections 3.4 and 4.3) it was shown that the models developed during this research programme were useful for some situations. In the following discussion these models will be compared further with the experimental results.

Figure 6.1 shows the joint block cracking load for different
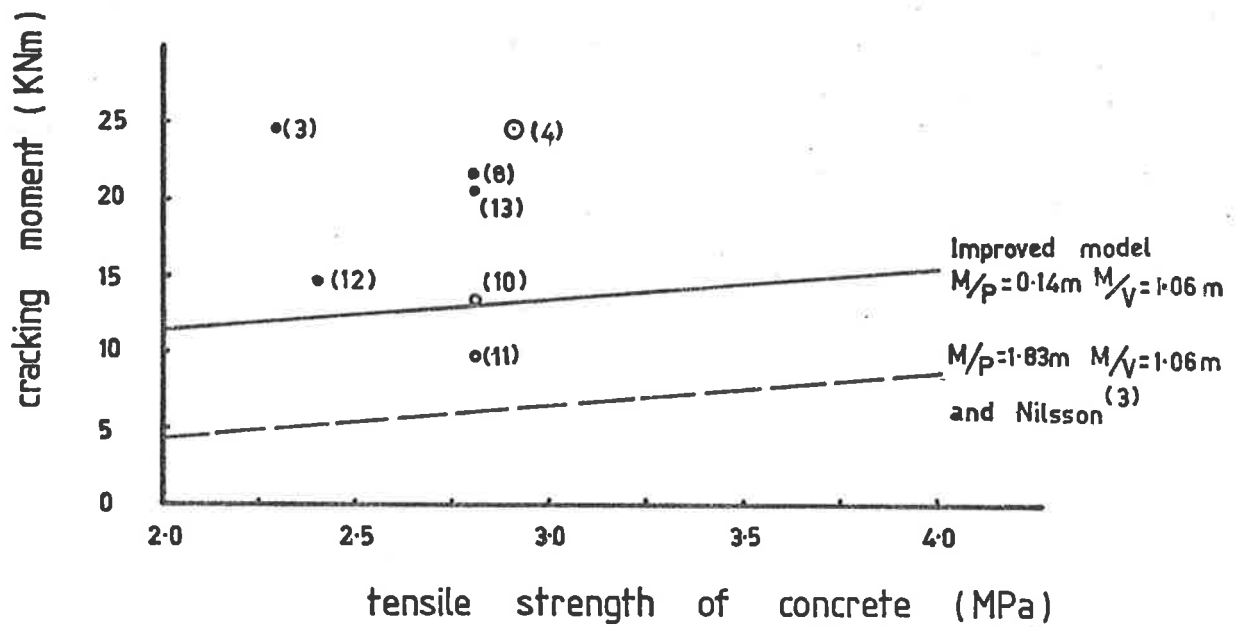
FIGURE 6.1 The load to cause a crack on the primary
diagonal of the joint block as determined
from models and testing.

specimens, as predicted by the improved model for joint block cracking and as determined by tests on the specimens. The experimental results indicated can be grouped as follows, according to the type of specimen and the loading conditions,

(1) beam steel bent into the joint block, low value of M/P

(2) beam steel bent into the joint block, high value of M/P

(3) beam steel bent out of the joint block, high value of M/P

By comparing the experimental results and model predictions the following is observed,

(1) For those specimens tested in this research programme the model underestimates the cracking load by at least 60 per cent. For some specimens which cracked the error is as great as 600 per cent.

(2) The model predicts increased resistance to cracking with lower M/P values. However, only one of the specimens tested with a large column prestress cracked (see Figure 6.1) although the model indicated that they should all have done so.

(3) The scatter of results from the specimens

with the reinforcement bent into the joint

block is as large as the variation in

cracking resistance predicted by the model

with concrete tensile strength as the variable.

Thus no conclusion can be reached on the effect

of the tensile strength of the concrete.

Previous discussion in Chapter 3 has indicated the close agreement between the improved model for diagonal cracking of the joint block, Nilsson's model and his test results. Further comparison between the improved model and Nilsson's model is made in Figure 6.1 where the predicted cracking load of some of the T-joint specimens (Series 1 and 2) is given. For those specimens with little column prestress, the predicted cracking loads from the two models are so close together that they have been plotted as a single line.

Nilsson's model uses the moment at the centre line of the joint block as the effective moment causing the diagonal crack. The improved model uses the moment at the face of the joint block and depending on the ratio of member length to joint block size makes the improved model more optimistic. However, Nilsson's model uses a stress distribution around the joint block which gives a diagonal cracking force of 0.79 times that in the improved model for the same moment at the face of the joint block. Also, the length of the zone of concrete in tension used in the two models is 10 percent greater in Nilsson's model. These effects nearly cancel in this case and similar results are obtained.

In addition the improved model takes into account the shear and axial forces in the members. When these forces are large and in the direction used in the tests, the improved model predicts a greatly increased strength over that obtained from Nilsson's model.

The improved model obviously has limitations in its ability to model the formation of a diagonal crack within the joint block. Although there is little test evidence available, the following points are considered to be instrumental in causing the limitations,

(1) neglecting the strength obtained from the presence of reinforcement and variations of its arrangement (the experimental results show that variations in the reinforcement arrangement produce a large effect),

(2) using an incorrect distribution of the stress in and around the joint block,

(3) neglecting the effect of displacement on the joint block (some of the specimens did not crack until large displacements occurred during yielding).

The non-linear F.E. model, as discussed previously in Chapter 4, has been shown to be able to predict the load-deflection curve very closely for those specimens which failed by beam hinging (see Figure 6.2). It is considered that the reason for the inability to show the effect of variations in the reinforcement arrangement within the joint block is that the failure in the model occurred outside of the joint block. For those specimens for which the failure was closely predicted, a crack pattern was obtained at increments of 1 mm beam displacement. Some of these patterns are shown in Figure 6.3 with the corresponding patterns from Specimen 8. Because of the limitations in the joint block of the F.E. model it is not reasonable to draw any independent conclusions from the predicted crack patterns on the likely performance of a specimen.
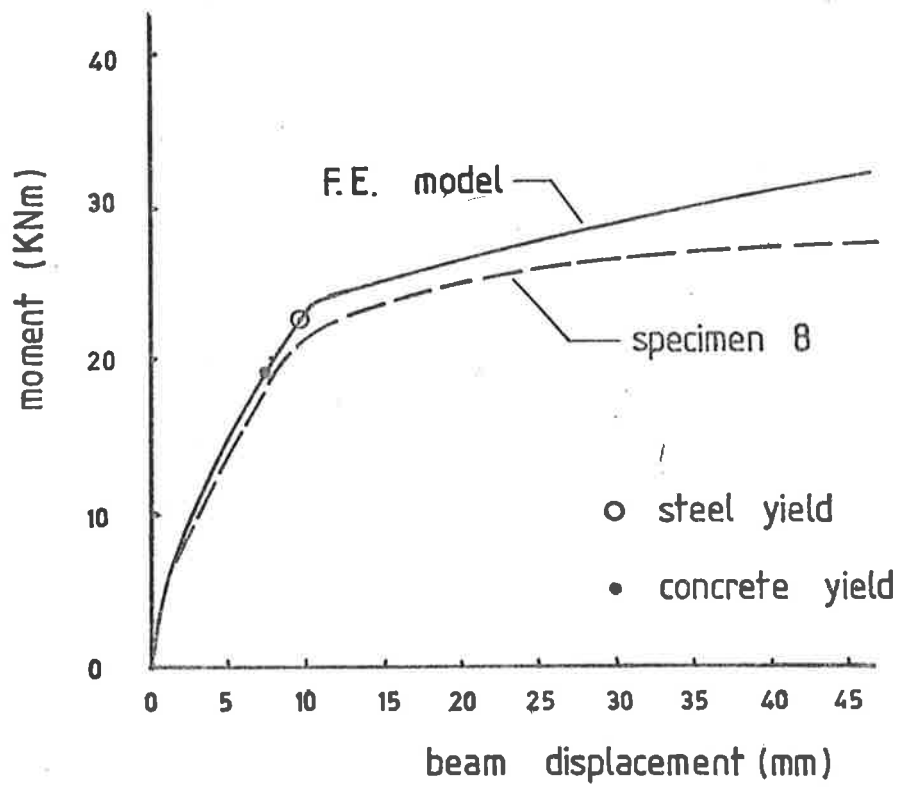
FIGURE 6.2   The load deflection curve for a
              T-joint specimen obtained from
              the F.E. model and testing.

6·4 KNm

18·5 KNm

10·9 KNm

21·7 KNm

8·8 KNm

22·7 KNm

18·1 KNm

Fig. 6.3(b)   The crack patterns in specimen 8

10·8 KNm

24·9 KNm

16·6 KNm

29·1 KNm

FIG 6.3(a) The crack patterns predicted by the
F.E. model.
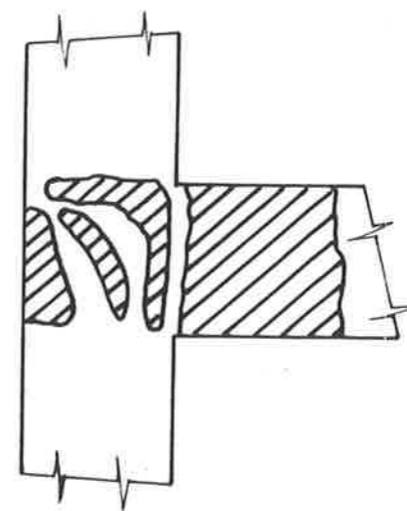
Fig. 6.3(c)   The areas of the joint in
which cracking occurred during
the tests.

The F.E. model indicates that the cracking originates in the opening corner. With increased load cracks form throughout the joint block and at the interfaces of the joint block and the members. There is no sudden appearance of a crack on the diagonal of the joint block but a gradual movement of the crack "front" parallel to the primary diagonal. If the areas of cracking in the test specimens (Areas 1 - 4 as described in Section 5) and those predicted by the model in Figure 6.3 are compared, it can be seen that there are no major disagreements. However, it is not possible to identify the separate areas of cracking within the joint block of the model, and the formation of the cracks in the joint block of the model may be by a vastly different mechanism than in the test specimen. Similarly, the cracks in Specimen 8 (as shown in Figure 6.3) can be associated with those predicted by the model. The model indicates that cracking is more widespread than is observed in the test specimen for any given load. This is because of the more uniform strength and stress within the model, whereas in a specimen there is always a plane of weakness.

Figure 6.2 indicates the load-deflection curve for those specimens which failed by beam hinging. The load at which the first steel and concrete elements yielded in the F.E. model are indicated in Figure 6.2. The concrete on the compression side of the beam was the first to yield but the accuracy of this may have been affected by the singularities in the F.E. mesh. Yielding occurred in the beam steel at the joint block end of the beam at a moment of 22.7 KNm. With increased displacement yielding occurred in the beam tension steel elements up to 100 mm inside the joint block. Yielding also occurred in some of the concrete elements in the joint block. These elements were located near the primary diagonal,

one being on the inside of the bend in the beam tension steel and the other on the upper side of the diagonal near the other end. This yielding may have been due to the action of the compressive strut on the primary diagonal but this is not conclusive because of limitations within the model, the small number of yielded gauss points and the small number of examples analysed.

The limitations of the model, as discussed in Chapter 4, are considered to be the inability to model bond slip, bends in the reinforcement, and geometric non-linearity. It would also be an advantage to be able to determine the width of the cracks in the model to aid in the comparison with the crack pattern in the test specimens and in determining the failure mechanism.

Overall, the correlation between the results of the F.E. modelling and the experimentation was not as good as had been initially hoped for. However, the limitations of the model have been established and this will aid future work in this field.

7. CONCLUSIONS AND SUGGESTIONS FOR FUTURE WORK

The aim of this research programme was to determine the performance characteristics of a joint commonly used in practice and also to determine the effect of variations in the reinforcement arrangement and M/P value.

Results of the fatigue tests on Type 2 specimens indicate that it will withstand at least 40,000 cycles of the yield load. No failures were recorded for any of the specimens of this type tested in fatigue. The M/P variations had little effect on a joint of this type because the damage was mainly confined to a hinge in the beam.

It was found that variations in the reinforcement arrangement have a large effect on the performance of a joint. Bending the beam steel out of the joint block produces a joint which is unsuitable for static or fatigue loading because of the weakness of the joint block in shear.

Under fatigue load, a reduction in the bond length on the beam tension steel resulted in bond failure when the column was lightly loaded. Thus, in accordance with the results of the Series 1 tests, it is recommended that where the column is lightly loaded the bond length on the beam steel is provided from the bend. A large column load was found to increase the bond strength of the beam tension steel.

The ability of the column load to reduce cracking on the primary diagonal of the joint block was observed in some specimens but as only a few tests were conducted the effect is not fully understood for all types of T-joint.

The improved model used to predict joint block cracking indicates that large column loads greatly increase the resistance to cracking.

However, in many instances the model was found to be very inaccurate.

The results of the non-linear F.E. modelling show that it is possible to predict the static performance of the joints which fail by beam hinging. However, without further development of the model to allow for bond slip and geometric non-linearity the model is not suitable for predicting failure within the joint block.

In practice, many of the T-joints within a building frame are restrained laterally by beams on the periphery of the building. Although previous research had shown that this improved seismic performance of the joint, this parameter was not studied in this test series but it should be included in any future research. During a cyclone the direction of the prevailing wind can reverse. The effect of only one application of load in the reverse direction before static test (Specimen 9) was found to greatly reduce the stiffness of the joint. Any future test series should investigate the effects of loading pattern on the performance of T-joints, particularly where the detail is recommended for use in areas where cyclones occur.

APPENDIX A.1   Captions on Figures and Tables

Chapter 1

Chapter 2

Chapter 3

Appendix A.1 continued....

Appendix A.1 continued.....

Chapter 4

Chapter 5

Appendix A.1   continued....

Appendix A.1 continued....

Appendix A.1 continued.....

Chapter 6

APPENDIX A.2   Computations using the Improved Model for Joint
                Block Cracking

    A.2.1   Computations to check improved model against
             Nilsson's model and test results for the cracking
             load of the joint block.
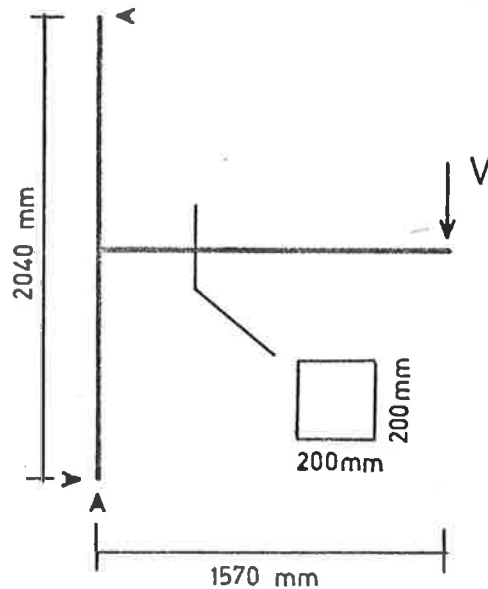
In this case :

$P = 0$

$V = M_b/S_b = M_b/1570$

$H_u = M_b/2040$

$M_b^* = M_b \times (1470/1570)$
$\quad\quad = 0.94\ M_b$

$M_u^* = (M_b/2) \times (920/1020)$
$\quad\quad = 0.45\ M_b = M_\ell$

$b = 200$ mm

$D = 200$ mm

$jd = 0.85 \times 173^{(3)}$
$\quad = 147$ mm

(diagram: 2040 mm vertical, 1570 mm horizontal, 200 mm × 200 mm block, point A, arrow V)

K = 0.66 (portion of joint block diagonal under tension as obtained

from Figure 3.6(a) - non-linear F.E. analysis)

Substituting into formula for peak stress on diagonal (Section 3.4.2)

$$f = M_b\ [\ 0.94/147\ \ + (0.45 \times 2)/147\ \ ]\ \times 3/(4 \times 200 \times 200 \times 0.66)$$

$$- M_b \times 1.5/(2 \times 200 \times 200 \times 2040) - M_b \times 1.5/(2 \times 200 \times 200 \times 1570)$$

$$f = 0.334 \times 10^{-6} \times Mb$$

Substituting the concrete tensile strengths from Nilsson's[3] tests,

i.e. 2.1, 2.6 and 2.4 MPa, gives the results in Table 3.2, Section 3.4.

    A.2.2   Calculations to determine the peak tensile stress
             on the joint block diagonal as given by the current
             model for joint block cracking

Dimensions of the specimen are those given in Figure 3.4 in

Section 3.2 for the non-linear F.E. analysis.

700mm

350mm

200mm

1mm
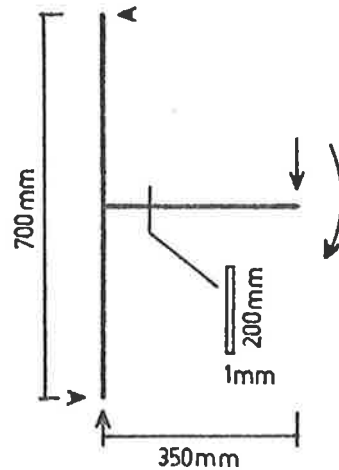
$S_b = S_u = S_\ell = 350$ mm

$D = 200$ mm

$j_d = 200 \times 0.66$

$= 132$ mm.

Case 1

$M_b/P = 0.2$ metres $M_b/V = 0.7$ metres $M_b = 1.0$ KNm

$K = 0.66$ (portion of joint block diagonal under tension

as obtained from Figure 3.6(a) - non-linear F.E.

analysis).

$M_b^* = 0.857$ kNm

$M_u^* = 0.357$ kNm $= M_\ell^*$

Substitute into equation for peak tensile stress (see Section 3.4.2)

$$f = 44.0 \text{ MPa}$$

Case 2

$M_b/P = 1.0$ metres $M_b/V = 0.7$ metres $M_b = 1.0$ KNm

$K = 0.66$ (portion of joint block diagonal under tension

as obtained from Figure 3.6(a) - non-linear F.E. analysis.

$M_b^* = 0.857$ kNm

$M_u^* = 0.357$ kNm $= M_\ell^*$

Substitute into equation for peak tensile stress (see Section 3.4.2)

$$f = 54.0 \text{ MPa}$$

APPENDIX A.3   Strength of Materials used in T-joint Specimens

| SPECIMEN | CONCRETE MIX 1 | | | | | | | | MIX 2 | | STEEL |
| | COMPRESSION | | | | BRAZILIAN | | | | CP^N | BRL^N | |
	C_1 (MPa)	C_2 (MPa)	C_3 (MPa)	F'_c (MPa)	T_1 (MPa)	T_2 (MPa)	T_3 (MPa)	Ft (MPa)	F'_c (MPa)	F_t (MPa)	F_y (MPa)
1	36.0	36.5	–	36.2	2.3	3.1	–	2.7	–	–	303
2	34.1	33.6	33.5	33.7	3.0	3.0	2.8	2.9	34.3	–	300
3	31.6	33.7	32.8	32.7	2.0	2.5	2.3	2.3	33.9	2.6	300
4	34.5	33.6	33.4	33.8	2.9	3.0	2.9	2.9	38.0	3.2	300
5	34.3	36.3	36.2	35.6	3.0	–	3.1	3.1	35.7	3.2	300
6	–	–	N O T		T E S T E D				–	–	300
7	–	–	N O T		T E S T E D				–	–	300
8	35.3	37.0	35.4	35.4	2.8	2.6	3.0	2.8	35.9	3.4	300
9	35.4	35.6	36.2	35.7	3.2	3.1	3.0	3.1	34.1	2.9	300
10	36.0	–	36.2	36.1	2.9	2.8	2.9	2.8	32.1	2.7	303
11	30.0	31.0	31.2	30.8	2.7	2.8	2.8	2.8	35.6	2.5	303
12	32.9	33.4	33.3	33.2	2.6	2.3	2.4	2.4	34.2	3.2	303
13	33.3	34.7	32.7	33.6	2.8	2.7	2.8	2.8	38.4	3.4	303
14	35.6	33.7	33.1	34.2	2.7	2.2	3.1	2.6	36.9	2.6	303
15	37.6	36.3	36.8	36.9	3.3	3.4	2.9	3.2	35.7	2.7	303

"F_y"   Yield strength of S16 Bars (MPa)
          (yield strength of S12 Bars - 298 MPa)
          (Proof strength of 6.3 mm   ligatures - 498 MPa)

"C" and "T"   Strength of concrete test cylinders (MPa)

"F'_c" and "F_t"   Average of individual test values for compressive
          and tensile concrete strength (MPa)

BIBLIOGRAPHY

1. Somerville, G. and Taylor, H.P.J. "The Influence of
   Reinforcement Detailing on the Strength of Concrete
   Structures", The Structural Engineer, No. 1. Vol. 50,
   Jan. 1972.

2. Taylor, H.P.J. and Clarke, J.L. "Some Detailing Problems
   in Concrete Frame Structures", The Structural Engineer,
   No. 1. Vol 54., Jan. 1976.

3. Nilsson, I.H.E. and Losberg, A. "Reinforced Concrete Corners
   and Joints subjected to Bending Moments", Journ. ASCE, Struct.
   Div. No. ST6, Vol. 102, June 1976.

4. Jirsa, J.O. and Marques, J.L.G. "A Study of Hooked Bar
   Anchorages in Beam-Column Joints", Project 33, Final Report,
   Dept. of Civil Engineering, University of Texas at Austin,
   1972.

5. Baldwin, J.W., (jr) and Viest, I.M. "Effect of Axial Compression on
   Shear Strength of Reinforced Concrete Frame Members", Journ.
   ACI , No. 5, Vol. 30, Proc. Vol. 55, Nov. 1958.

6. Burnett, E.F.P. and Trenberth, R.J. "Column Load Influence on
   Reinforced Concrete Beam-Column Connection", Journ. ACI , Proc.
   No. 2. Vol. 69, Feb. 1972.

7. Brooks, D.S. and Hirst, M.J.S. "Low Cycle Fatigue behaviour
   of joints in Reinforced Concrete Frames", Fifth Australasian
   Conference on the Mechanics of Structures and Materials,
   University of Canterbury, Christchurch, New Zealand, Aug. 1977.

8. Park, R. and Paulay, T. "Reinforced Concrete Structures",
    New York, Wiley, 1975.

9. Park, R. and Paulay, T. "Behaviour of Reinforced Concrete
    External Beam Column Joints under Cyclic Loading",
    Earthquake Engineering Symposium, Rome 1973.

10. Megget, L.M. and Park, R. "Reinforced Concrete Exterior Beam-
    Column Joints under Seismic Loading", New Zealand Engineering,
    No. 11, Vol. 26, Nov. 1971.

11. Hanson, N.W. and Connor, H.W. "Seismic Resistance of Reinforced
    Concrete Beam-Column Joints", Journ. ASCE. Struct. Div,
    No. ST5, Vol. 93, Oct. 1967.

12. Hawkins, N.M. (Ed). "Reinforced Concrete Structures in Seismic
    Zones", American Concrete Institute Publication SP-53,
    Detroit, 1977.

13. Kunze, W.E., Sbarounis, J.A., Amrhein, J.E. "The March 27 Alaskan
    Earthquake - Effects on Structures in Anchorage", Journ. of
    ACI, Proc. No. 6, Vol. 62, June 1965.

14. "Seismic Problems in Structural Engineering", Proceedings of a
    Seminar arranged by the Departments of Civil Engineering and
    External Studies, University of Canterbury, Christchurch,
    New Zealand.

15. Hanson, R.D., and Degenkolb H.J., "The Venezuela Earthquake,
    July 29, 1967", American Iron and Steel Institute, New York,
    1969.

16. ACI Committee 318 "Building Code Requirements for Reinforced
    Concrete (ACI 318-63)", American Concrete Institute, Detroit,
    1963.

17. ACI Committee 318, "Building Code Requirements for Reinforced Concrete (ACI 318-71)", American Concrete Institute, Detroit, 1971.

18. Award, M.E. and Hilsdorf, H.K., "Strength and Deformation Characteristics of Plain Concrete subjected to High Repeated and Sustained Loads", Abeles Symposium - Fatigue of Concrete, ACI Publication SP-41, Detroit, 1974.

19. Shah, S.P. and Chandra, S. "Fracture of Concrete subjected to Cyclic and Sustained Loading", Journ. ACI, Proc No. 10, Vol. 67, Oct. 1970.

20. Raithby, K.D. and Galloway, J.W. "Effects of Moisture Condition, Age and Rate of Loading on Fatigue of Plain Concrete", Abeles Symposium - Fatigue of Concrete, ACI Publication SP-41, Detroit, 1974.

21. Murdock, J.W. "A Critical Review of Research on Fatigue of Plain Concrete", University of Illinois Engineering Research Station, Bulletin 475, 1965.

22. Nordby, G.M. "Fatigue of Concrete - A Review of Research", Journ. ACI, No. 2, Vol. 30, Proc. Vol. 55, Aug. 1958.

23. Kesler, C.E. "Effect of Speed of Testing on Flexural Fatigue Strength of Plain Concrete", Proc. Highway Research Board, Vol. 32, 1953.

24. Sparks, P.R. and Menzies, J.B. "The Effect of Rate of Loading upon the Static and Fatigue Strengths of Plain Concrete in Compression", Magazine of Concrete Research, No. 83, Vol. 25, June 1973.

25. Chang, T.S. and Kesler, C.E. "Fatigue Behaviour of Reinforced Concrete Beams", Journ. ACI, No. 2, Vol. 30, Proc. Vol. 55, Aug. 1958.

26. Hilsdorf, H.K. and Kesler, C.E. "Fatigue Strength of Concrete under varying Flexural Stresses", Journ. ACI, Proc. No. 10, Vol. 63, Oct. 1966.

27. Stelson, T.E. and Cernica, J.N. "Fatigue Properties of Concrete Beams", Journ. ACI, No. 2, Vol. 30, Proc. Vol. 55, Aug. 1958.

28. Takhar, S.S., Jordan, I.J. and Gamble, B.R. "Fatigue of Concrete under Lateral Confining Pressure", Abeles Symposium - Fatigue of Concrete, ACI Publication SP-41, Detroit, 1974.

29. Spooner, D.C. "Stress-Strain-Time Relationships for Concrete" Magazine of Concrete Research, No. 75-76, Vol. 23, June - Sept. 1971.

30. Miner, M.A. "Cumulative Damage in Fatigue", Journ. of App. Mech, Trans. ASME, Vol. 67, Sept. 1945.

31. ACI Committee 215, "Considerations for Design of Concrete Structures subjected to Fatigue Loading", Journ ACI, Proc. No. 3, Vol. 71, March 1974.

32. SAA "SAA Loading Code AS 1170, Part 1 - 1971 Dead and Live Loads", Standards Assoc. of Australia, Sydney 1971.

33. SAA "SAA Loading Code AS 1170, Part 2 - 1975 Wind Forces", Standards Assoc. of Australia, Sydney 1975.

34. SAA "SAA Concrete Structures Code AS 1480 - 1974", Standards Assoc. of Australia, Sydney 1974.

35. Cope, R.J. and Vasudeva Rao, P. "Non-linear Finite Element Analysis of Concrete Slab Structures", Proc. Inst. of Civil Engineers, Part 2, Vol. 63, March 1977.

36. Darwin Reconstruction Committee, "Darwin Area Building Manual", December 1975.

37. SAA "SAA Steel Structures Code AS 1250 - 1975" , Standards Assoc. of Australia, Sydney 1975.

38. SAA "Methods of Testing Concrete AS 1012, Part 9 - 1973, Determination of Compressive Strength of Concrete Specimens", Standards Assoc. of Australia, Sydney 1973.

39. SAA "Methods of Testing Concrete AS 1012, Part 10 - 1972, Determination of Indirect Tensile Strength of Concrete, (Brazil or Splitting Test)" , Standards Assoc. of Australia, Sydney 1972.

40. SAA "Steel Reinforcing Bars for Concrete AS 1302 - 1977", Standards Assoc. of Australia, Sydney 1977.

41. SAA "Hard-drawn Steel Reinforcing Wire for Concrete AS 1303 - 1973" , Standards Assoc. of Australia, Sydney 1973.